General Disclaimer

One or more of the Following Statements may affect this Document

- This document has been reproduced from the best copy furnished by the organizational source. It is being released in the interest of making available as much information as possible.

- This document may contain data, which exceeds the sheet parameters. It was furnished in this condition by the organizational source and is the best copy available.

- This document may contain tone-on-tone or color graphs, charts and/or pictures, which have been reproduced in black and white.

- This document is paginated as submitted by the original source.

- Portions of this document are not fully legible due to the historical nature of some of the material. However, it is the best reproduction available from the original submission.

MODERATE TEMPERATURE RECHARGEABLE SODIUM BATTERIES

FINAL REPORT

For the period October 1978 - January 1983

Contract No. NAS3-21726

K.M. Abraham
M.W. Rupich
L. Pitts
J.E. Elliott

EIC Laboratories, Inc.
111 Chapel Street
Newton, Massachusetts 02158

Prepared for
NATIONAL AERONAUTICS AND SPACE ADMINISTRATION
Lewis Research Center
Cleveland, Ohio 44135

July 1983

MODERATE TEMPERATURE RECHARGEABLE SODIUM BATTERIES

FINAL REPORT

For the period October 1978 - January 1983

Contract No. NAS3-21726

K. M. Abraham
M. W. Rupich
L. Pitts
J. E. Elliott

EIC Laboratories, Inc.
111 Chapel Street
Newton, Massachusetts 02158

Prepared for

NATIONAL AERONAUTICS AND SPACE ADMINISTRATION
Lewis Research Center
Cleveland, Ohio 44135

July 1983

1. Report No.	2. Government Accession No.	3. Recipient's Catalog No.
NASA CR 168220		

4. Title and Subtitle	5. Report Date
MODERATE TEMPERATURE RECHARGEABLE SODIUM BATTERIES	July 1983
	6. Performing Organization Code

7. Author(s)	8. Performing Organization Report No.
K. M. Abraham, M. W. Rupich, L. Pitts and J. E. Elliott	
	10. Work Unit No.

9. Performing Organization Name and Address	11. Contract or Grant No.
EIC Laboratories, Inc. 111 Chapel Street Newton, Massachusetts 02158	NAS3-21726
	13. Type of Report and Period Covered
12. Sponsoring Agency Name and Address	Final, OCT 78-JAN 83
NASA Lewis Research Center 21000 Brookpark Road Cleveland, Ohio 44135	14. Sponsoring Agency Code 506-55-52

15. Supplementary Notes

Final Report - Project Manager: J. Singer, 106-1, Lewis Research Center, NASA, Cleveland, OH 44135

16. Abstract

This report summarizes the research performed on moderate temperature rechargeable Na batteries of the general configuration

$$Na_{(\ell)} \,/\, \beta''\text{-}Al_2O_3 \,/\, \begin{matrix}Na^+\text{-containing}\\ \text{electrolyte}\end{matrix} \,/\, \begin{matrix}\text{Transition metal}\\ \text{sulfide}\end{matrix}$$

A major aspect of the work concerned the positive electrode for which transition metal chalcogenides were studied in organic and inorganic electrolytes.

Cells utilizing the organic electrolyte, NaI in triglyme, operated at ~130°C with Na^+-intercalating cathodes. However, their rate and stability were inadequate. $NaAlCl_4$ was found to be a highly useful electrolyte for cell operation at 165-190°C. Na^+-intercalating chalcogenides reacted with $NaAlCl_4$ during cycling to form stable phases. Thus, VS_2 became essentially VS_2Cl, with reversible capacity of ~2.8 e^-/V, and a mid-discharge voltage of ~2.5V and >100 deep discharge cycles were readily achieved. A positive electrode consisting of VCl_3 and S plus $NaAlCl_4$ was subjected to deep-discharge cycles >300 times and it demonstrated identity with the in-situ-formed VS_xCl_y cathode.

NiS_2 and NiS which are not Na^+-intercalating structures formed highly reversible electrodes in $NaAlCl_4$. The indicated discharge mechanism implies a theoretical capacity $4e^-/Ni$ for NiS_2 and $2e^-/Ni$ for NiS. The mid-discharge potentials are, respectively, 2.4V and 2.1V. A Na/NiS_2 cell cycling at a C/5 rate has exceeded 500 deep discharge cycles with $2.5e^-/Ni$ average utilization.

A 4 A-hr nominal capacity prototype Na/NiS_2 cell was tested at 190°C. It was voluntarily terminated after 80 cycles. Further development, particularly of cathode structure and hardware should produce a battery capable of at least 50 W-hr/lb and more than 1000 cycles.

17. Key Words (Suggested by Author(s))	18. Distribution Statement
Sodium battery. Transition metal sulfide cathodes, NiS, NiS_2, VS_xCl_y. Rechargeable sodium battery for below 200°C.	Unclassified - Unlimited

19. Security Classif. (of this report)	20. Security Classif. (of this page)	21. No. of Pages	22. Price*
Unclassified	Unclassified	96	

* For sale by the National Technical Information Service, Springfield, Virginia 22161

TABLE OF CONTENTS

LIST OF ILLUSTRATIONS

LIST OF TABLES

ABSTRACT

This report summarizes the research performed on NASA Contract NAS3-21726, dealing with the development of moderate temperature rechargeable Na batteries. The configuration of the battery is

$$\text{Liquid Na} \,/\, \beta''\text{-}Al_2O_3 \,/\, \begin{matrix}\text{Na}^+\text{-containing} \\ \text{electrolyte}\end{matrix} \,/\, \begin{matrix}\text{Transition metal} \\ \text{sulfide}\end{matrix}$$

Depending on the electrolyte used, the battery operates at a temperature in the range of 130-200°C.

A major aspect of the work involved identification and characterization of high energy density rechargeable positive electrodes (cathodes). Na^+-intercalating, layered, transition metal chalcogenides, typified by VS_2, have been studied in both an organic and an inorganic electrolyte.

The organic electrolyte consisted of a solution of IM NaI in triglyme. Cells were operated at ~130°C, utilizing the Na^+-intercalating cathodes, VS_2, TiS_2, $Cr_{0.5}V_{0.5}S_2$, NbS_2, $TiSe_2$ or VSe_2. The organic electrolyte has been identified with inadequate thermal stability, causing restrictions on long term operations of the cells, and with limited rate capabilities because of its poor conductivity. In addition, the Na^+-intercalation reaction at 130°C, in most of the chalcogenides investigated, results in nucleation of irreversible phases, reducing the energy densities of the cells.

In order to circumvent the limitations of the organic electrolyte, we have used molten $NaAlCl_4$ as an alternative. These cells were operated at 165-190°C. We have discovered that the layered disulfide, VS_2, reacts with $NaAlCl_4$ during early stages of cell cycling. However, the *in situ* formed VS_xCl_y cathode material exhibits high capacity, and excellent rate and rechargeability characteristics. The composition of the cathode material approximates VS_2Cl. It exhibits a reversible capacity of ~2.8e^-/vanadium and a mid-discharge voltage of ~2.6V. The excellent reversibility of the positive electrode has been demonstrated by more than 100 deep discharge/charge cycles in a cell operating at about the C/10 rate.

A simple method to produce a high capacity VS_xCl_y cathode has been developed. It consists of assembling the cell initially with a positive electrode composed of VCl_3 and S, taken in a mole ratio of 1:2, and $NaAlCl_4$. The theoretical specific capacity of the "VCl_3 + 2S" cathode is 4e^-/vanadium, and the mid-discharge potential is 2.6V. One cell utilizing this electrode has exceeded 300 deep discharge/charge cycles. Its rate capability compares with that of the *in situ* formed VS_xCl_y cathode.

The non-Na^+-intercalating nickel sulfides, NiS_2 and NiS have been identified as highly reversible positive electrodes in molten $NaAlCl_4$. These cells were operated at ~190°C. The cathode reactions involve a displacement process, resulting in Na_2S and a lower nickel sulfide or Ni as products. The theoretical capacity of NiS_2 is $4e^-/Ni$ and that of NiS, $2e^-/Ni$. The mid-discharge potential of the Na/NiS_2 cell is 2.4V and that of the Na/NiS cell 2.1V. A Na/NiS_2 cell, cycling at the C/5 rate, has exceeded 500 deep discharge/charge cycles. The average NiS_2 utilization in this cell was ~$2.5e^-/Ni$.

Reversibility of the NiS cathode has been demonstrated by more than 100 deep discharge/charge cycles in a Na/NiS cell.

A prototype Na/NiS_2 cell having a nominal capacity of 4 A-hr has been constructed and tested at 190°C. This cell was repeatedly discharged and charged more then 80 times before being voluntarily terminated. Cathode structure and hardware improvements have been identified as key items for further development of the Na/NiS_2 battery. This latter battery is capable of delivering $\geq$50 W-hr/lb and >1000 deep discharge/charge cycles.

1.0 INTRODUCTION

Continued evolutions in such areas of space technology as space stations, advanced communication satellites, and interplanatory space probes demand highly reliable power sources. Qualities that are required of these power sources are high energy density, high power density, and long cycle and shelf lifes. Rechargeable batteries with Li and Na anodes have been recognized as potential candidates for many of these NASA applications.

Among the alkali metal anode batteries, a relatively well advanced system is the Liquid Na/Molten S Cell (1). It operates in the temperature range of 300-400°C. At this temperature, the active materials are highly corrosive. As a result, materials management is a persistent problem in the further advancement of that battery.

A Na battery which operates in the moderate temperature range of 130-200°C is an alternative to the high temperature system. Possible advantages include lower corrosion rates, and easier thermal and materials management. The commercial availability of the higher conducting Na-β"-Al_2O_3 solid electrolyte (over Na-β-Al_2O_3), and recent advances in technology to fabricate thinner solid electrolytes make moderate temperature Na cells a potentially feasible concept. Major breakthroughs required are in the area of positive electrode materials (cathodes).

The moderate temperature Na cell being discussed in this report has the general configuration,

$$\text{Liquid Na} \,/\, \beta\text{"-}Al_2O_3 \,/\, \begin{matrix}\text{Na}^+\text{-containing} \\ \text{electrolyte}\end{matrix} \,/\, \begin{matrix}\text{Transition} \\ \text{metal sulfide}\end{matrix}$$

A near-term goal of the project has been to demonstrate a rechargeable moderate temperature Na battery with a specific energy of 60^+ Whr/lb, a rate capability of C/5 or faster, and a cycle life exceeding 500 deep discharge/charge cycles.

Our work on NASA Contract NAS3-21726 was initially aimed at developing high energy density Na-intercalation cathodes. Accordingly, many layered transition metal disulfides and diselenides - VS_2, TiS_2, $Cr_{0.5}V_{0.5}S_2$, NbS_2, $TiSe_2$ and VSe_2 - were evaluated for their cathodic behavior in a Na cell utilizing an organic electrolyte, composed of triglyme with 1M NaI (2). Extensive studies of these chalcogenide cathodes in the organic electrolyte have revealed that cells based on organic electrolytes have somewhat limited practical use. The thermal stability range of most organic electrolytes is less than adequate. Because of poor conductivities of organic solutions, the cells have only moderate rate capabilities.

In order to circumvent the problems with the organic electrolyte, we have evaluated molten $NaAlCl_4$ as an alternative. This study has led to an extremely fruitful area of research. In early studies we explored the layered chalcogenide, VS_2 as the positive electrode. We have discovered unique chemical and electrochemical reactions between molten $NaAlCl_4$ and VS_2, resulting in novel high energy density cathode materials showing excellent electrochemical reversibility. The results are presented in this report.

In continuing our work, we have investigated the use of non-Na-intercalating transition metal chalcogenides such as NiS_2, FeS_2 and CuS as cathodes in molten $NaAlCl_4$. This study has led to the demonstration of more than 500 deep discharge/charge cycles for Na/NiS_2 cell. Detailed results of this investigation, including mechanistic aspects of cathode reactions, rate-capacity relationships of the positive electrode, and cell cycle life are presented.

2.0 INTERCALATION POSITIVE ELECTRODES IN TRIGLYME/NaI

The cathode reaction in a Na cell utilizing an intercalation positive electrode involves the insertion of Na^+ into the interstices of the cathode material crystal lattice - the Van der Waals gaps in the case of layered transition metal chalcogenides - as depicted in equation [1].

$$xNa^+ + ne^- + MY_n \underset{\text{charge}}{\overset{\text{discharge}}{\rightleftharpoons}} Na_xMY_n \qquad [1]$$

The species MY_n in equation [1] is a layered transition metal chalcogenide. An ideal intercalation reaction, by definition involving little or no structural change of the cathode material, is highly reversible. In practice, fractional irreversibilities may appear due to factors such as a slight perturbation of the bonding within the crystal lattice, a slight expansion of the lattice, and crystallographic phase changes of the material. It is, therefore, necessary to experimentally determine the reversible capacity of each material.

Our studies were carried out in a cell of the configuration,

$$\text{Liquid Na} \,/\, \beta''\text{-}Al_2O_3 \,/\, \text{Triglyme, 1M NaI} \,/\, \begin{matrix}\text{Layered}\\ \text{transition}\\ \text{metal chalcogenide}\end{matrix}$$

The operating temperature of the battery was ~130°C. The layered transition metal chalcogenides included TiS_2, VS_2, $Cr_{0.5}V_{0.5}S_2$, $Nb_{1.1}S_2$, $TiSe_2$ and VSe_2. The results obtained with these materials have been published in a series of papers in the Journal of Electrochem. Soc. (3-5), and have been summarized in a recent review, published in Solid State Ionics (2). The latter paper is included in the appendix of this report in order to acquaint the reader with this new and potentially fruitful area of research. The major conclusions of our work on intercalation cathodes in Triglyme/NaI electrolyte are the following:

- At moderate temperatures, i.e., ~130°C, the rechargeability of the intercalation electrode is limited by crystallographic phase changes of the cathode material. The intercalated Na associated with only certain phases have been found to be reversible in most chalcogenides. As a result, the useful capacities of many dichalcogenides are considerably less than anticipated on the basis of structural considerations.

- The organic electrolyte does not have adequate conductivity to permit cell discharges at high rates to give high energy and powder densities. In addition, the long term stability of the organic electrolyte in the 130-150°C range is projected to be only moderate.

The directions which we followed in order to achieve the original goals of the program were:

- Use of alternative electrolytes with higher conductivities and better thermal stabilities. The choice of molten $NaAlCl_4$ turned out to be an excellent one.

- Performing cell operations at a somewhat higher temperature than 130°C, employed with organic electrolyte cells. Cells utilizing molten $NaAlCl_4$ have been operated in the temperature range of 165-190°C.

3.0 MODERATE TEMPERATURE Na CELLS WITH LAYERED METAL CHALCOGENIDE POSITIVE ELECTRODES IN MOLTEN $NaAlCl_4$

In order to take advantage of the higher thermal stability and better ionic conductivity of inorganic molten salts, we have investigated the cycling behavior of layered metal chalcogenides in molten $NaAlCl_4$.

The acid-base properties of molten chloroaluminates can be varied by the initial mole ratio of NaCl and $AlCl_3$ (6). The Lewis acidity is expressed in terms of $pCl = -\log[Cl^-]$. The melts having $pCl > 2.7$ are acidic and those having $pCl < 2.7$ are basic. Near the 1:1 $AlCl_3$/NaCl mole ratio, the acid-base properties can be described by the equilibrium.

$$2AlCl_4^- \rightarrow Al_2Cl_7^- + Cl^- \qquad [2]$$

The $[Al_2Cl_7^-]$ changes from $\sim 10^{-4}$M to ~1M in going from a NaCl saturated (~49.8 m/o $AlCl_3$ at 175°C) melt to a 52 m/o $AlCl_3$ melt.

Some initial studies, which were carried out with VS_2 at 165°C, in an acidic melt, prepared from 40 mole-percent (m/o) NaCl and 60 m/o $AlCl_3$, indicated poor cathode capacity and rechargeability. Therefore, the acidic melt was abandoned.* All further Na cell studies were carried out in a basic electrolyte, prepared from a NaCl saturated NaCl/$AlCl_3$ melt, composed of 51 m/o NaCl and 49 m/o $AlCl_3$.

Some properties of the 50.50 NaCl/$AlCl_3$ melt and Na-β"-Al_2O_3 are presented in Table 1.

3.1 Experimental

All air and moisture sensitive materials were handled using standard techniques and equipment, designed for the manipulation of air sensitive compounds. All electrochemical experiments were carried out in a glove box (Vacuum Atmospheres Corporation), maintained with an argon atmosphere which was continuously circulated through a drying column.

3.1.1 Synthesis and Characterization of Transition Metal Sulfides

Crystalline VS_2, TiS_2 and VSe_2. Crystalline VS_2 and TiS_2 were prepared as described previously (3). VSe_2 was purchased from Cerac, Inc. Milwaukee, WI. They were characterized by X-ray diffraction data (5).

*It would be useful to re-examine the chemistry and electrochemistry of layered metal chalcogenides in acidic NaCl/$AlCl_3$ melts.

Table 1

Some Properties of $NaAlCl_4$ and Na-β"-Al_2O_3*

Electrolyte	Temperature (^oK)	Property		
		Viscosity (c.p)	Density (g/ml)	Conductivity (ohm^{-1} cm^{-1})
$NaCl/AlCl_3$ 50:50	460	2.65	1.3	0.462
Na-β"-Al_2O_3	573	-	3.2	0.16

*From Ceramatec, Inc., Salt Lake city, UT.

Amorphous VS_2. a-VS_2 was prepared according to equation 3 using a procedure developed by Chianelli and Dines (7).

$$VCl_4 + 2Li_2S_{(s)} \xrightarrow{THF} VS_2 \cdot THF_{(s)} + 4LiCl \qquad [3]$$

The rate of reaction 3 is very much dependent on the crystallinity of Li_2S. With highly crystalline Li_2S almost no reaction occurs at 20°C. The a-VS_2 used in our studies was prepared by stirring a slight excess of VCl_4 in THF with Li_2S (Cerac; Cat. #1080) for 16 hours at ambient temperatures. The $VS_2 \cdot THF$ product was vacuum filtered and repeatedly washed with THF to remove all the LiCl. The unsolvated a-VS_2 was obtained quantitatively by heating the solvated product under vacuum at 210°C for four hours.

Elemental analysis of the product indicated a stoichiometry of $VS_{1.99}$ and less than 0.4 w/o LiCl contamination. An X-ray diffraction analysis confirmed the amorphous nature of the material.

Amorphous MoS_3. Amorphous MoS_3 was prepared by thermal decomposition of $(NH_4)_2MoS_4$ in an argon atmosphere at 200°C for three hours (8). The ammonium thiomolybdate was prepared by passing hydrogen sulfide through an aqueous ammoniacal solution of ammonium paramolybdate at ambient temperatures. The red crystals of $(NH_4)_2MoS_4$, which separated from solution, were analyzed by thermogravimetric analysis. The first weight loss which begins at 200°C accounted for 26.0% of the weight compared to the theoretical 25.2% expected for the reaction

$$(NH_4)_2MoS_4 \rightarrow MoS_3 + (NH_4)_2S \uparrow \qquad [4]$$

The second weight loss, which begins at 400°C, results in the formation of MoS_2, with loss of sulfur. The weight loss calculated from the thermogram was 38.4% compared to a theoretical 38.8%. The weight loss of $(NH_4)_2MoS_4$ in the preparation of the MoS_3 used in cell studies was 26.6%, in good agreement with reaction 4. Elemental analysis of the MoS_3 product confirmed its stoichiometry; found: Mo, 49.86; S, 50.10; calculated: Mo, 49.94; S, 50.03.

The MoS_3 product exhibited no X-ray diffraction lines as expected. An SEM photograph revealed its highly porous, noncrystalline structure.

Sodium Vanadium Disulfide, $NaVS_2$. Crystalline VS_2 was added to a 30% excess of Na naphthalide in THF (0.3M). The slurry was stirred for three days and then the $NaVS_2$ was removed by vacuum filtration, washed with THF, and dried under vacuum at 70°C for 24 hours. Elemental analysis indicated a composition of $Na_{0.95}VS_2$. It was also characterized by X-ray diffraction data (5).

NbS_2Cl_2. NbS_2Cl_2 was prepared according to reaction 5 (9).

$$Nb + S_2Cl_2 \rightarrow NbS_2Cl_2 \qquad [5]$$

The X-ray pattern for NbS_2Cl_2 is given in Table 2.

3.1.2 Electrolyte Preparation

Sodium Tetrachloroaluminate, $NaAlCl_4$. The $NaAlCl_4$ electrolyte was prepared by heating a NaCl (51 m/o)/$AlCl_3$ (49 m/o) mixture at 190°C to form a liquid. The melt was then purified by constant current electrolysis at 10 mA (0.5 mA/cm^2) between two Al disc electrodes for 72-96 hours. The resulting clear liquid was cooled and the solid was ground to a fine white powder, and stored in a glove box until use.

3.1.3 Electrochemical Cell

A typical cell (Fig. 1) consisted of an outer pyrex compartment which contained the $NaAlCl_4$ electrolyte and the positive electrode, and an inner compartment, fabricated from a β''-Al_2O_3 Na^+-conductor tube (Ceramatec Cat. No. CT16A), which contained the sodium. The cell after assembly was placed in a thermostated oven, maintained at 165 ± 5°C.

The cathodes were fabricated in a graphite-felt (Union Carbide, WDF felt) matrix. The cathode material powder was sifted into the graphite felt of known area and the felt, in turn, was wrapped around the β''-Al_2O_3 tube. An amount of $NaAlCl_4$*, sufficient to completely wet the carbon felt, was added. A tungsten wire, in contact with carbon felt, served as the positive electrical lead from the cell.

The β''-Al_2O_3 tube anode compartment contained a large excess of Na and a tungsten wire current collector. The β''-Al_2O_3 tube was first filled with chunks of Na metal (Alfa-Ventron, packed in Argon) which had been skimmed of its oxide coating with a sharp knife. The tube was then heated to 400°C for ~24 hr in order to allow good wetting of the β''-Al_2O_3 with liquid Na.

The anode compartment of the cell was sealed with a silicone rubber plug and the cathode compartment with a Teflon-seal. All cells were assembled and operated in a glove box having an Argon atmosphere.

3.2 Results and Discussion

3.2.1 The Na/VS_2 Cell

Cell studies were carried out with crystalline VS_2, amorphous VS_2 and $NaVS_2$ as cathodes.

*The $NaAlCl_4$ powder is usually mixed with a small amount of NaCl to ensure melt basicity.

Table 2

X-Ray Powder Pattern of NbS_2Cl_2

EIC Synthesized NbS_2Cl_2		NbS_2Cl_2*	
d, Å	I/I_o	d, Å	I/I_o
6.19	100	6.24	80
5.82	20		
5.15	20	5.28	60
4.82	20	4.82	60
3.11	50	3.14	60
2.59	60	2.61	90
2.40	10	2.42	30
2.17	10	2.19	50
2.05	90	2.09	80
2.01	20	2.03	50
1.92	10	1.93	40
1.83	20	1.83	60
1.65	10	1.67	40
1.56	10		
1.52	10		
1.38	5		
1.36	5		
1.26	5		

*From reference 9.

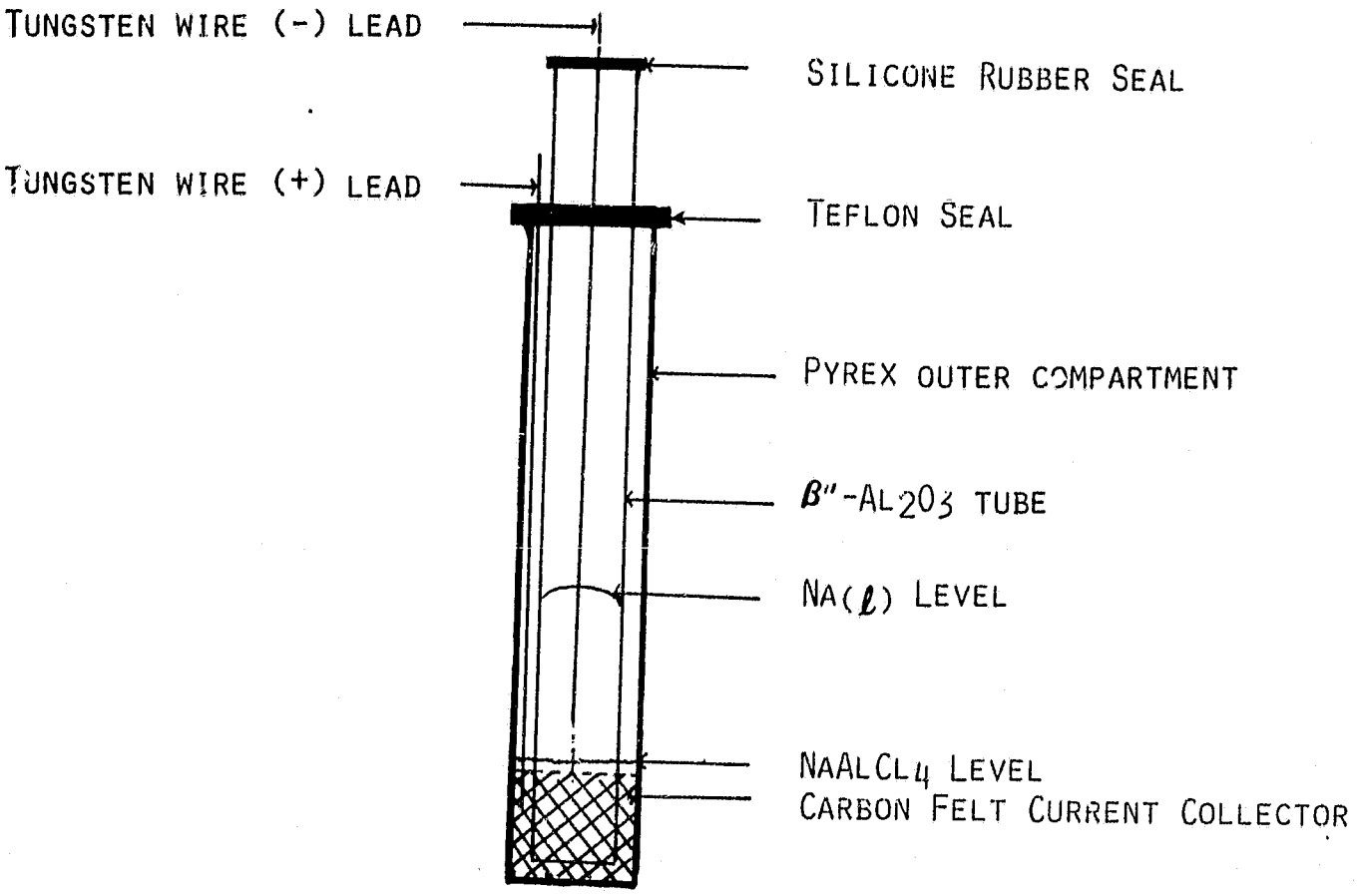

Fig. 1. A laboratory sodium cell.

3.2.1.1 Crystalline VS_2 Cathode

Figure 2 depicts the cycling behavior of a Na/VS_2 cell at 165°C. The cathode contained 0.52 g crystalline VS_2 in contact with ~8 g $NaAlCl_4$* electrolyte. The Na/VS_2 cell exhibits an open-circuit voltage of 3.05V at 165°C. The first discharge of the cell to 1.8V usually yields capacities between 0.90 and 0.7 electrons/vanadium (e^-/V) at current densities between 1 and 5 mA/cm^2. The discharge proceeds with three voltage regions - a downward sloping region between 2.8 and 2.4V, with ~8% of the capacity, another downward sloping region between 2.4 and 2.V, with ~25% of the capacity, and a plateau at 2.2V with the remaining capacity. The mid-discharge voltage is slightly above 2.2V. The first recharge to 3.5V usually corresponds to 100% of the discharge. The recharge occurs in three major voltage regions - an upward sloping region between 1.8V and 2.2V, with ~20% of the capacity, a second upward sloping region between 2.2 and 3.1V, with ~20% of the capacity, and a plateau at 3.2V, with the remaining capacity. The discharge and recharge curves exhibit considerable hysteresis (cycle 1 in Fig. 2). Repeated cycling of the Na/VS_2 cell between 1.8 and 3.5V results in a gradual increase in cathode capacity with the mid-discharge voltage moving to higher values and the mid-charge voltage moving to lower values. The capacity increases to values between 1.2 and $1.3e^-/V$ in about 10 cycles. These characteristics are illustrated in the first, second and the tenth cycle of the cell in Figure 2.

It was found, however, that if, after the first discharge to 1.8V, the cell is allowed to stand on open circuit at 165°C, instead of immediately recharging it, the OCV increases from 1.9V to a constant value of 2.3V in a period of ~75 hours. This is indicated in Figure 3 (cycle 1) which depicts the cycling behavior of another Na/VS_2 cell, very much similar to the one above. This behavior seems to indicate that a reaction between the discharged cathode and $NaAlCl_4$ takes place. Moreover, the recharge capacity of the cell after this open circuit stand is about twice that of the previous discharge, i.e., $1.6e^-/V$ for the cell in Figure 2. Most of the recharge occurs in a plateau at ~3.2V. During the next few cycles the discharge capacity to 1.8V increases to even higher values, with the respective recharges to 3.5V showing capacities higher than the discharges. The capacity then reaches a constant value of ~2.6 to $2.8e^-/V$ in 5 to 8 cycles. The cycling of the cell then becomes 100% coulombically efficient. The mid-discharge voltage is ~2.5V and the mid-charge voltage is ~2.8V. The discharge proceeds in four major voltage steps (cycles 6 and 28 in Fig. 3). The cell exhibits excellent rechargeability.

3.2.1.2 Amorphous VS_2 Cathode

Amorphous VS_2 was investigated to determine whether the morphology of the initial VS_2 had any effect on the cycling characteristics of the cathode.

*The background capacity due to $NaAlCl_4$ alone on graphite felt under identical conditions is practically nil.

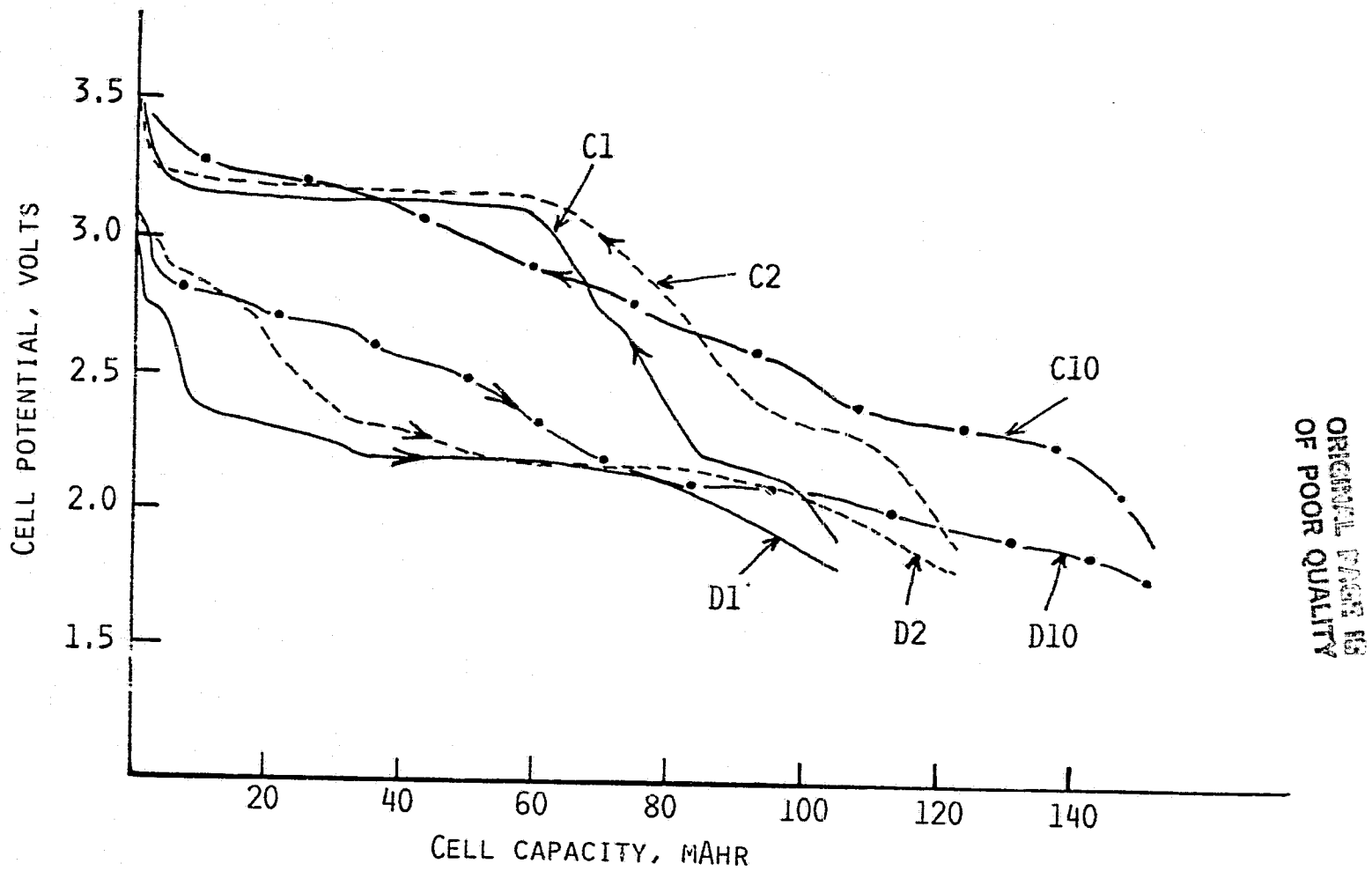

Fig. 2. Galvanostatic cycling curves for a liquid Na/β"-Al_2O_3/$NaAlCl_4$, VS_2 cell at 165°C. Voltage limits, 1.8 and 3.5V. Curves marked D's are discharges and those marked C's are charges. Current = 16 mA (2 mA/cm^2). The VS_2 cathode has 120 mAh le^- theoretical capacity.

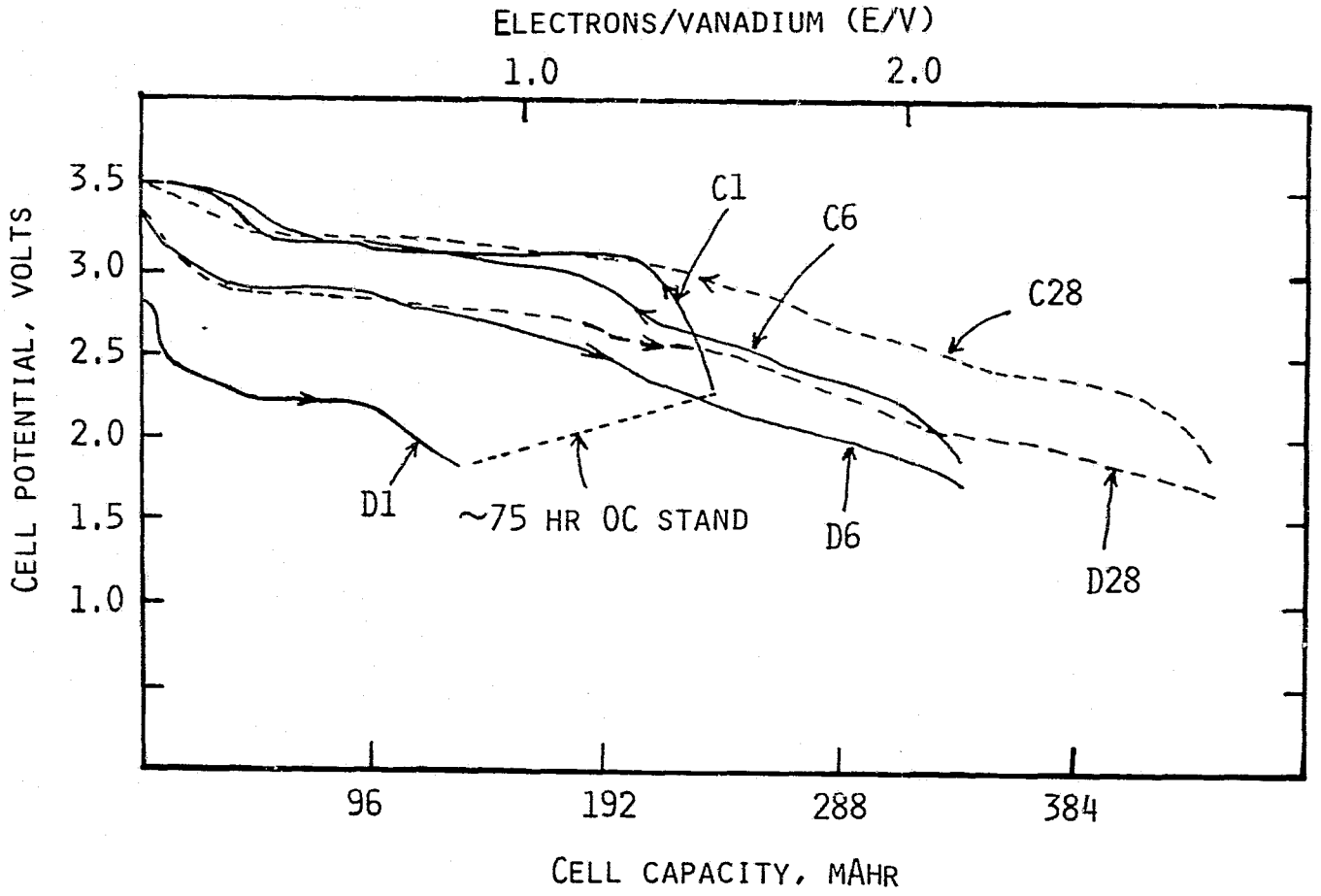

Fig. 3. Galvanostatic cycling curves for a liquid Na/β"-Al_2O_3/$NaAlCl_4$, VS_2 cell at 165°C prior to and after the open circuit (OC) stand. Curves marked D's are discharges and those marked C's are charges. Voltage limits, 1.8 and 3.5V. Current = 16 mA (2 mA/cm^2).

The cell for this (No. 302-33) was constructed with 0.33 g VS_2 (77 mA-Hr, $1e^-$ theoretical capacity). As before the cell contained a larger excess of $NaAlCl_4$. Figures 4 and 5 depict typical cycles of the cell. The OCV of the cell at 165°C was 3.03V. The first discharge at 8 mA (1.0 mA/cm^2) resulted in a capacity of 96 mA-Hr ($1.2e^-/V$). The first recharge resulted in slightly more than double this capacity, amounting to $2.5e^-/V$. This recharge behavior of the amorphous VS_2 cell is reminiscent of the same behavior of crystalline VS_2 cells after the long open-circuit stand following the first discharge. It appears that with a-VS_2, the reaction between the discharged cathode and $NaAlCl_4$ occurs at a much faster rate (the same time scale as the discharge rate) than that in the case of the crystalline VS_2 cathode.

The average cathode capacity during the 49 cycles following the first recharge amounted to the full utilization of the capacity in the first recharge, i.e., $2.5e^-/V$. Figure 5 shows some of the later cycles of the cell.

3.2.1.3 $NaVS_2$ Cathode

The cycling behavior of an Na/VS_2 cell at 165°C was investigated utilizing $NaVS_2$ as the initial cathode. The $NaVS_2$ used in these experiments was prepared by the reaction between an excess of Na-naphthalide and VS_2 in THF (5). The $NaVS_2$ product had been washed with THF and dried in vacuo at ~80°C.

The cell, No. 88, was assembled with a cathode containing 3.62 mmoles (97 mA-Hr, $1e^-$/vanadium) of $NaVS_2$ and an excess of $NaAlCl_4$. The open-circuit-voltage (OCV) of the cell was 1.90V at 165°C. The lower open-circuit voltage is in agreement with a lower oxidation state for V, i.e., V^{+3} in $NaVS_2$, as opposed to V^{+4} in VS_2. The cell, after heating to 165°C, was left on open circuit for ~16 hr during which time the OCV increased to 2.30V. This behavior is similar to the behavior of the cells initially setup with VS_2, discussed earlier. It appears that a reaction between $NaVS_2$ and $NaAlCl_4$ occurs at 165°C.

The cycling of the cell began with an initial charge to 3.5V, followed by cycling between 1.8V and 3.5V. The current was 8 mA, corresponding to a current density of 1 mA/cm^2. The data are given in Figure 6. The capacity in the first charge to 3.5V was 125 mAh ($1.3e^-/VS_2$). The first discharge to 1.8V yielded a capacity equivalent to 1.9 e^-/VS_2. The capacity in the second charge was more than that in the discharge, being $2.3e^-/VS_2$. In the second discharge a higher capacity of $2.4e^-/VS_2$ was obtained. The charge/discharge curves, shown in Figure 6, are very much similar to those of the cell presented in Figure 3, initially set up with VS_2.

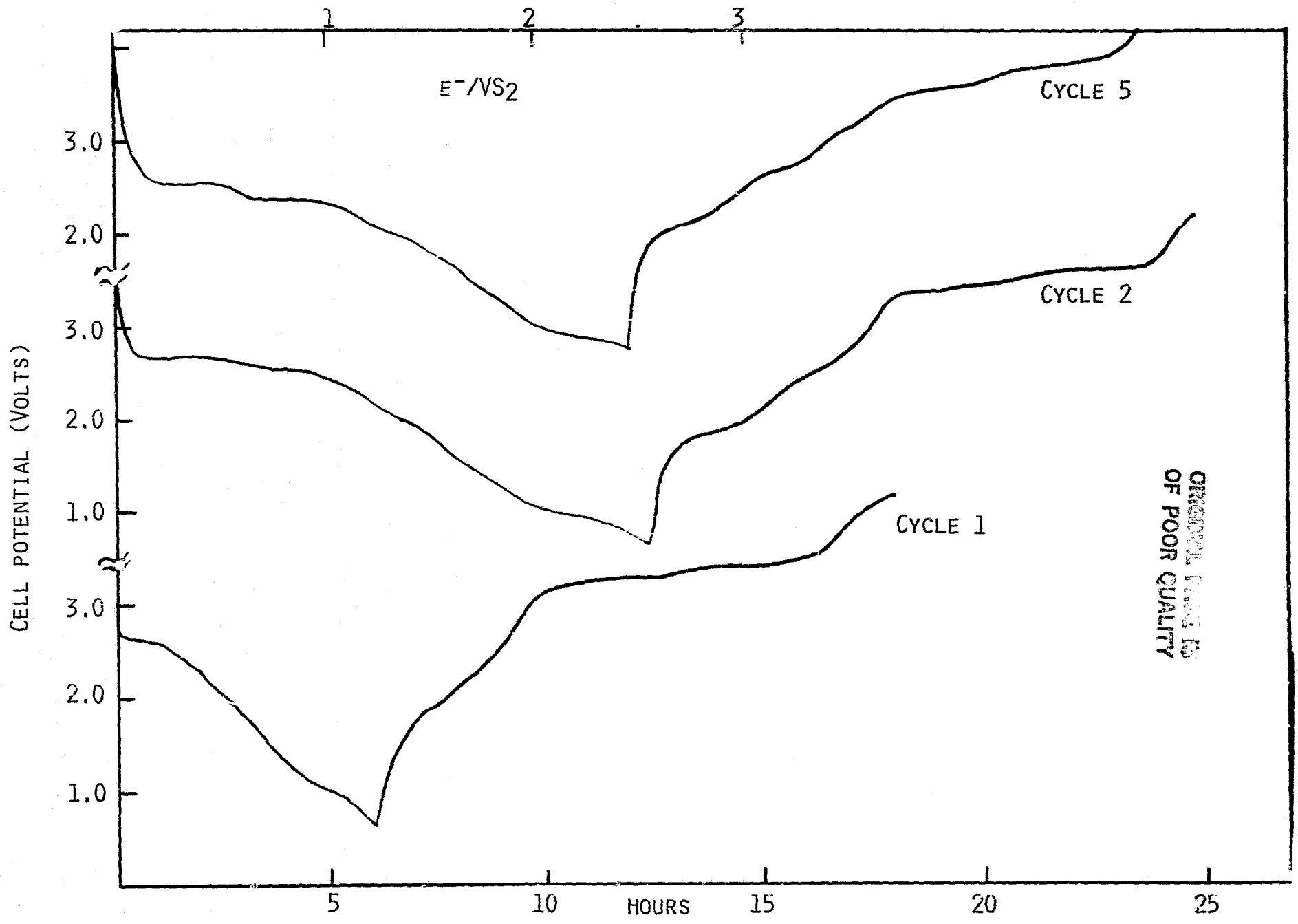

Fig. 4. Galvanostatic cycles 1, 2 and 5 of Na/a-VS_2 Cell No. 302-33. Cycling limits: 3.4-1.75V; current, 16 mA (1 mA/cm^2).

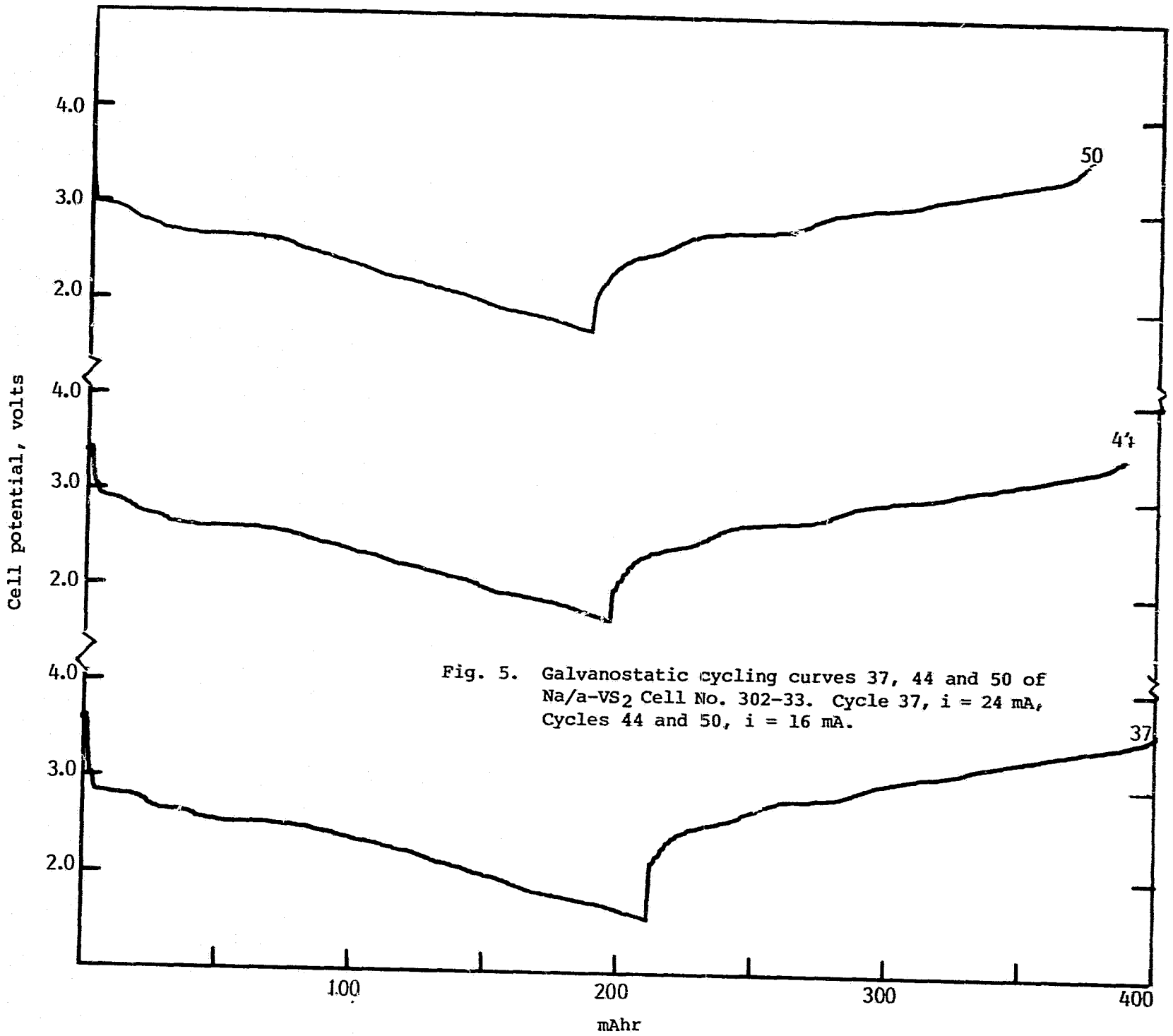

Fig. 5. Galvanostatic cycling curves 37, 44 and 50 of Na/a-VS_2 Cell No. 302-33. Cycle 37, i = 24 mA, Cycles 44 and 50, i = 16 mA.

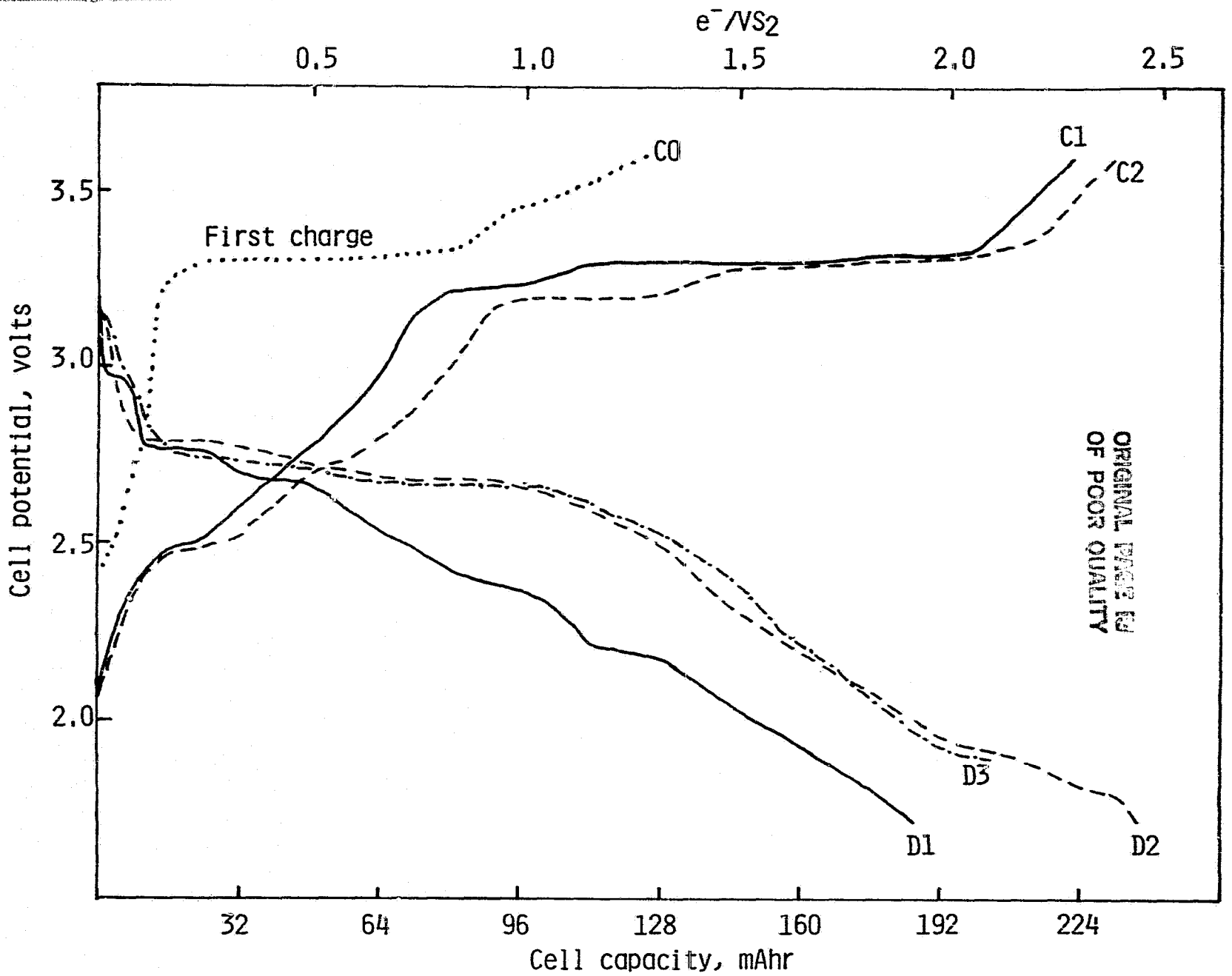

Fig. 6. Galvanostatic cycling curves for $Na/NaVS_2$ Cell No. 88. Curves marked D's are discharges and those marked C's are charges. The cell cycling began with a charge first. Current: 8 mA (1 mA/cm^2). Voltage limits: 1.8V-3.5V.

3.2.2 Mechanism of the VS_2 Cathode Cycling

3.2.2.1 Discharge Potentials in Organic Electrolyte Versus in $NaAlCl_4$

The discharge of VS_2 in triglyme/NaI at 130°C has been established as involving an intercalation process with a maximum capacity of $1e^-/VS_2$ (3). The open circuit voltage of the cell in the organic electrolyte is 2.4V and the mid-discharge voltage is ~1.8V. The recharge voltage profile, for all practical purposes, is a mirror image of the discharge, and the voltage separation between the discharge and charge curves can be mostly accounted for by iR effects.

The first discharge of VS_2 in molten $NaAlCl_4$ is significantly different. The OCV at 165°C is 3.05V. The mid-discharge potential at current densities comparable to that used in the organic electrolyte is ~2.3V, and practically all of the cell capacity is obtained above 1.8V.

3.2.2.2 Discharge/Charge Reactions in Molten $NaAlCl_4$

It is apparent that an intercalation mechanism does not occur in the first discharge of VS_2 in $NaAlCl_4$. The first discharge may be visualized as a displacement process, as shown in equation [6], involving a utilization of one Na per VS_2.

$$2VS_2 + 2Na^+ + 2e^- \rightarrow V_2S_3 + Na_2S \qquad [6]$$

The formation of V_2S_3 may occur through other V-S phases, including V_5S_8 (10). Indeed, at some discharge rates the final product could be V_5S_8. The reduction of VS_2 to V_2S_3 involves $1e^-/VS_2$, while a reduction to V_5S_8 involves $0.8e^-/VS_2$.

The Na_2S formed in a basic $NaAlCl_4$ melt would most probably be converted to $NaAlSCl_2$, according to reaction [7] (11).

$$Na_2S + NaAlCl_4 \rightarrow NaAlSCl_2 + 2NaCl \qquad [7]$$

We have direct evidence from X-ray data for a reaction such as that shown in equation [7]. The X-ray diffraction pattern of the reaction product from $NaAlCl_4$ and Na_2S, obtained by heating a 1:1 mixture of the reactants at 165°C, does not show lines due to either $NaAlCl_4$ or Na_2S (Table 3).

The overall cathode reaction in early stages of VS_2 cycling (Fig. 2) may be represented as in equation [8].

$$2VS_2 + 2Na^+ + 2e^- + NaAlCl_4 \rightleftarrows V_2S_3 + 2NaCl + NaAlSCl_2 \qquad [8]$$

Table 3

Debye-Scherrer X-Ray Diffraction Data for a 1:1 $NaAlCl_4/Na_2S$ Mixture Heated at 165°C

$NaAlCl_4/Na_2S$ Product		Na_2S		$NaAlCl_4$	
d, Å	I/I_o	d, Å	I/I_o	d, Å	I/I_o
				5.30	23
				4.93	23
		3.77	63	3.62	40
3.14	10	3.28	13	3.10	100
3.02	7			2.95	86
2.72	100			2.80	57
				2.55	71
				2.47	29
		2.31	100	2.30	23
				2.22	23
2.12	< 5	1.98	25	2.10	29
2.01	< 5			1.87	23
1.94	80	1.63	20	1.64	100
1.67	65				
1.57	40	1.50	10		
1.38	20				
1.24	50				
1.14	30				

When the discharged cathode, containing V_2S_3, is allowed to stand on open circuit at 165°C, a reaction between V_2S_3 and $NaAlCl_4$ appears to take place. In analogy to the process shown in equation [7], the reaction at open circuit may be represented as in equation [9].

$$V_2S_3 + NaAlCl_4 \rightarrow 2VSCl + NaAlSCl_2 \qquad [9]$$

The proposed reaction is in agreement with a significantly higher recharge capacity observed after an open circuit stand. We have no direct proof for the formation of VSCl. However, compounds such as VOCl, CrOCl, FeOCl etc. have been described in the literature (12). Identification of the VSCl species by isolation from the molten salt media has been difficult. We have not been able to develop a satisfactory method for the separation of the Al and V products, although most of the starting molten salt, $NaAlCl_4$, could be removed by washing the cathode with CH_3CN.

It appears that when the initial cathode is $NaVS_2$, the open circuit reactions involving $NaAlCl_4$ are those in equations [10] and [11].

$$2NaVS_2 + NaAlCl_4 \rightarrow V_2S_3 + 2NaCl + NaAlSCl_2 \qquad [10]$$

$$V_2S_3 + NaAlCl_4 \rightarrow 2VSCl + NaAlSCl_2 \qquad [11]$$

It is reasonable to consider $NaVS_2$ as $1/2Na_2S \cdot 1/2V_2S_3$. With that analogy the similarity between reactions [7] and [10] is clear.

Recharge reactions which follow the chemical reactions on open circuit stand appear to be the following:

$$2NaCl + NaAlSCl_2 \rightarrow NaAlCl_4 + S + 2Na^+ + 2e^- \qquad [12]$$

$$VSCl + S \rightarrow VS_2Cl \qquad [13]$$

Subsequent to the <u>in situ</u> synthesis of VS_2Cl, which is complete in about the first ten cycles, cell cycling seem to involve a redox process as shown in reaction [14].

$$VS_2Cl + 2.8Na^+ + 2.8e^- + 1.4NaAlCl_4 \rightarrow VS_{0.6}Cl + 1.4NaAlSCl_2 + 2.8NaCl \qquad [14]$$

The $2.8e^-$ reduction process shown in equation [14] is based solely on observed capacities of cells. An alternative reduction stoichiometry to form VS, involving $3e^-$, is equally possible (equation [15]).

$$VS_2Cl + 3Na^+ + 3e^- + NaAlCl_4 \rightarrow VS + 3NaCl + NaAlSCl_2 \qquad [15]$$

3.2.2.3 Characterization of the High Capacity Vanadium Species

Attempts to isolate the high capacity cathode and (completely) characterize it have not been successful. The major problem involved

an incomplete removal of the molten salt by almost all of the organic solvents used for extracting it. In the case of solvents such as CH_3CN, dissolution of $NaAlCl_4$ was accompanied by its dissociation so that the isolated material always contained NaCl. This made X-ray and elemental analysis data ambiguous.

X-ray analyses of cycled VS_2 cathodes (both crystalline and amorphous) have revealed crystalline products; but the compounds have not yet been indexed for any particular species. The X-ray data from three different cells are shown in Table 4. In one case the cathode had been washed with CH_3CN, but the washings had shown a green color suggesting that some vanadium species, probably a chloride, might have been extracted out. However, it is not known whether the green compounds resulted from decomposition during washing or if it actually is a product of cell reactions.

Elemental analysis was carried out on three different cathode samples. The analytical results are given in Table 5. All cells were terminated at the end of a charge; however, they had been cycled to different extents, i.e., different number of cycles. The analyzed compositions in Table 5 have been obtained after substracting out excess $NaAlCl_4$. We have no evidence that the small amount of Al in the two samples is significant. If we assume that the small amount of Al is present as $AlCl_3$, then the compositions of the cathodes in the three cases, each exhibiting $\sim 2.5e^-/VS_2$, are $VS_{2.3}Cl_{1.61}$, $VS_{2.4}Cl_{1.31}$ and $VS_{2.7}Cl_{1.6}$. Clearly, there is a substantial inconsistency. However, two major conclusions can be drawn from the elemental analysis results:

- A vanadium-sulfur-halide is produced <u>in situ</u> during early stages of cycling. It is this material which exhibits the higher capacity cycling behavior.

- The S/Cl atom ratio in the material is >1, in reasonable agreement with the proposed composition VS_2Cl, shown in equation 13.

We do not know of any previously characterized vanadium-sulfur-chlorides. However, the compounds NbS_2Cl_2, TaS_2Cl_2 and $NbSe_2Cl_2$ are known (9). These compounds apparently crystallize as pseudo-one-dimensional fibers. Cycling behavior of NbS_2Cl_2 has been investigated by us (see later). The cycling curves of NbS_2Cl_2, beginning with the second cycle, show considerable similarity to those of the higher capacity, <u>in situ</u> formed, "VS_2" cathode.

Hereafter the higher capacity vanadium cathode will be denoted as VS_xCl_y.

Table 4

X-Ray Powder Diffraction Data of Cycled VS_2 Cathodes

Cathode from Cell A[1]		Cathode from Cell B[2]		Cathode from Cell C[3]	
d, A	I/I_o	d, A	I/I_o	d, A	I/I_o
				7.37	10
5.75	30	5.75	6	5.86	50
5.27*	100	5.21*	5	5.21*	10
4.98	5	4.90*	3		
4.59	5	4.39	1	4.90*	10
3.56*	50	3.88	8		
3.24	10	3.67*	8		
3.11*	90	3.41	2		
2.94	100	3.28	100	3.24	20
2.87*	90	3.14*	1	3.08*	10
2.78	70	2.97	2		
2.53*	60	2.83	60	2.81**	100
2.48*	10	2.64	1	2.67	40
2.40	10	2.56*	10		
2.29*	20	2.31	40		
2.20*	5	2.19	10		
2.10*	20	2.07*	35	2.08	30
2.01	10	2.00	50	1.99*	90
1.96	10	1.94	12		
1.87*	5	1.84*	1		
1.75	40	1.82	2		
1.65*	50	1.79	8	1.76	60
1.62	30	1.68	3		
1.55*	< 5	1.65*	4	1.62**	80
1.52*	5	1.63	6		
1.49	5	1.55*	1		
1.20	5	1.52*	2		
		1.48	3	1.46	60
		1.47	4		
		1.26	7	1.41	70
		1.23	5	1.26	60
		1.15	7	1.15	40

[1]Initial cathode VS_2, terminated at the end of the 50th charge, capacity $2.5e^-/VS_2$.

[2]Initial cathode $NaVS_2$, terminated at the end of the 5th charge, capacity $2.6e^-/VS_2$.

[3]Initial cathode VS_2, terminated at the end of the 9th charge; cathode was washed with CH_3CN to remove $NaAlCl_4$.

*At least partially due to $NaAlCl_4$.

**At least partially due to NaCl.

Table 5

Results of Elemental Analysis of Cycled Cathodes

Sample Number	Analyzed Composition
1*	$VS_{2.3}Cl_2Al_{0.13}$
2**	$VS_{2.4}Cl_{1.7}Al_{0.13}$
3***	$VS_{2.7}Cl_{1.6}$

*Same sample as in B in Table 4. That is, cell started as $NaVS_2$.
**Cell cycled 17 times; the capacity was $2.24e^-/VS_2$.
***Same sample as in C in Table 3; i.e., after washing with CH_3CN.

3.2.3 Comparison of the Cycling Behavior of VS_xCl_y with NbS_2Cl_2 in $NaAlCl_4$

A Na/NbS_2Cl_2 cell was constructed with a cathode containing 0.35 g of NbS_2Cl_2 (40 mAhr, $1e^-/Nb$) in a carbon felt matrix. The OCV of the cell at 165°C was 3.2V. The cell was galvanostatically cycled at 10 mA (1 mA/cm^2) between voltage limits of 1.8 and 3.7V. The cycle curves are given in Figure 7. Although the OCV is 3.2V, upon initiating the discharge the cell shows a relatively rapid polarization to a plateau of ~2.05V. The rest of the discharge proceeds mostly at this plateau with a capacity of ~$2.2e^-/Nb$ to a cut off of 1.8V. The recharge to 3.6V is 100% efficient. The second and subsequent discharges yield a reversible capacity of ~$2.8e^-/NbS_2Cl_2$. A comparison of the fourth cycle of the Na/NbS_2Cl_2 cell with the 8th cycle of a Na/VS_2 cell, containing *in situ* synthesized VS_xCl_y, is depicted in Figure 8. The similarities are quite clear.

The cycling data, including capacity and voltage profiles, indicate only too clearly that NbS_2Cl_2 undergoes a structural change after the first cycle. The cathode composition after the first cycle, apparently, is very much similar to that of the VS_xCl_y cathode.

- Mechanism of the Cycling of NbS_2Cl_2

NbS_2Cl_2 was treated with Na-naphthalide in THF at room temperature. The reaction products were analyzed by X-rays. For up to two equivalents of Na per mole of NbS_2Cl_2, the X-ray data (Table 6) showed very little change suggesting the formation of intercalated products. At higher concentrations of Na uptakes, however, the X-ray data indicated both Na_2S and NaCl in the product, indicating a decomposition of the NbS_2Cl_2 lattice. We have investigated the discharge behavior of NbS_2Cl_2 in triglyme/NaI at 130°C and found a discharge plateau at ~2V as in molten $NaAlCl_4$ at 165°C. The discharge capacity was only $1e^-/NbS_2Cl_2$ (2).

A capacity of ~$2e^-/NbS_2Cl_2$ in the first discharge in molten $NaAlCl_4$ at 165°C, and an apparent change in cathode composition subsequent to the first charge, resulting in greater capacities and higher voltages in the following cycles, can be explained as follows:

$$NbS_2Cl_2 + 2Na^+ + 2e^- + 0.5NaAlCl_4$$

$$\xrightarrow{\text{First discharge}} NbS_{1.5}Cl + 0.5NaAlSCl_2 + 2NaCl \qquad [16]$$

$$0.5NaAlSCl_2 + 2NaCl \xrightarrow{\text{First charge}} 0.5NaAlCl_4 + 0.5S + 0.5Cl_2 + 2Na \qquad [17]$$

$$NbS_{1.5}Cl + 0.5S \rightarrow NbS_2Cl \qquad [18]$$

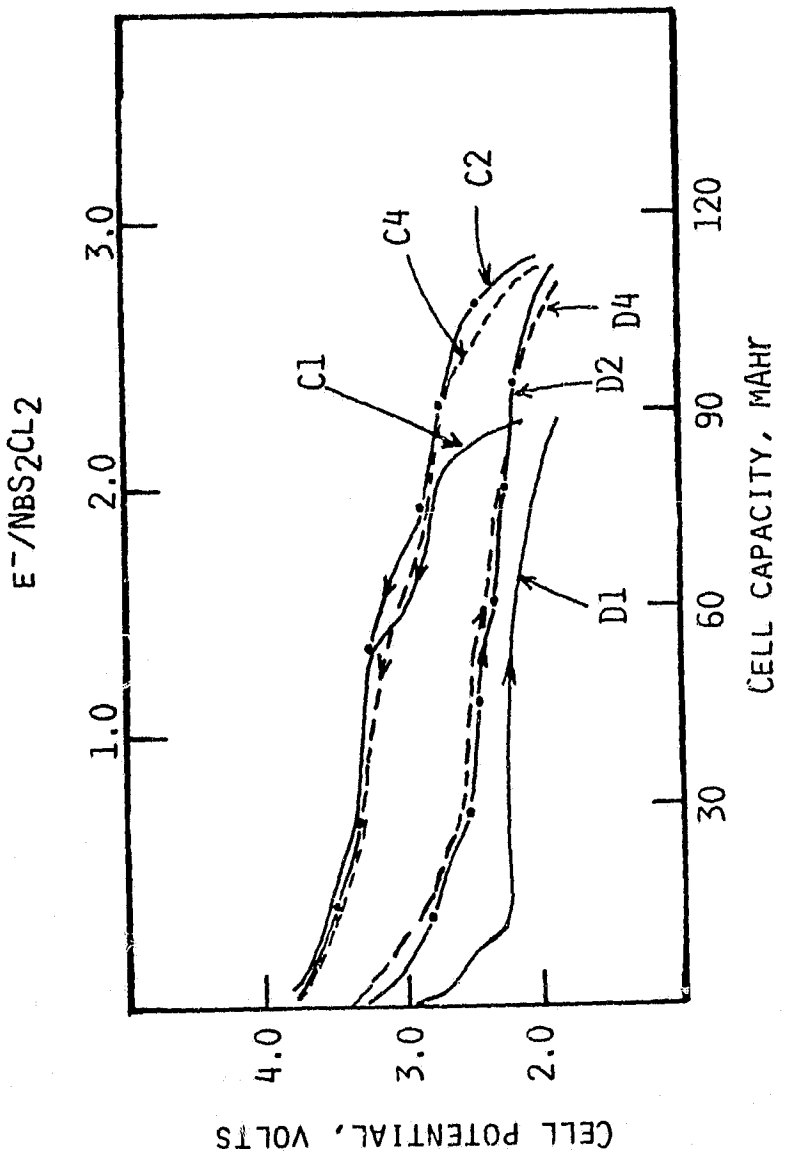

Fig. 7. The first four cycles of a Na/NbS_2Cl_2 cell at 165°C. Current density, 1 mA/cm^2. Voltage limits: 1.8-3.6V.

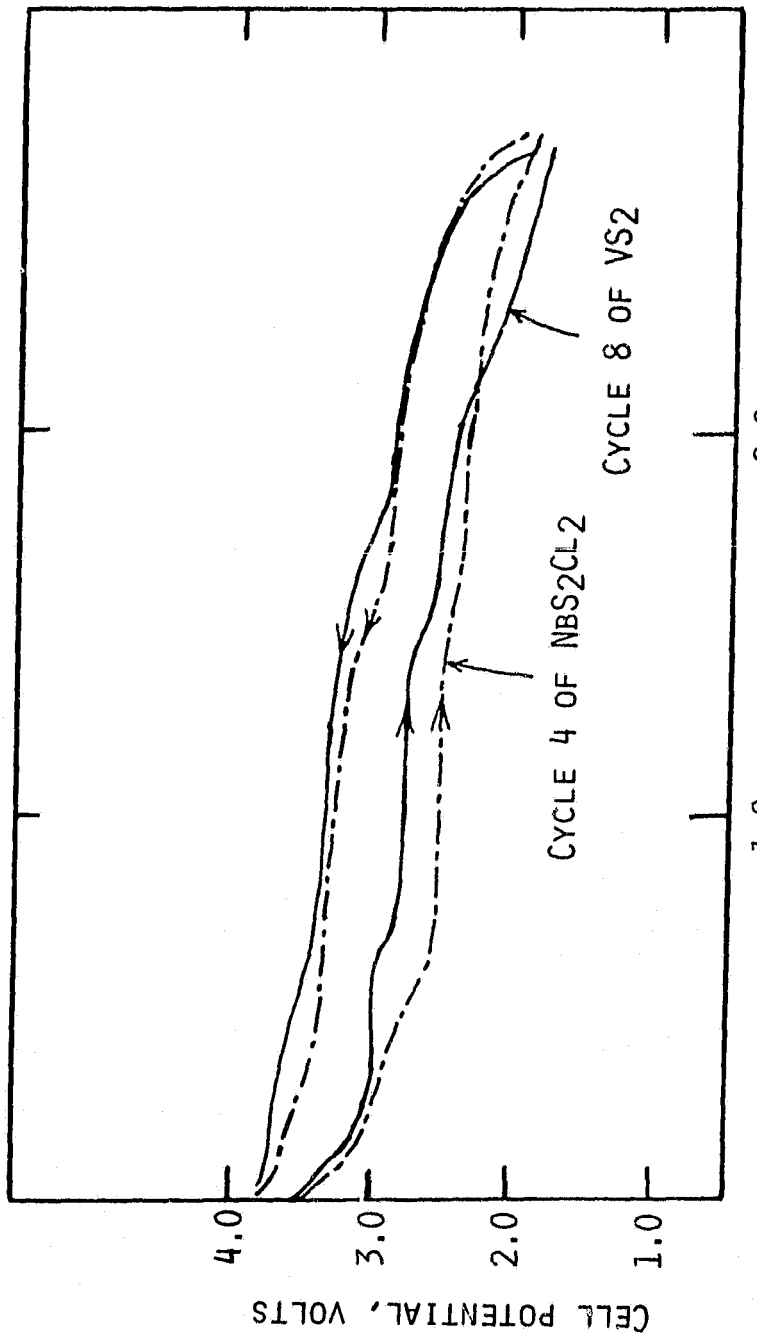

Fig. 8. Comparison of VS_xCl_y and NbS_2Cl_2.

Table 6

X-Ray Powder Diffraction Data of NbS_2Cl_2 Cathodes

EIC Synthesized NbS_2Cl_2		$Na_2NbS_2Cl_2$[1]		Cathode[2] Discharged Once		Cathode[2] Cycled Once		Cathode[2] Cycled 22 Times and Terminated at a Charge	
d, Å	I/I_0	d, Å	I/I_0	d, Å	I/I_0	d, Å	I/I_0	d, Å	I/I_0
6.19	100	6.31	100	6.32	30	6.28	80	6.55	10
5.82	20	5.45	30	3.24	20	5.09	20	3.24	10
5.15	20	5.18	70	3.09	20	3.20	10	3.08	10
4.82	20	4.87	60	2.80	100	2.80	100	2.79	100
3.11	50	3.14	90	2.17	10	2.06	30	2.05	20
2.59	60	2.82	80	1.98	90	1.99	60	1.98	90
2.40	10	2.60	80	1.67	10	1.62	40	1.62	70
2.17	10	2.41	20	1.62	60	1.51	20	1.40	50
2.05	90	2.20	20	1.40	50	1.40	10	1.26	80
2.01	20	2.06	70	1.25	80	1.29	10	1.15	70
1.92	10	2.01	60	1.15	70	1.26	50		
1.83	20	1.90	10			1.15	40		
1.65	10	1.82	20						
1.56	10	1.56	20						
1.52	10	1.52	20						
1.38	5	1.36	10						
1.36	5	1.26	10						
1.26	5	1.16	10						

[1]Obtained from reaction with a stoichiometric amount of Na-naphthalide in THF.
[2]In $NaAlCl_4$ at 165°C.

Thus, NbS_2Cl apparently is formed at the end of the first charge which then cycles with a capacity of ~2.8e^-/Nb as in the case of the VS_xCl_y cathode. It should be noted this mechanistic scheme is purely conjectural; other schemes could be formulated to explain the experimental results. Sinitsyna et al. (17) prepared NbS_2Cl from $NbCl_5$ and S in benzene. It shows an IR absorption band at 535 cm^{-1} (17).

X-ray data for NbS_2Cl_2 cathodes, obtained after various stages of cycling, are given in Table 6. It has not yet been possible to assign the pattern of the cycled cathodes to any particular NbS_xCl_y composition. Elemental analysis results were inconclusive because of difficulties in separating the material from the electrolyte.

3.2.4 Comparison of the Cycling Behavior of VS_xCl_y with S, VCl_3, and VCl_3 + S Mixtures

In order to further elucidate the cycling mechanism of the VS_2 cathode in molten $NaAlCl_4$ and to ascertain their potential usefulness as rechargeable cathodes in molten $NaAlCl_4$, cycling behavior of S, VCl_3, and mixtures of VCl_3 + S was investigated at ~165°C. The experimental data are summarized in Table 7 and Figure 9. All experiments were carried out in a cell having a flooded electrolyte level. The experimental cell setup was the same as in the studies of the VS_2 cathode.

The data in Figure 9 depict the first cycles of the various cells. Except in the cell with S alone as the cathode, no significant changes are observed between first and following cycles. In the S cell, the first discharge shows a two step process. But, only one potential step is observed in the first charge and in all further cycles beginning with the second discharge. The average discharge potential is ~2.55V and the charge potential, ~2.8V. All the experiments described in Table 7 and Figure 9 were carried out in duplicate and the reproducibility of the results was very good.

The discharge of VCl_3, occurring in two potential steps with each encompassing nearly equal capacities, seems to indicate reactions [19] and [20] as the most probable processes.

$$VCl_3 + Na^+ + e^- \rightarrow VCl_2 + NaCl \qquad [19]$$

$$VCl_2 + Na^+ + e^- \rightarrow VCl + NaCl \qquad [20]$$

However, the total discharge capacity is only ~0.7e^-/VCl_3. This suggests that some of the VCl_3 may react with the discharge product Cl^-, to form complexes such as VCl_4^- or VCl_6^{-3}. These latter species have been identified by others in molten salts comprising alkali metal halides and VCl_3 (13). An overall process in the discharge of Na/VCl_3 cells that accounts for the observed capacity may be as shown in equation [21].

Table 7

Utilizations of VCl_3 + S Mixtures in Na Cells at 165°C

VCl_3:S Mole Ratio		Total Discharge Capacity Expressed as e^-/VCl_3	Excess Discharge Capacity Due to S*, e^-/S	Capacity in the 3.2V Recharge Plateau Expressed as e^-/VCl_3	Capacity in the 3.2V Plateau $-0.7e^-/VCl_3$, Expressed as Moles of S**
VCl_3	Sulfur				
1	0.00	0.70	-	0.70	0
1	0.50	1.75	3.10	1.41	0.35
1	0.75	2.30	2.13	1.74	0.52
1	1.00	2.40	1.70	1.82	0.56
1	2.00	3.60	1.45	2.05	0.67
1	3.00	5.44	1.58	2.30	0.80
0	1.00	-	1.04	-	0

*Total discharge capacity $-0.7e^-$ due to VCl_3 divided by moles of S.
**Assume a $2e^-/S$ reaction.

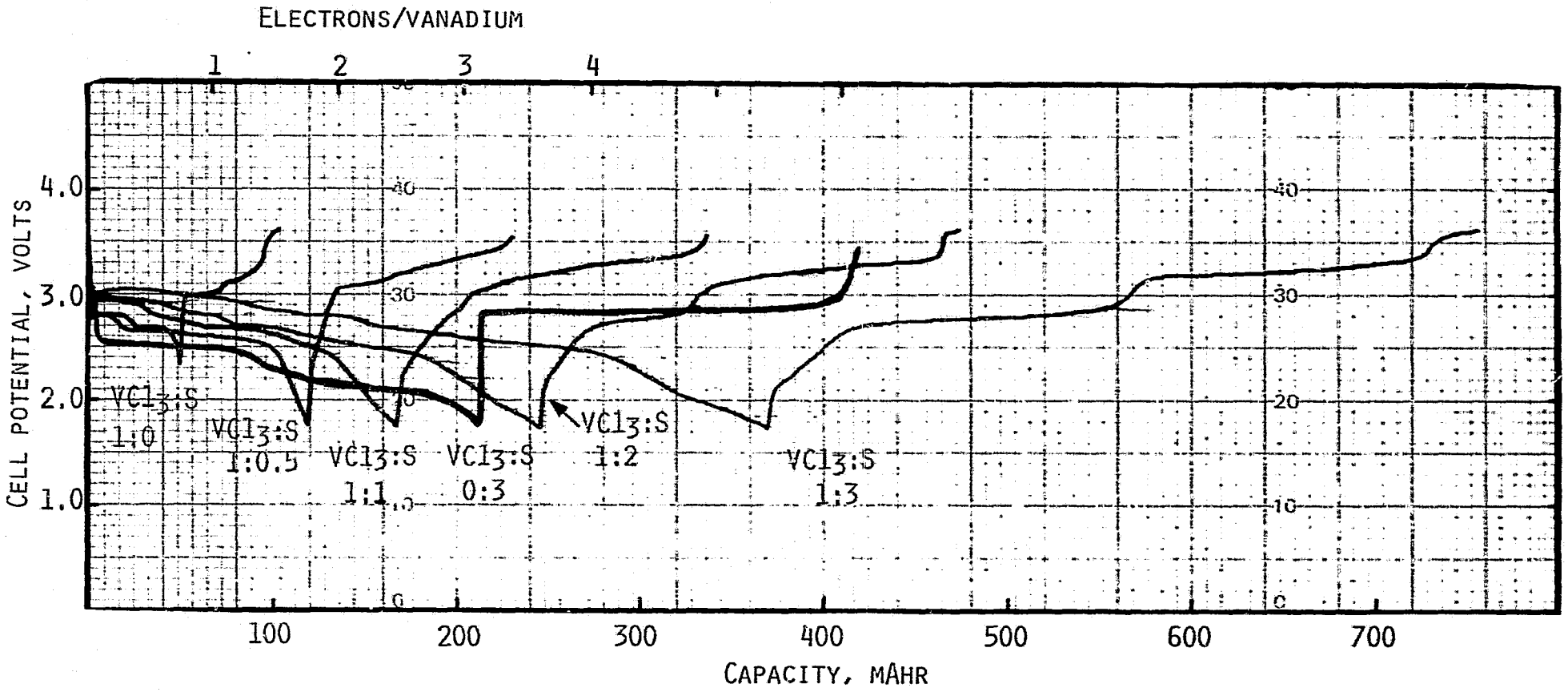

Fig. 9. The first cycles of sodium cells with cathodes of VCl_3, S, and "VCl_3 + S" mixtures.

$$3VCl_3 + 2Na^+ + 2e^- \rightarrow VCl + 2VCl_4^- \quad [21]$$

In the discharge of cathodes with mixtures of VCl_3 and S, the following additional reactions may occur:*

$$S + 2Na^+ + 2e^- \rightarrow Na_2S \quad [22]$$

$$Na_2S + NaVCl_4 \rightarrow NaVSCl_2 + 2NaCl \quad [23]$$

Complexation of VCl with S and/or the occurrence of reaction [23] would explain the nearly $2e^-/S$ utilization in "VCl_3 + S" mixtures, as opposed to only $\sim 1e^-/S$ with S itself. Such reactions could also account for the higher average cell potentials observed with "VCl_3 + S" mixtures than that expected from the individual potentials of VCl_3 and S cells.

The recharge capacity involved in the 3.2V plateau approaches the maximum value in the 1:0.75 "VCl_3 + S" cathode. Indeed, it is clear from the values in column 3 of Table 7 that beginning with the 1:1 "VCl_3 + S" cathode, one sees cycling of elemental S also. Thus, in the 1:2 VCl_3:S cathode about 40% of the recharge, and in the 1:3 mixture about 58% of the recharge occurs at a constant potential of ~2.8V. The latter is the same as the recharge potential in the Na/S cell. Assuming that the recharge capacity in excess of $0.7e^-/VCl_3$, associated with the 3.2V plateau, is due to complexed S, then we find a reaction stoichiometry of ~0.7 mole S per mole of VCl_3. This is in fair agreement with the formation of VS_2Cl following reaction [21]. Other evidences which support the reactions proposed above are the disappearance of free VCl_3 at the end of discharge (X-ray data and absence of the VCl_3-$3CH_3CN$ complex, ν_{max} 694 nm) and the appearance of VCl_3 at the end of a charge of "VCl_3 + S" cathode ($VCl_3 \cdot 3CH_3CN$ complex).

In one experiment with a 1:1 VCl_3:S cathode mix, terminated at the end of a discharge, the acetonitrile washings showed the presence of a green complex with an absorption maximum at 618 nm. All VCl_3 had been used up as indicated by the absence of the 694 nm absorption.

The mechanism suggested for the redox chemistry of VCl_3/S mixtures is obviously based on incomplete evidence. It is presented here as a working model, merely to base further studies on. A rather complex and rich redox chemistry for VCl_3, and VCl_3 + S mixtures in $NaAlCl_4$ is envisioned in view of the numerous chlorocomplexes and polynuclear vanadium chloride species known (13).

*The S may in fact complex with VCl to form VS_xCl_y-type species, utilizing in the order of two moles of S/mole of VCl, as in the VS_2 cathode discussed earlier. Thus, the S reduction in equation [22] may actually involve VS_xCl_y.

There is considerable similarity between the cycling behavior of "VCl_3 + S" mixtures and the in situ formed VS_xCl_y cathode. Much further work is needed for a full elucidation of the relationships, if any, between the two cathode systems. The rate and rechargeability aspects of the "VCl_3 + S" electrode and the in situ formed VS_xCl_y cathode are discussed in the next section.

3.2.5 Rate and Rechargeability of Na/VS_2, $Na/"VCl_3 + xS"$, and Na/NbS_2Cl_2 Cells

Preprototype cells, having the configuration, Liquid $Na/\beta"-Al_2O_3/NaAlCl_4$, $MS_x(MS_xCl_y)$, have been constructed and tested at ~165°C to evaluate the following:

- Maximum deliverable capacity of cells with each cathode.
- The optimum $NaAlCl_4$ to cathode material ratio.
- The long-term reversibility of each cathode system.

3.2.5.1 The Na/VS_2 Cell with In Situ Synthesized VS_xCl_y

- Maximum Capacity: Results of several experiments have indicated that the maximum capacity obtainable from a Na/VS_2 cell is equivalent to ~2.8e^-/metal. The proposed reaction mechanism suggests that the discharge reaction would utilize ~2.0 moles of $NaAlCl_4$ per mole of VS_2 (see equations 6-14). The corresponding energy density, with an average cell voltage of 2.6V, is 366 Whr/Kg. If the in situ formed VS_xCl_y could be synthesized ex situ, then, about 0.5 mole of $NaAlCl_4$ would be removed from the discharge reaction, increasing the energy density to 446 Whr/Kg.

- Optimum $NaAlCl_4$ to VS_2 Mole Ratio: The electrolyte in the VS_2 cell has two roles: (1) it reacts with VS_2 to produce the actual high capacity cathode material, approximating the composition VS_2Cl; and (2) it helps maintain proper Na^+ transport in the cathode compartment. The lowest experimentally obtained value would be the minimum amount of electrolyte required for adequately meeting both of the criteria.

Cell cycling experiments have been carried out with cathode compositions comprised of $NaAlCl_4/VS_2$ mole ratios of 2, 3 and >>3. The results obtained are summarized in Table 8. In our cells with unoptimized cathode structures, a $NaAlCl_4$ to VS_2 ratio of ~3:1 was required for the highest cell capacity at reasonable rates of discharge.

- Long-Term Cycling Behavior of a Na/VS_2 Cell: This was investigated in a cell constructed with 0.54 g VS_2 (126 mA-Hr, 1e^-/V capacity), sifted into a graphite felt cathode current collector (~0.12 g),

Table 8

Effect of $NaAlCl_4/VS_2$ Ratio on Cell Capacity

$NaAlCl_4/VS_2$ Mole Ratio	Current Density (mA/cm^2)	Maximum Cell Capacity (e^-/Vanadium)*
2	1.0	1.4
3	1.0	2.5
>> 3	1.0	2.8

*Average of several requirements.

wrapped around the outer periphery of the $\beta"$-Al_2O_3 tube. The cathode area facing the $\beta"$-Al_2O_3 solid electrolyte was 10 cm^2. Five grams of $NaAlCl_4$ were added to the cathode compartment. The cell was cycled at 165°C. The voltage limits were 1.8V and 3.6V.

The cycling data, plotted as cathode utilization versus cycle number are given in Figure 10. After the first discharge the cell was placed on open circuit for ~72 hours. Subsequently, the capacity increased to $2.4e^-/VS_2$ by the 5th cycle. Then the cathode utilization remained steady for more than 125 deep discharge/charge cycles. Some typical cycles, obtained at a current density of 3 mA/cm^2, are given in Figure 11. The 3 mA/cm^2 discharge corresponds to a 10 hour rate. Note that there is only a very small decrease in cathode utilization when the current density is increased to 10 mA/cm^2.

• Rate-Capacity Behavior of a Na/VS_2 Cell: This was evaluated in the above cell after it had completed 125 deep discharge/charge cycles. The cell capacity was evaluated at current densities between 3 and 20 mA/cm^2. Each discharge was followed by a charge at 3 mA/cm^2 to 3.6V; all recharges were all 100 percent efficient.

The data are given in Figures 12 and 13. Even at 20 mA/cm^2 (~ a 1-hr rate) the cell capacity is about 60% of the maximum capacity, obtained at 3 mA/cm^2.

The cycling behavior and the rate-capacity data discussed above illustrate some of the excellent features of the Na/VS_2 battery system.

3.2.5.2 The Na/"VCl_3 + xS" Cell

All cell cycling studies to-date have been carried out with a cathode composition, comprised of 1 mole of VCl_3 and 2 moles of S.

• Capacity of the "VCl_3 + 2S" Cathode: The reversible capacity of the system was investigated using a mixture, consisting of 0.4 g VCl_3 and 0.16 gm S, dispersed into a graphite felt current collector. The Cathode contained a large excess of $NaAlCl_4$. The experiment was carried out at 165°C. The first cycle of the cell is given in Figure 14.

The OCV of the cell was 3.1V at 165°C. The first discharge of the cell, shown in Figure 14, occurred in four regions. The first two regions span the voltage plateaus of 3.05 and 2.85V, each with a capacity of 84 mA-hr. The last two regions appear with sloping potential profiles, between 2.7-2.5V and 2.5-1.8V, and involve capacities of 34 mA-hr and 60 mA-hr respectively. The total capacity of the discharge was equivalent to $3.9e^-/V$. The charge also proceeded in four similar potential steps.

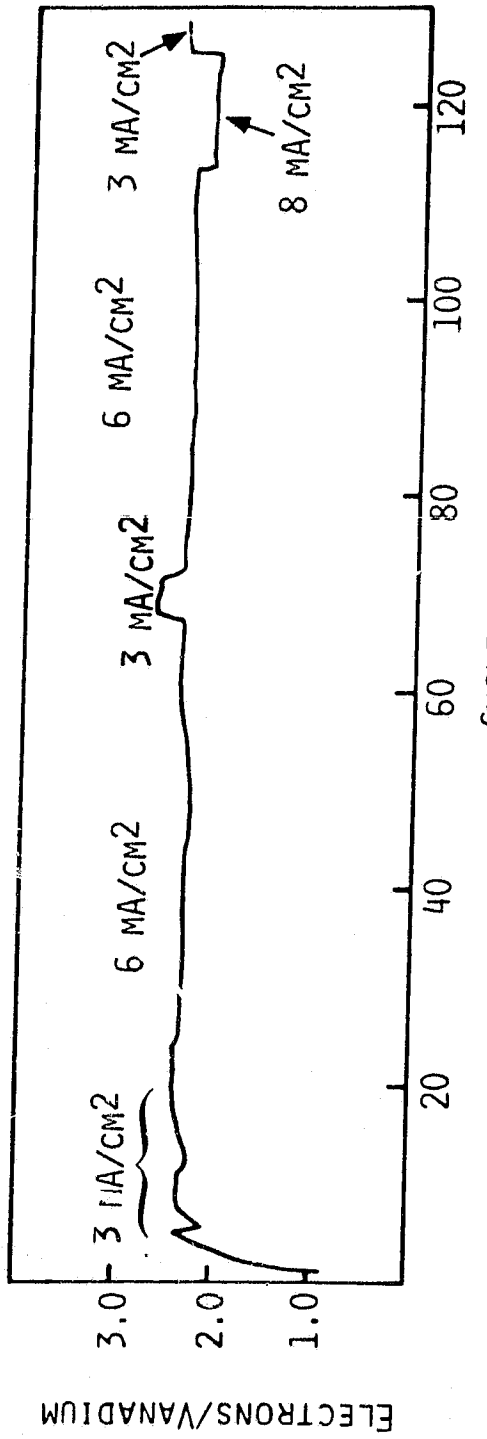

Fig. 10. Cathode utilization versus cycle number in a Na/VS_2 cell at 165°C. Voltage limits; 1.8-3.6V.

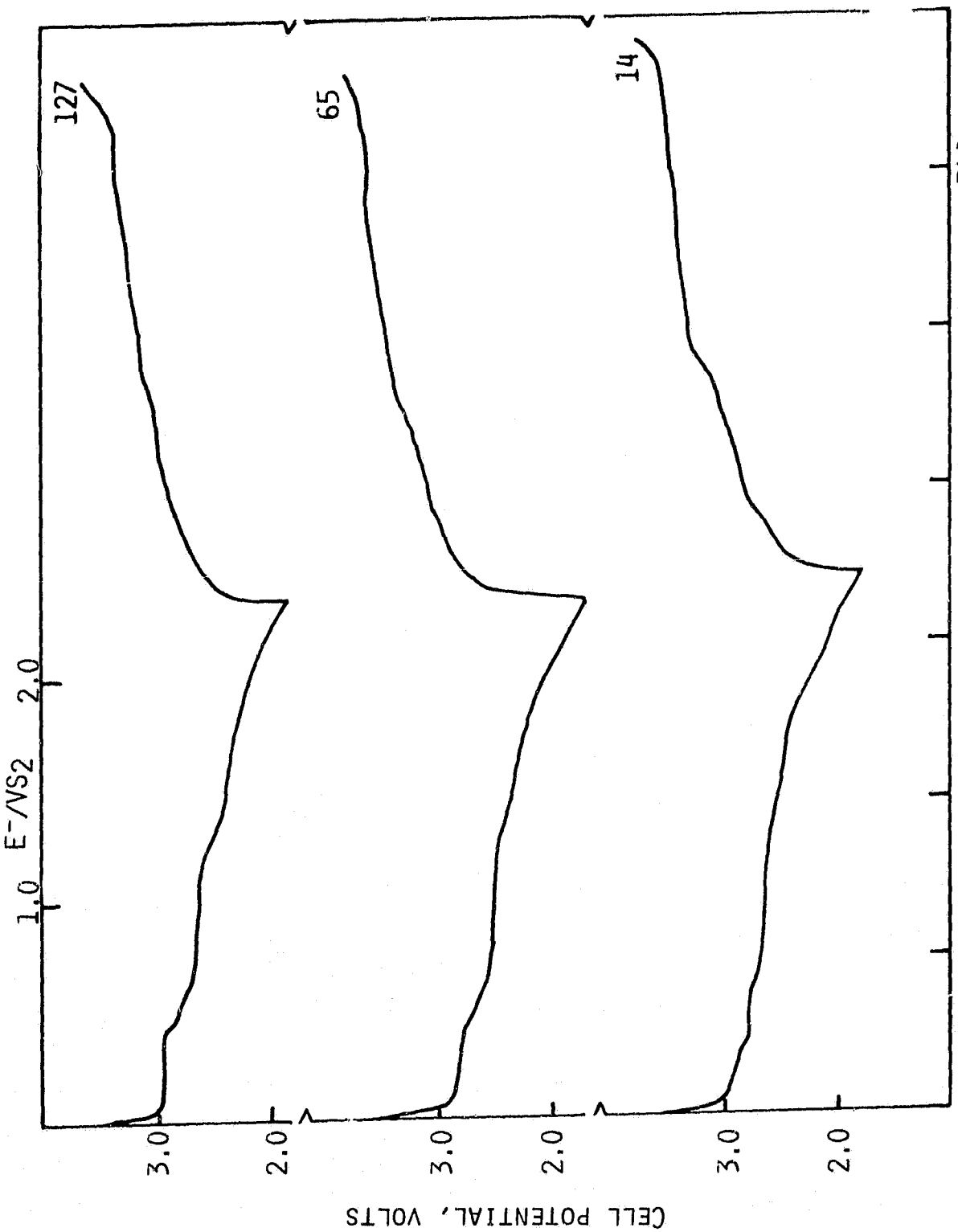

Fig. 11. Typical cycles of the Na/VS_2 cell shown in Fig. 10. Current density; 3 mA/cm^2. Voltage limits, 1.8-3.6V.

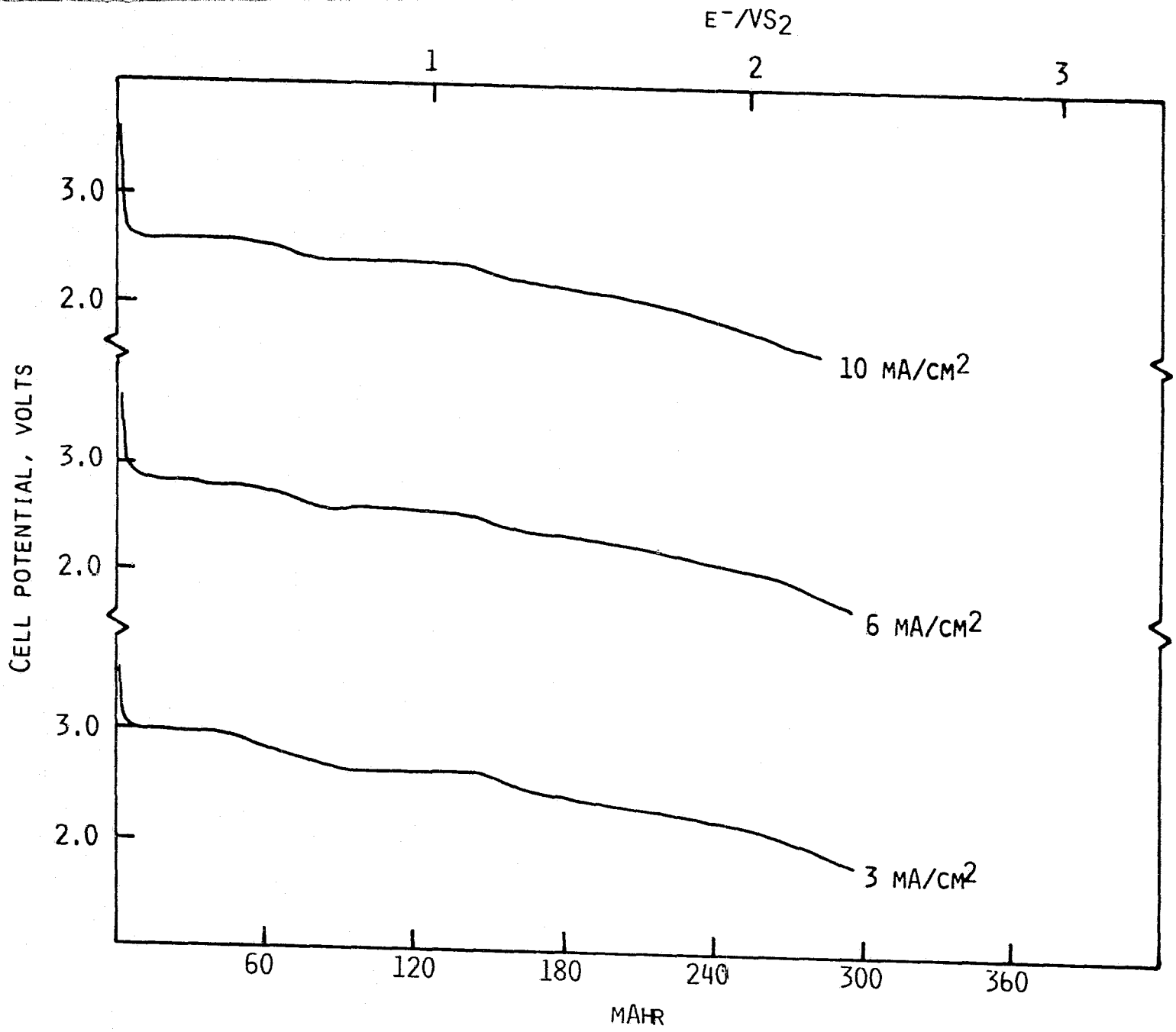

Fig. 12. Cathode utilization at various current densities in the Na/VS_2 cell shown in Fig. 10.

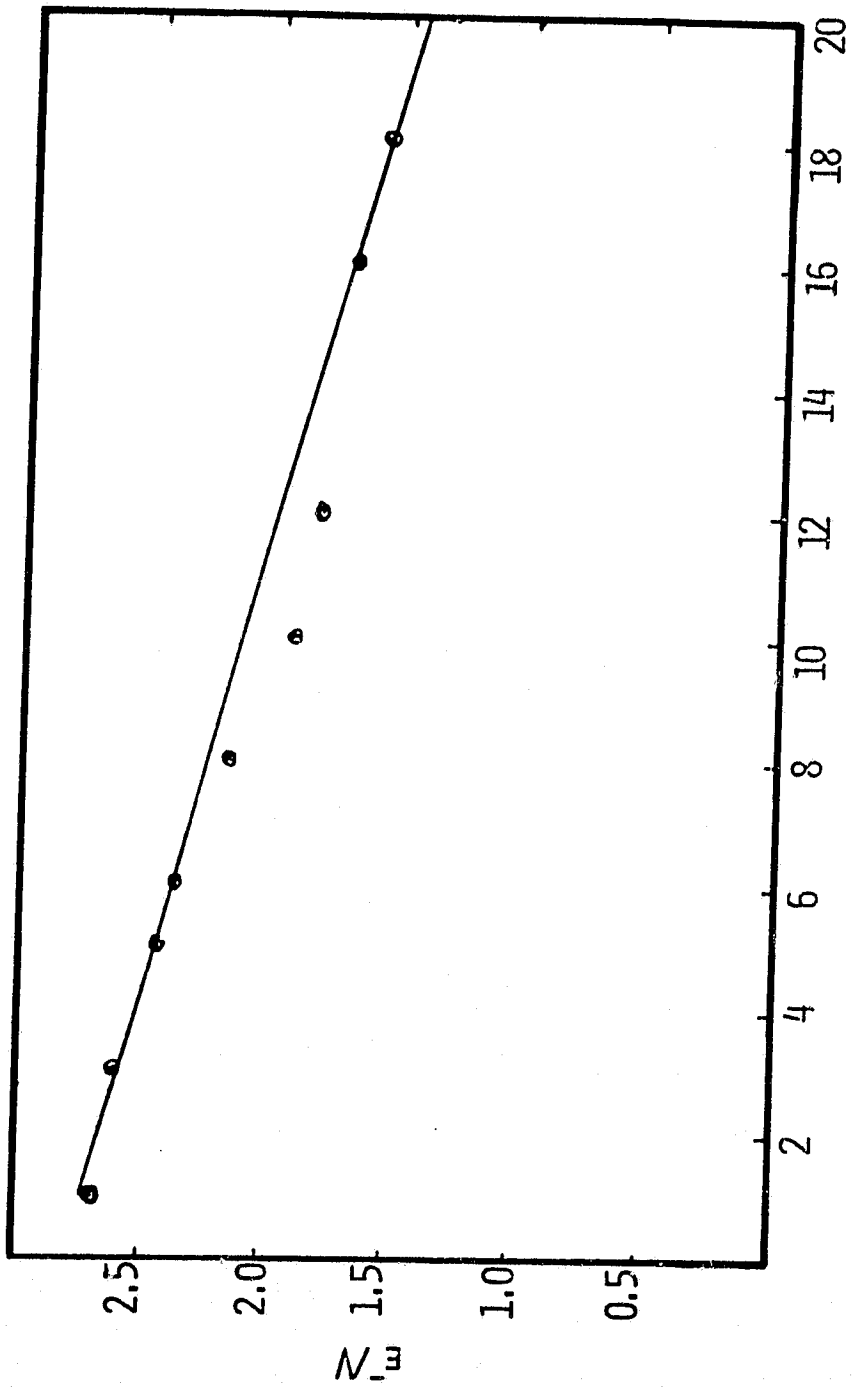

Fig. 13. Cathode utilization versus current density in the Na/VS_2 cell shown in Fig. 10.

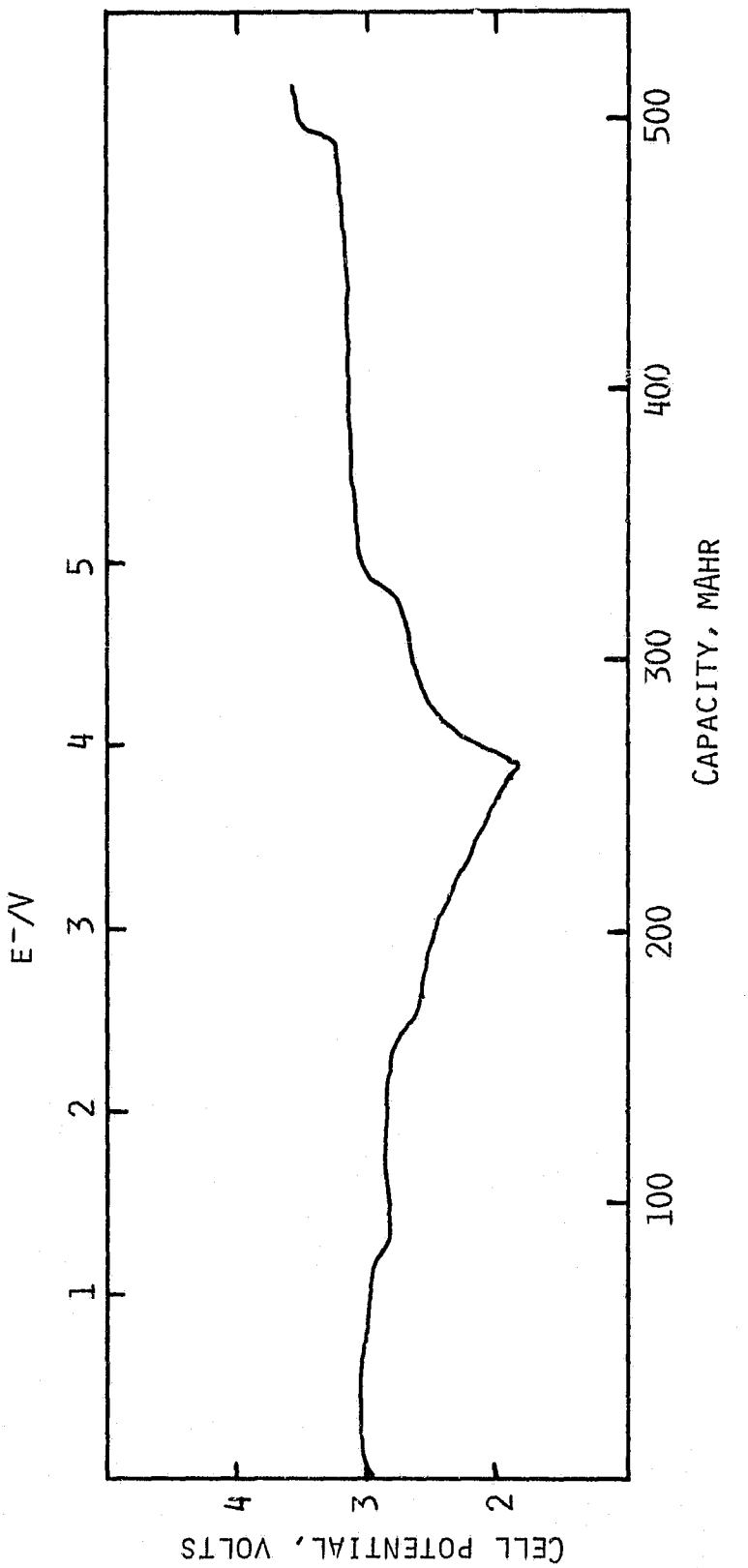

Fig. 14. The first galvanostatic cycle of a Na/"VCl_3 + 2S" cell. Current = 10 mA (1 mA/cm^2); voltage limits, 1.8-3.6V.

There was no change in the capacity or voltage profiles through 20 cycles. The data for the 20 cycles are given in Table 9.

The cell was disassembled and analyzed after the 20th charge. Sulfur could not be removed from the cathode either by extraction with CS_2 or by sublimation (150°C, 15 mmHg). This observation further supports our belief that the electrode reaction does not simply consist of the individual cycling of S and VCl_3.

- The Rate and Rechargeability of the "VCl_3 + 2S" Cathode:

The cell for this study was constructed with a cathode mix, composed of 0.4 g VCl_3 and 0.16 g S (S/V mole ratio of 2). The positive mix also contained 1.92 gm $NaAlCl_4$. The carbon felt current collector, facing the β"-Al_2O_3 tube, had an area of 8.5 cm^2. Initially, the cycling was carried out at 165°C.

In the first several cycles, current density was varied between 2 and 20 mA/cm^2. A plot of cathode utilization versus current density is shown in Figure 15. Some typical cycles are given in Figure 16. The excellent rate capability of the system is clearly indicated by these data.

The discharge capacity of 240 mA-hr is equivalent to a specific capacity of 28 $mA\text{-}hr/cm^2$.

Subsequent to the rate/capacity studies, the cell was cycled at a discharge current of 170 mA (20 mA/cm^2) and a recharge current of 85 mA (10 mA/cm^2). The voltage limits were 1.5 and 3.7V. The capacity, which was equivalent to $2.9e^-$/vanadium at the beginning of the 20 mA/cm^2 cycling, remained at ~$2.5e^-$/V, even after 150 cycles. Beginning with cycle 180, the current density was changed to 10 mA/cm^2 for both discharge and charge. The lowered current density resulted in an increase in cathode utilization to ~$2.7e^-$/V. The cycling of the cell was continued until it exceeded 300 cycles. The full cycling data are given in Figure 17. Some cycles are given in Figure 18.

The cell was voluntarily terminated after the 302nd cycle as the data had already demonstrated, to our satisfaction, the excellent rate and rechargeability of the "VCl_3 + 2S" cathode. The energy densities achieved in a prototype "VCl_3 + 2S" cell are discussed in Section 3.2.6.

3.2.5.3 Capacity, Rate and Rechargeability of the Na/NbS_2Cl_2 Cell

The maximum capacity of NbS_2Cl_2, as determined from discharges in cells containing a relatively large excess of $NaAlCl_4$ at low current densities at 165°C, is $2.8e^-/NbS_2Cl_2$.

Table 9

Cycling Data of Na/"VCl_3 + 2S" Cell

Cathode: 0.40 gm VCl_3 and 0.16 gm S on carbon felt.

Current: Cycles 1-4, 10 mA (1 mA/cm^2); cycles 5-22, 40 mA.

Voltage Limits: 1.8-3.6V

	Discharge Capacity		Charge Capacity
Cycle Number	mAh	e^-/V	mAh
1	262	3.9	250
2	252	3.7	258
3	263	3.9	269
4	251	3.7	241
5	242	3.6	248
6	244	3.6	238
7	242	3.6	248
8	250	3.7	254
9	255	3.8	255
10	255	3.8	235
11	231	3.4	239
12	242	3.6	230
13	234	3.4	234
14	234	3.4	237
15	240	3.5	238
16	243	3.6	241
17	244	3.6	246
18	246	3.6	239
19	244	3.6	240
20	243	3.6	236
21	236	3.5	221
22	220	3.2	221

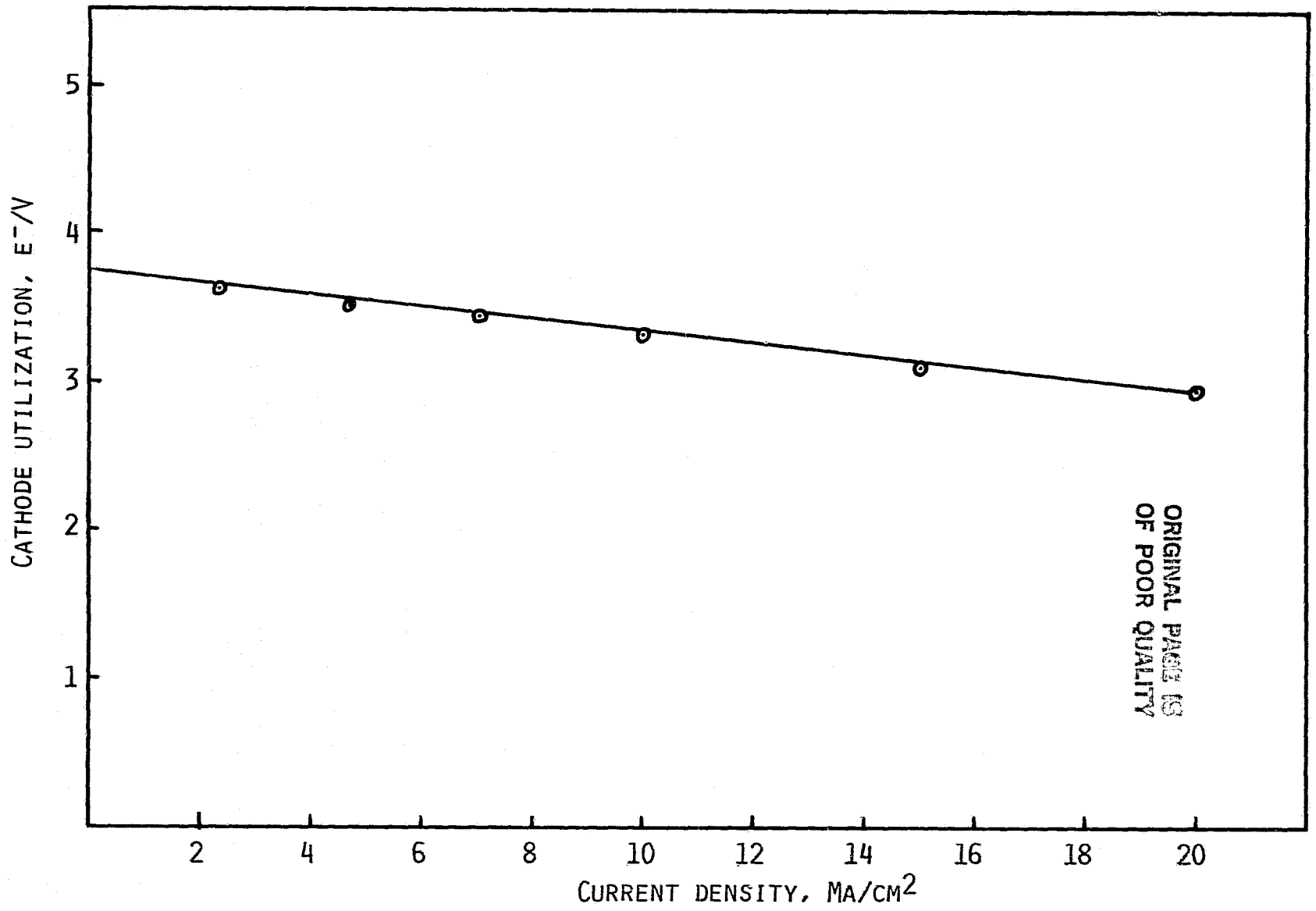

Fig. 15. Cathode utilization (e^-/V) versus current density for Na/"VCl_3 + 2S", Cell No. 365-64. Cathode area is 8.5 cm^2.

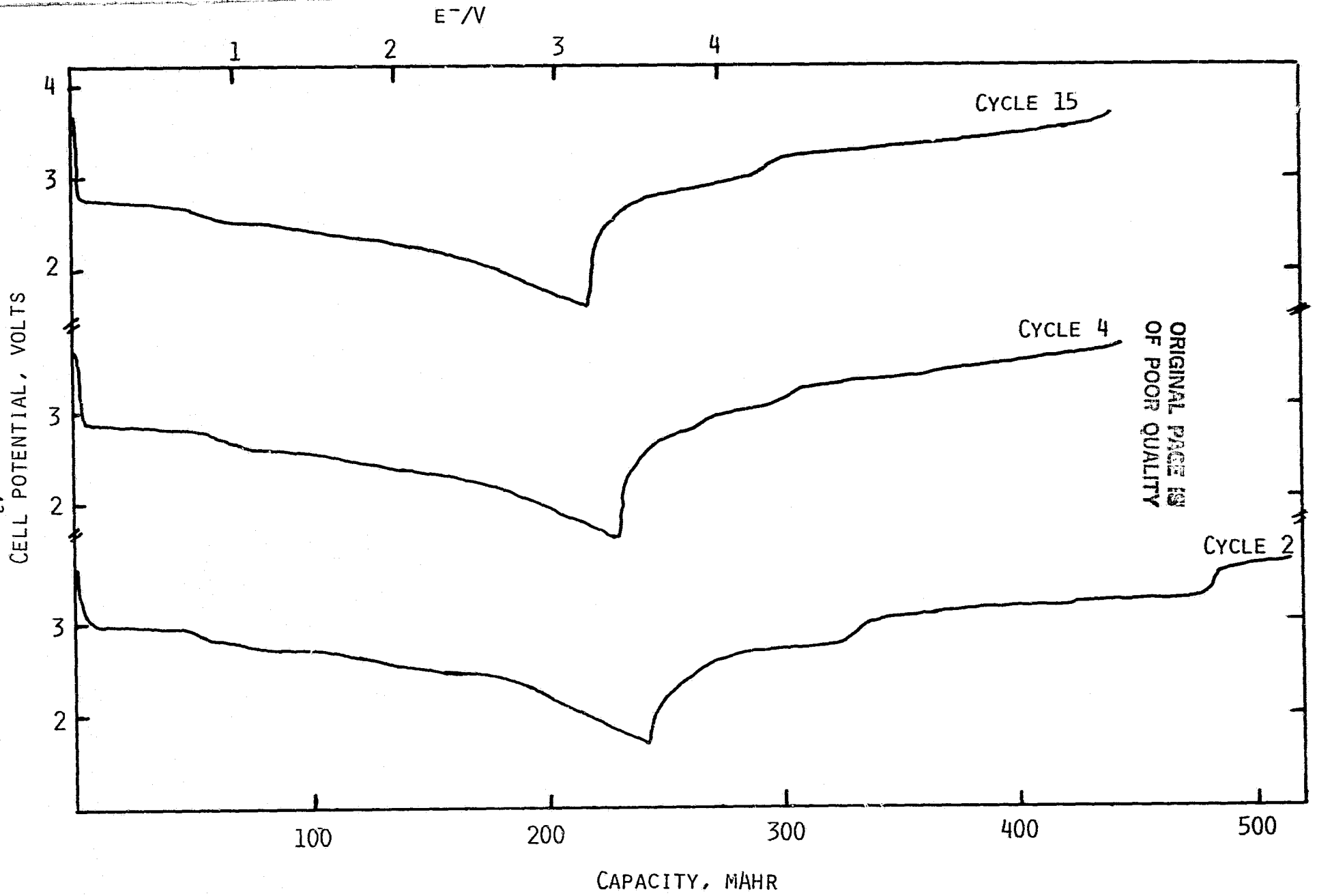

Fig. 16. Galvanostatic cycling curves of Na/"VCl_3 + 2S", Cell No. 365-64. Current density: cycle 2, 2.4 mA/cm^2; cycle 4, 7 mA/cm^2; and cycle 15, 10 mA/cm^2.

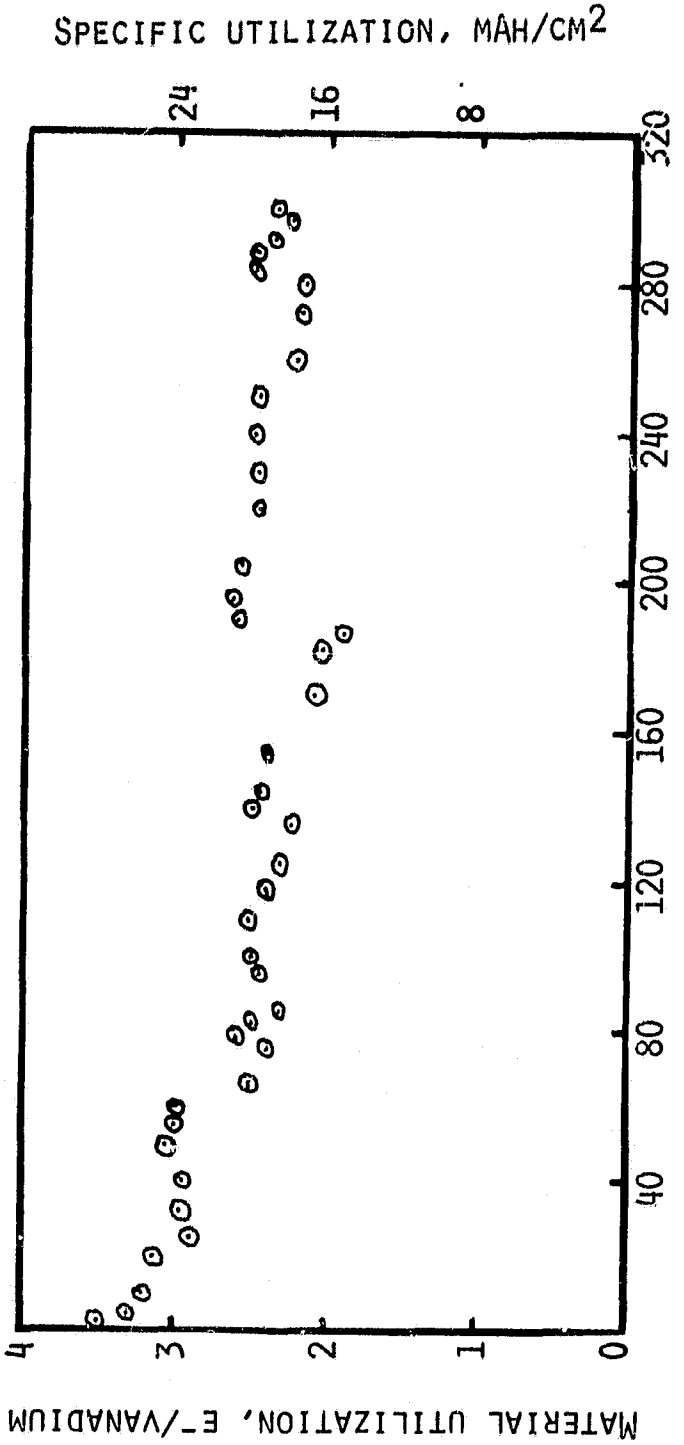

Fig. 17. Cathode utilization versus cycle number for $Na/"VCl_3$ + 2S", Cell No. 365-64. In the first 22 cycles current density was varied between 2.35 and 15 mA/cm^2. In cycles 23-186, id = 20 mA/cm^2, ic = 10 mA/cm^2. In cycles 187-283, id = ic = 10 mA/cm^2. In cycles 284-289, id = ic = 2.35 mA/cm^2. In cycles 290-303 id = ic = 5 mA/cm^2.

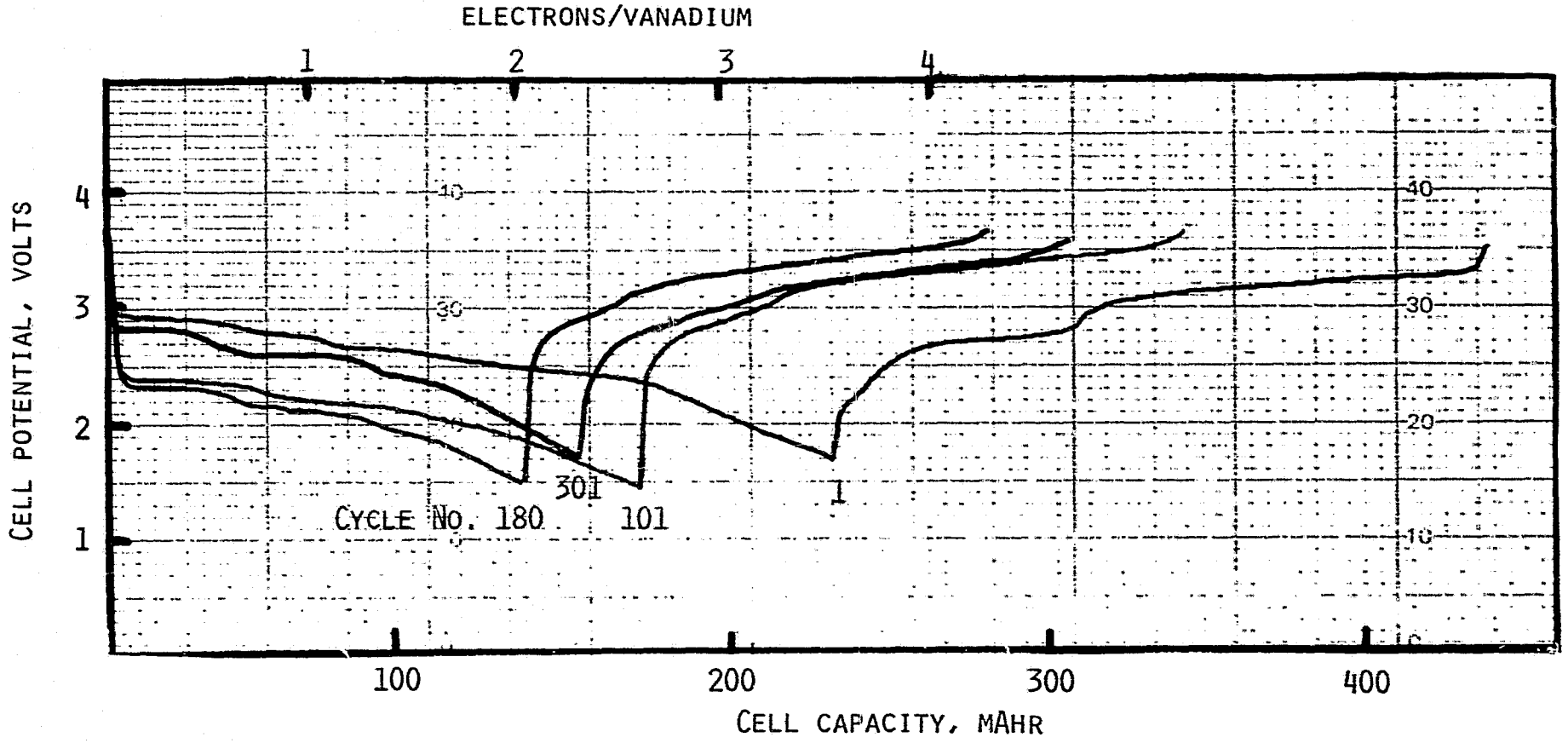

Fig. 18. Typical cycles of Na/"VCl_3 + 2S", Cell No. 364-64. Current: cycle 1, 20 mA (2.35 mA/cm^2); cycle 101, id = 170 mA (20 mA/cm^2), ic = 85 (10 mA/cm^2); cycle 180, id = ic = 85 mA (10 mA/cm^2), cycle 301, id = ic = 42.5 mA (5 mA/cm^2).

Cell capacities were evaluated as a function of $NaAlCl_4/NbS_2Cl_2$ mole ratios also. The results are given in Table 10. Even at a $NaAlCl_4/NbS_2Cl_2$ mole ratio of 2, the cathode exhibits >80% of its maximum capacity. However, rate capabilities are better at ratios ≥ 3.

The rate-capacity characteristics of a Na/NbS_2Cl_2 cell with a $NaAlCl_4/NbS_2Cl_2$ mole ratio of 3 are depicted in Figure 19. Discharge capacities were evaluated at current densities between 1.4 and 13 mA/cm^2. The recharge to 3.6V after each discharge was carried out at 3 mA/cm^2. Even at 13 mA/cm^2, the utilization is $1.5e^-/NbS_2Cl_2$ or still 65% of the maximum low-rate capacity. The mid-discharge voltage is 2.3V at 1.4 mA/cm^2 and 1.8V at 13 mA/cm^2. It should be noted that a part of the excessive polarization at the high current density is due to iR effects in the $\beta"$-Al_2O_3 tube.

- Long-Term Cycling of a Na/NbS_2Cl_2 Cell: A plot of cathode utilization versus cycle number for a Na/NbS_2Cl_2 cell, cycled at 165°C, is given in Figure 20. The cell has exceeded 250 deep discharge/charge cycles. The third and 241st cycle are given in Figure 21. The excellent reversibility of the NbS_2Cl_2 cathode is evident from these data.

3.2.6 Prototype Na/"VCl_3 + 2S" Cell

A schematic representation of the prototype cell is given in Figure 22. The cell has been constructed in an inside-out configuration with Na contained in the outer compartment. The inside-out configuration eliminates materials incompatibility problems arising from the corrosive nature of the $NaAlCl_4$ melt.

The cell was designed around the $\beta"$-Al_2O_3 tube we had been using in all our experiments. The tube (Ceramatec Cat. No. CT16A) dimensions are: OD, 16 mm; ID, 13 mm; length, 200 cm. The outer Na anode compartment was constructed of 316 stainless steel. The anode compartment was sealed to the $\beta"$-Al_2O_3 tube by a series of silicone O-rings in a 316 stainless steel sleeve. The stainless steel outer compartment also served as the anode current collector and current lead. The cathode lead was a vitreous carbon rod. The cathode current collector was fabricated from a matrix of graphite felt (2.5 cm x 5 cm) with the cathode plus electrolyte salt mix dispersed into it.

The cathode mix comprised 1.83 g VCl_3, 0.75 g S and 6.71 g $NaAlCl_4$. The cycling was carried out at 190°C. The first cycle was obtained at 2 mA/cm^2. A capacity of 1.27 Ah corresponds to a 100% utilization of the positive mix (based on $4e^-/V$ for the "VCl_3 + 2S" positive). The discharge rates and capacities for the first 20 cycles are given in Table 11. The charge current density was maintained at 5.8 mA/cm^2. The rather poor capacities in cycles 2-5 resulted from inefficiencies in the recharge, carried out at 10 mA/cm^2. This was eliminated when the charge current density was lowered to 5 mA/cm^2.

Table 10

Effect of $NaAlCl_4/NbS_2Cl_2$ Ratio on Cell Capacity

$NaAlCl_4/NbS_2Cl_2$ Mole Ratio	Current Density (mA/cm^2)	Maximum Cell Capacity (e^-/NbS_2Cl_2)
2	1	2.3
	3	2.1
3*	3	2.1**
>> 3	1	2.8
	3	2.6

*This ratio was achieved by adding another mole of $NaAlCl_4$ to the first cell.
**Cell voltage is higher by ~150 mV.

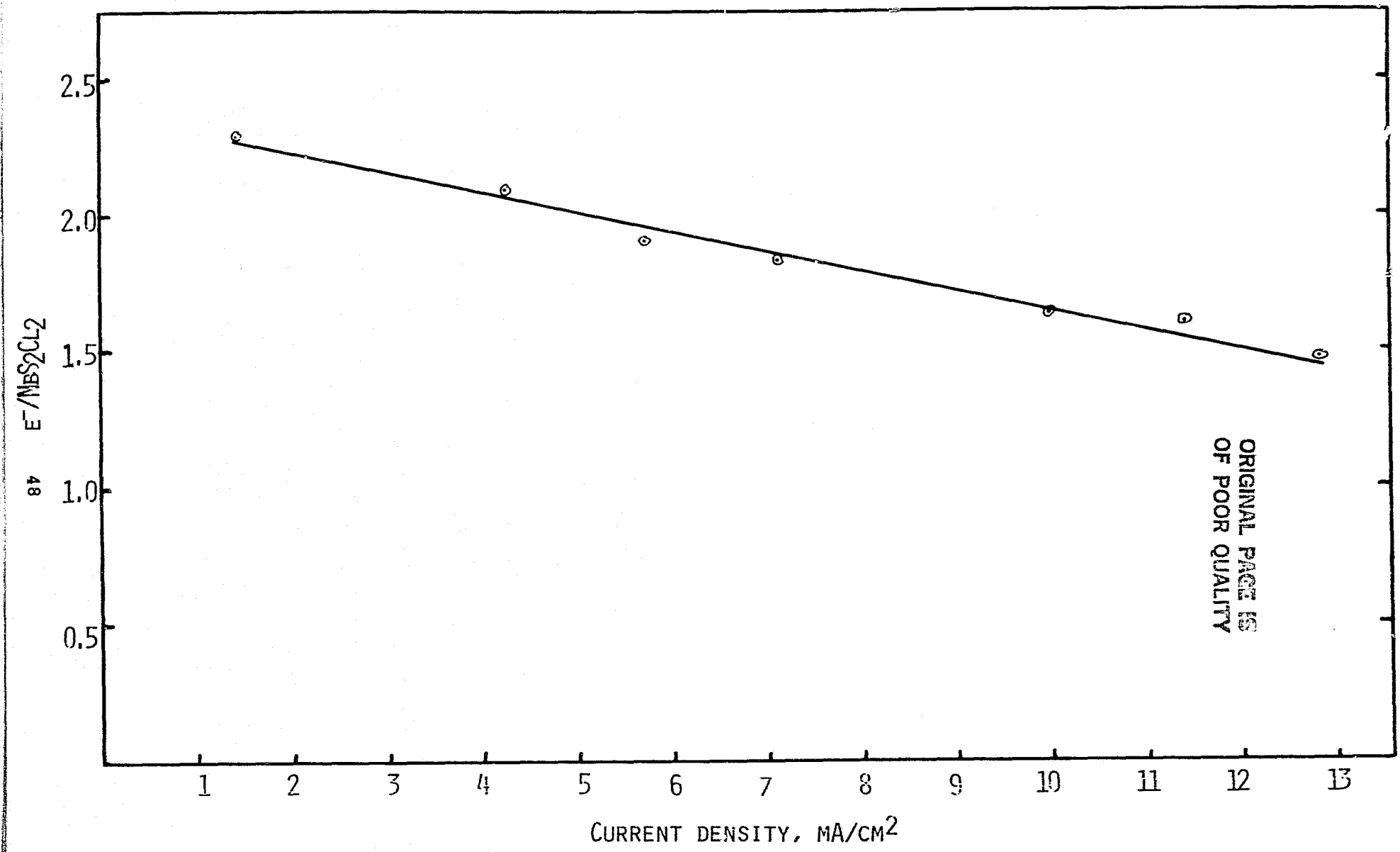

Fig. 19. Cathode utilization versus discharge current density for Na/NbS_2Cl_2 Cell No. 365-10. Cathode area 7 cm^2.

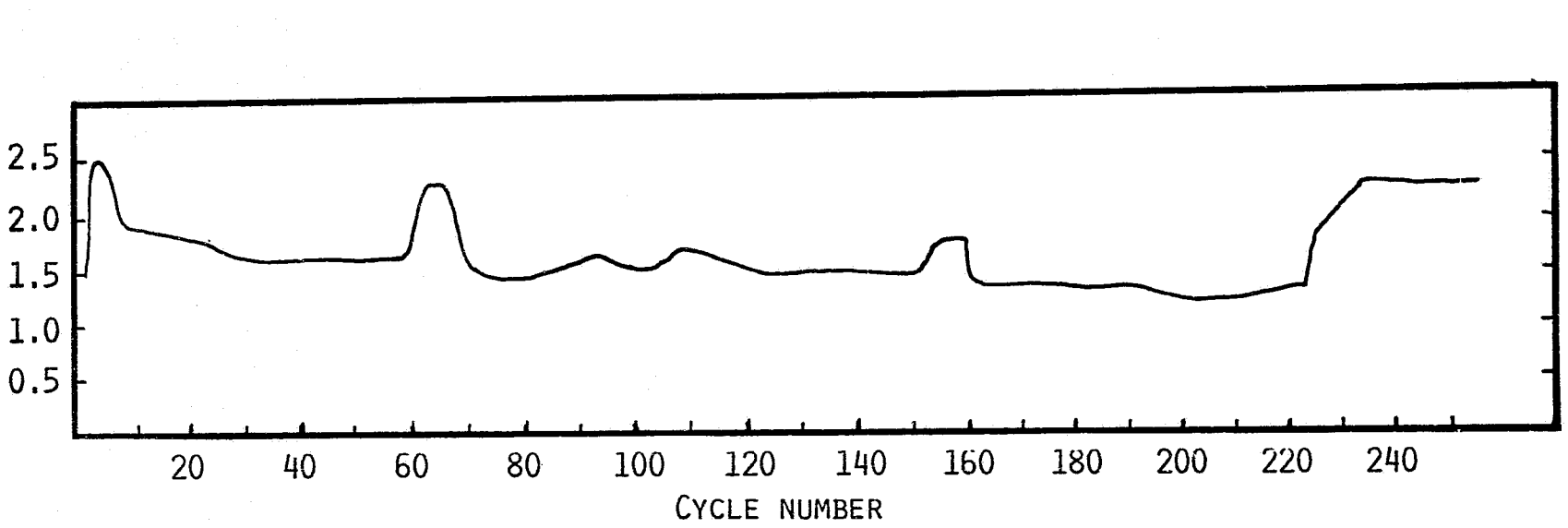

Fig. 20. Cathode utilization versus cycle number for a Na/NbS_2Cl_2 cell. Discharge current: cycles 1-8, 62-64, 151-155, and 224-250, 10 mA (1 mA/cm^2); cycles 9-61 and 65-150, 30 mA; cycles 156-223, 50 mA. Charge current: 10 mA.

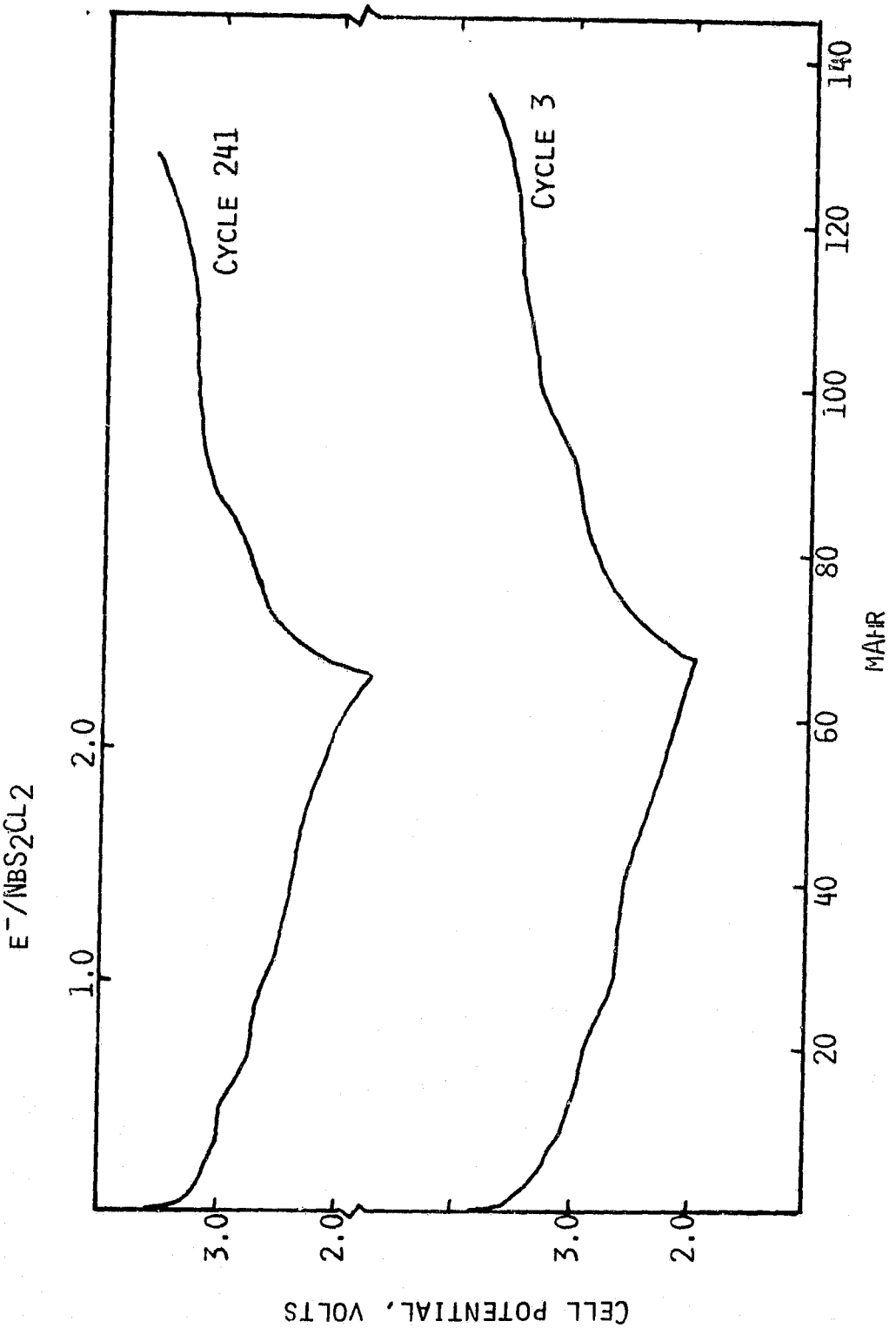

Fig. 21. Galvanostatic cycles 3 and 241 of a Na/NbS_2Cl_2 cell. id = ic = 10 mA (1 mA/cm^2).

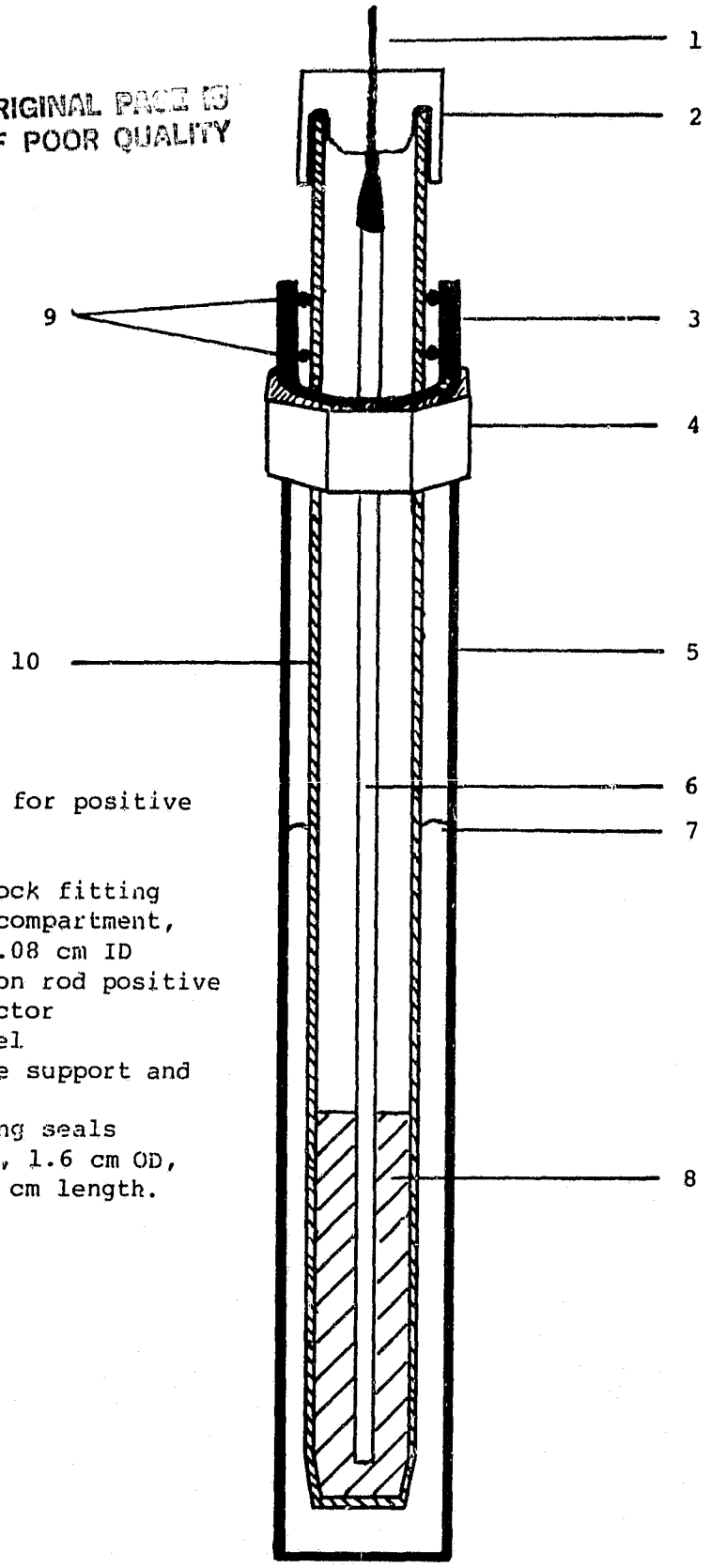

1. Positive lead
2. Silicone seal for positive compartment
3. 316 SS sleeve
4. 316 SS Swagelock fitting
5. 316 SS outer compartment, 2.67 cm OD, 2.08 cm ID
6. Vitreous carbon rod positive current collector
7. Liquid Na level
8. Carbon cathode support and positive mix.
9. Silicone O-ring seals
10. β''-Al_2O_3 tube, 1.6 cm OD, 1.3 cm ID, 20 cm length.

Fig. 22. Full scale drawing of a prototype Na cell.

Table 11

Cycling Data for Na/"VCl_3 + 2S" Cell No. 365-79

Cathode: 1.83g VCl_3, 0.75g S, 6.71g $NaAlCl_4$ (1.25 Ah based on $4e^-/V$); cathode area facing $\beta"$-Al_2O_3, 12.5 cm^2.

Cycle Number	Current Density (mA/cm^2)	Capacity (mAh)	Specific Energy* (Wh/Kg)
1	2	1275	330
2	10	881	197
3	10	350	82
4	10	394	92
5	5	439	103
6	5	1108	248
7	7.5	979	219
8	↓	968	216
9	↓	990	221
10	↓	950	212
11	↓	956	214
12	↓	1026	228
13	↓	1001	224
14	↓	974	218
15	↓	950	211
16	12.5	816	182
17	↓	820	193
18	↓	810	181
19	↓	804	180
20	↓	720	160

*Weight of active materials include Na. The cell hardware weights are not included in the calculation.

With continued cycling at 12.5 mA/cm^2 for discharge and 8 mA/cm^2 for charge (beginning with Cycle No. 16), there was a gradual loss in capacity, attributable largely to iR polarization losses. The cathode structure, it appears, was not appropriately optimized for high current operations. The cycling was terminated when the cell exceeded 100 cycles. It was decided that more extensive cycling of the Na/"VCl_3 + 2S" system should be carried out with cells constructed with further optimized cathode structures. The complete cycling data are shown in Figure 23 and some cycles are given in Figure 24.

The specific energies calculated for the first 20 discharges, based on the weights of all active materials including $NaAlCl_4$ and Na, are given in Table 11. With optimized hardware and thinner β"-Al_2O_3 tubes, it would reasonable to expect specific energies in the range of 110-150 Whr/Kg in practical cells.

3.2.7 The Na/Amorphous Molybdenum Trisulfide (a-MoS_3) Cell

In view of the unusual chemistry observed with the layered disulfide, VS_2, we have investigated the cycling behavior of a-MoS_3 in molten $NaAlCl_4$ at 165°C. Amorphous MoS_3 is especially interesting electrochemically since it has shown unusually high cathode capacities in Li cells utilizing non-aqueous organic electrolytes at ambient temperatures (14).

A Na/MoS_3 cell was setup in the usual manner utilizing a graphite felt current collector for the cathode. The cathode contained 0.59 g (82 mA-hr/1e$^-$)MoS_3. The OCV of the cell was 3.25V at 165°C. The cycling data are given in Table 12, and some typical cycles are given in Figure 25. The cell exhibits a reversible capacity of ~1e$^-$/MoS_3 to a discharge limit of ~1.7V. The higher average cell voltages than those found in organic electrolyte cells (14) suggest a probable displacement type discharge process.

$$MoS_3 + Na^+ + e^- + 0.5NaAlCl_4 \rightarrow MoS_{2.5} + 0.5NaAlSCl_2 + NaCl \quad [24]$$

Interestingly enough, further reactions of the discharge product with $NaAlCl_4$, as in the case of VS_2, do not seem to occur.

Indeed, the behavior of MoS_3 resembles that of non-Na intercalating materials such as NiS_2, discussed in this section, which undergoes displacement type electrode reactions. The reasons for the differences in the electrochemistry of Na-intercalating chalcogenides in organics and molten $NaAlCl_4$ electrolytes, as well as the differences in the behavior of VS_2 versus MoS_3 in molten $NaAlCl_4$ are not yet well understood.

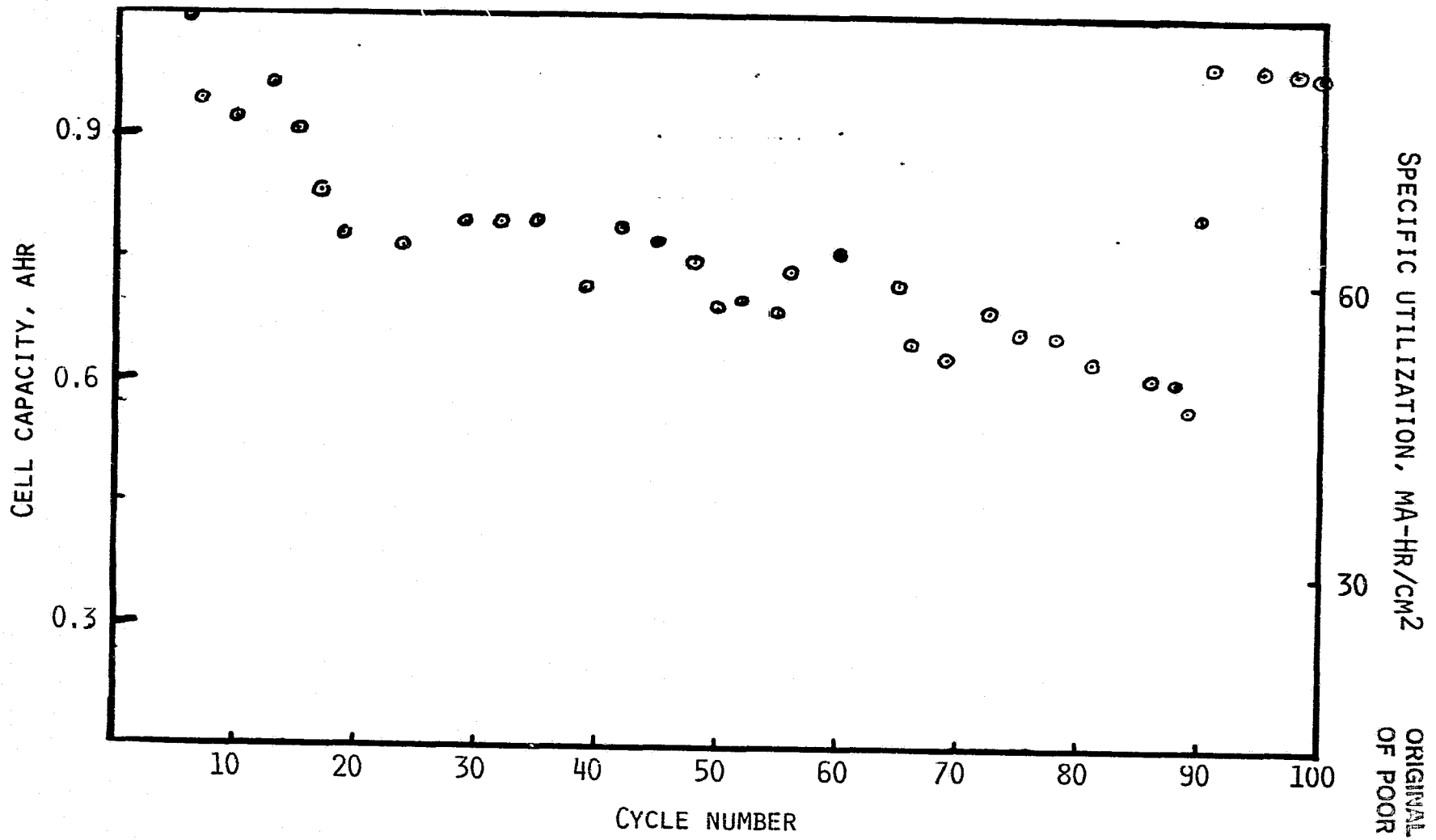

Fig. 23. Capacity versus cycle number for prototype Cell No. 365-79, current density: cycle 1, id = ic = 2 mA/cm^2; cycles 16-80, id = 12.5 mA/cm^2, ic = 8 mA/cm^2; cycles 90-101, id = ic = 2 mA/cm^2.

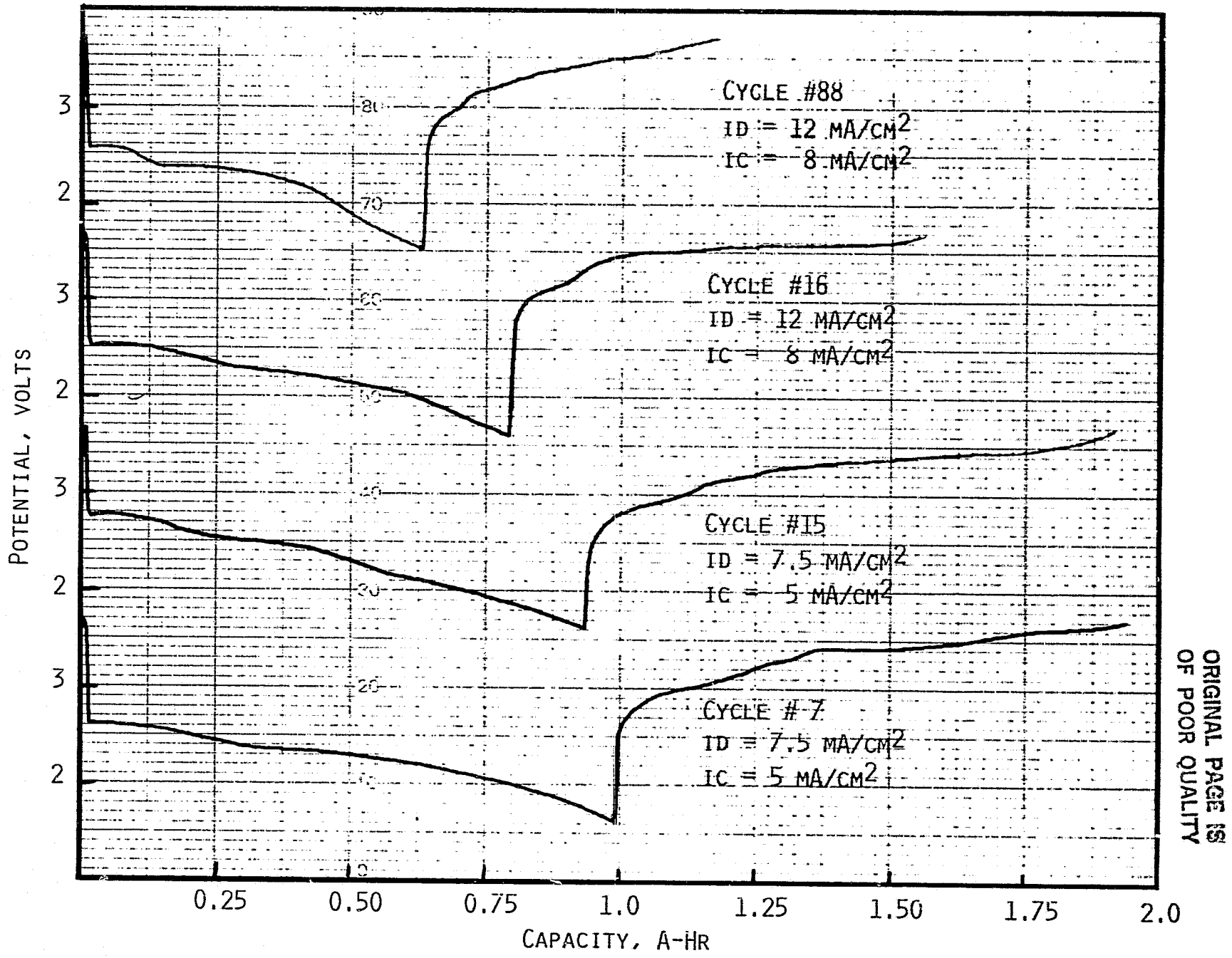

Fig. 24. Some cycles of Cell No. 365-79.

Table 12

Cycling Data for a Na/MoS_3 Cell at 165°C

Cathode: 0.59 gm MoS_3 (82.3 mA.hr)
Current: id = ic = 10 mA (1 mA/cm^2)
Voltage Limits: Cycles 1-9, 2.2-1.8V; cycles 10-38, 3.3-1.7V

Discharge Capacity			Charge Capacity
Cycle Number	mAh	Utilization e^-/MoS_3	mAh
1	86	1.04	63
2	77	0.93	69
3	78	0.95	75
4	77	0.94	75
5	82	1.00	78
6	81	0.98	82
7	84	1.02	84
8	90	1.09	88
9	87	1.06	86
10	95	1.15	93
11	98	1.19	98
12	101	1.23	99
13	98	1.19	98
14	99	1.20	101
15	99	1.20	101
16	96	1.17	96
17	96	1.17	96
18	96	1.17	96
19	95	1.15	96
20	86	1.04	86
21	86	1.08	84
22	89	1.08	87
23	84	1.02	84
24	84	1.02	83
25	83	1.01	84
26	84	1.02	84
27	84	1.02	81
28	81	0.98	80
29	83	1.01	81
30	79	0.96	79
31	81	0.98	81
32	78	0.95	78
33	78	0.95	77
34	79	0.96	77
35	68	0.83	69
36	70	0.85	69
37	70	0.85	70
38	70	0.85	68
39	68	0.83	65
40	62	0.75	61

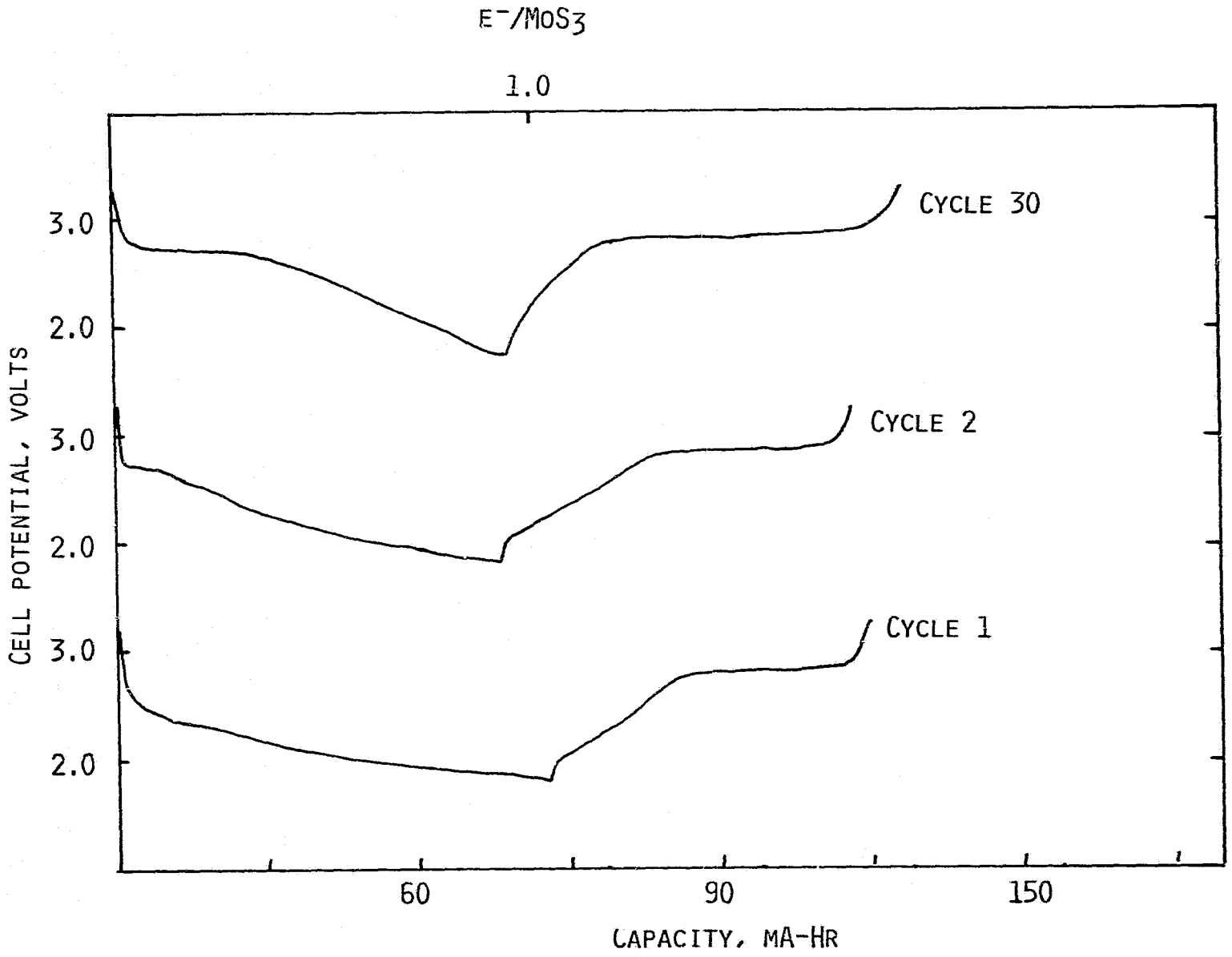

Fig. 25. Galvanostatic cycles 1, 2, and 30 of the Na/MoS_3 cell with a carbon current collector. Current: id = ic = 10 mA (1 mA/cm^2).

4.0 MODERATE TEMPERATURE Na CELLS WITH NiS_2 AND NiS AS CATHODES IN MOLTEN $NaAlCl_4$

In view of the unusual electrochemistry exhibited by Na-intercalating transition metal chalcogenides such as VS_2 in molten $NaAlCl_4$ at ~165°C, we have investigated the electrochemical properties of the apparently non-Na-intercalating sulfides, NiS_2 and NiS, in the same electrolyte medium. Nickel sulfides have been studied by others (15) as cathodes for high temperature Li batteries employing Li-Al alloy anodes. Since the molten salt electrolyte employed in those Li cells consists of melts of simple alkali metal halide mixtures, a rather straightforward cathode chemistry with little involvement of the molten salt would be expected. Such a behavior has been found for NiS_2 in molten LiCl-KCl electrolytes (16).

In a molten salt medium composed of potentially reactive complex salts such as $NaAlCl_4$, the electrode chemistry could be very complex, and interesting. The use of nickel sulfides as cathodes could result in rechargeable Na cells with very high energy densities at moderately high temperatures.

Most of studies to-date have been carried out with NiS_2. The cathodic properties of NiS have been examined briefly.

4.1 Experimental

The general experimental procedures were the same as described in the previous section. Cell construction and operation were also carried out as already discussed.

The nickel sulfides were obtained from Alfa-Ventron, Beverly, MA. The NiS_2 is believed to have a cubic structure (ASTM File No. 11-99) and the NiS, a hexagonal structure (ASTM File No. 2-1280).

4.2 Results and Discussion

4.2.1 Cycling Behavior of the Na/β"-Al_2O_3/$NaAlCl_4$, NiS_2 Cell

The Na/NiS_2 cell exhibits an open-circuit voltage of 3.0V at 165°C. However, this value is in the vicinity of the OCV's we have seen for several other transition metal sulfides in molten $NaAlCl_4$, and it may reflect the small amount of S which is present in the sample rather than the true reduction potential of the disulfide. Cycling behavior of the two cells discussed below serves to illustrate the overall features of the Na/NiS_2 system.

Cell No. 365-133 was constructed with 0.30 g NiS_2 (65.5 mA-Hr/$1e^-$) and ~2.50 g $NaAlCl_4$. The cell exhibited an OCV of 2.99V at 165°C. The cell was cycled at a current of 10 mA or 1 mA/cm^2 between voltage limits of 1.7 and 3.0V.

The first four cycles of Cell No. 365-133 are depicted in Figure 26. The capacity of 150 mA-Hr in the first discharge corresponds to a utilization of $2.3e^-/NiS_2$. The mid-discharge potential is 2.4V. The capacity in the second discharge is $2.1e^-/NiS_2$ and the fourth $1.9e^-/NiS_2$. The discharge voltage profiles show some minor changes on going from the first to the second discharge, and virtually no charge thereafter.

In cells cycled to a recharge limit of 3.0V, the discharge capacity decreased by ~10% in going from the first to the second cycle, and by smaller amounts in the next few cycles. The average rechargeable capacity has been determined to be slightly less than $2e^-/NiS_2$.

We have found a different behavior when the recharge limit is 3.5V. There is a slight increase in capacity on going from the first to the second cycle. Furthermore the NiS_2 utilization shows practically no decline with continued cycling. Reversible NiS_2 utilizations exceeding $3e^-/NiS_2$ can be achieved under these circumstances. This behavior is indicated in Figure 27 which displays the cycling behavior of Cell No. 302-149, identical in construction to 365-133. The utilization in the second cycle of this cell is slightly more than $3e^-/NiS_2$. The additional capacity appears as a high voltage plateau at the beginning of the discharge.

4.2.2 Mechanism of the Cycling of the NiS_2 Cathode

4.2.2.1 X-Ray Analysis of Cycled Cathodes

In order to identify the discharge products, and the various intermediate phases, X-ray analyses were carried out on cycled cathodes. The cathodes were discharged/charged to various depths, washed first with CH_3CN to remove $NaAlCl_4$, and then with dilute ammonia. The latter step was intended to remove the NaCl which was present after the CH_3CN wash.

The X-ray data for the cathode from Cell No. 365-133 (see Fig. 26) are given in Table 13. The cathode had been cycled nine times and ended at the end of the ninth charge. Based on the total coulombic capacities in the nine discharges and charges, the cathode had undergone a net discharge by $0.25e^-$. This implies an average composition of $NiS_{1.88}$ for the cathode sample X-rayed. The data in Table 13 can be assigned to a mixture, composed mostly of NiS_2 and small amounts of Ni_3S_4.

ORIGINAL PAGE IS
OF POOR QUALITY

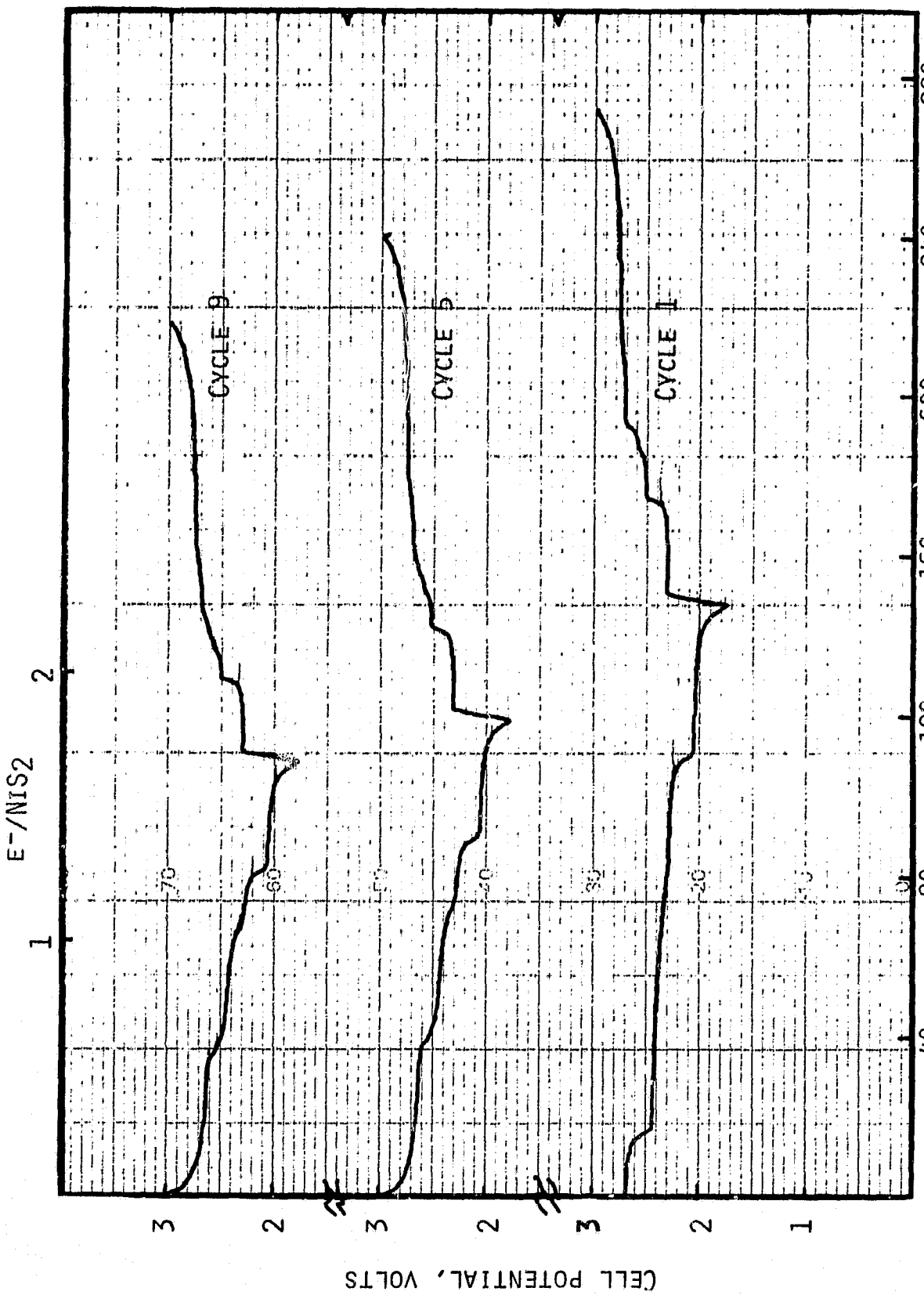

Fig. 26. The utilization in a NiS_2 cathode (Cell No. 365-133) cycling with a recharge limit of 3.0V. The discharge limit is 1.7V. Current density; id = ic = 1 mA/cm^2.

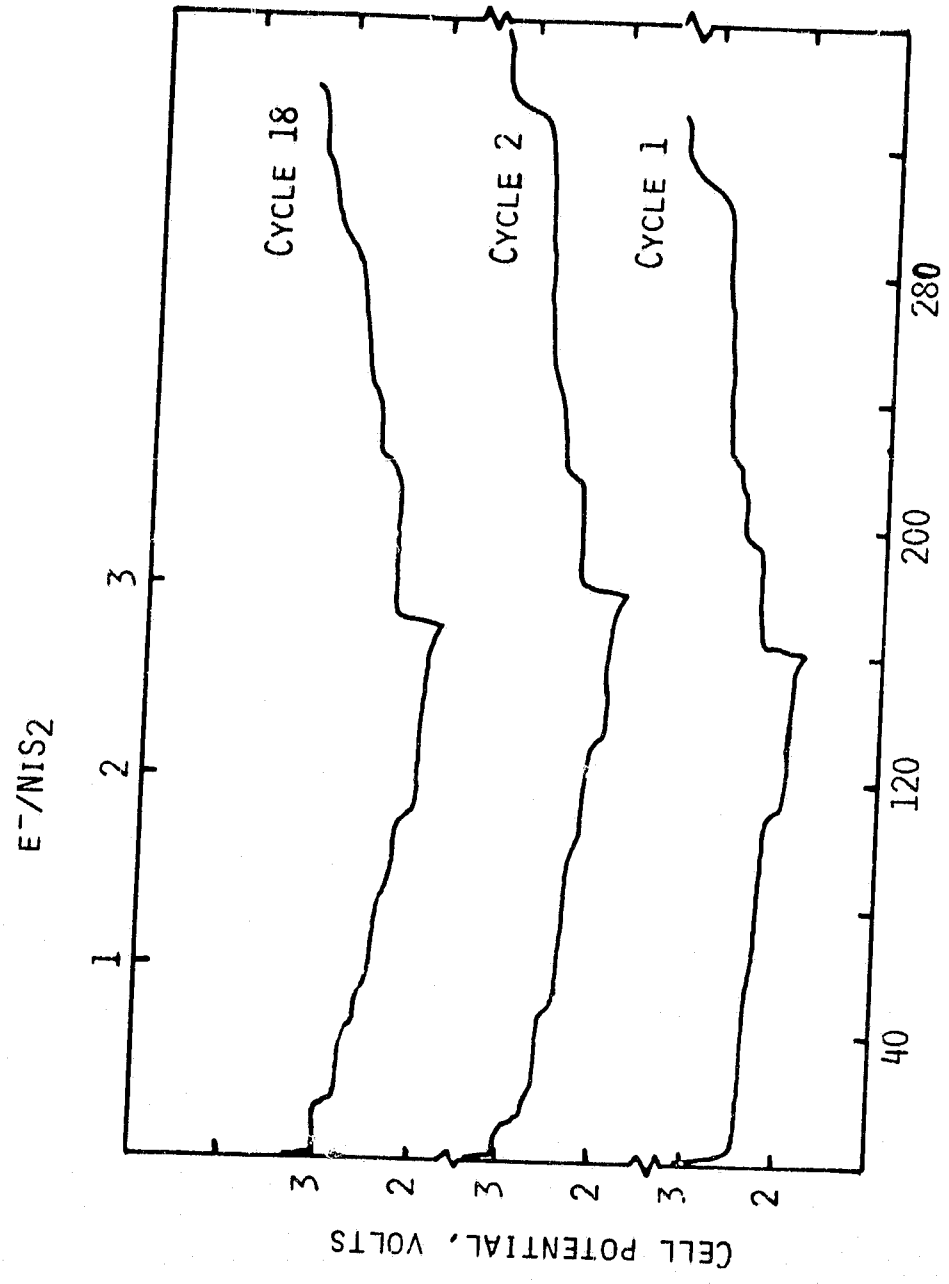

Fig. 27. Cycles of Na/NiS_2 Cell No. 302-149 at ~170°C. Current: id = ic = 1 mA/cm^2; voltage limits: 1.7-3.5V.

Table 13

X-Ray Diffraction Data for the Cathode from Cell No. 365-133 Ended on Top of a Charge Half-Cycle

Cathode		Original NiS_2		Ni_3S_4	
d, Å	I/I_o	d, Å	I/I_o	d, Å	I/I_o
5.40	< 10			5.5	20
4.33	10				
3.96	< 10				
3.56	< 10			3.34	40
3.26	10	3.27	20		
2.81	100	2.83	100	2.85	90
2.60	40	2.54	40		
2.36	10			2.36	90
2.31	30	2.32	40		
2.00	60	2.00	50	1.94	30
1.82	10			1.82	90
1.71	90	1.71	80		
1.67	20	1.63	20	1.67	100
1.57	20			1.60	10
1.52	20	1.52	30	1.44	50
1.30	10	1.30	20	1.37	60
1.26	10	1.27	20		
1.24	< 10	1.23	20	1.27	30
1.16	10	1.16	30	1.23	80
1.09	60	1.09	60	1.18	70

Another cell, No. 365-128, was cycled once, and then its second discharge was ended at 2.1V, prior to the onset of the 2.0V discharge plateau. The cell was disassembled and, after workup, the cathode was X-rayed. The utilization in the second discharge was $1.8e^-/NiS_2$. Thus, the calculated cathode composition is $NiS_{1.1}$. The X-ray data are displayed in Table 14, and are compared with that of NiS and Ni_3S_2. Clearly, the major component is NiS. Small amounts of Ni_3S_4 and Ni_3S_2 are also probably present.

In some cases after a discharge to 2.1V, the cathode mostly contained Ni_3S_2. It is accurate to say that Ni_3S_4, NiS and Ni_3S_2 are intermediate phases in the discharge of NiS_2 in molten $NaAlCl_4$ at ~165°C.

4.2.2.2 Cycling Behavior of the NiS Cathode

The X-ray data presented above clearly show NiS as an intermediate phase in the discharge of NiS_2. This has been confirmed by comparing the cycling behavior of NiS with that of NiS_2.

A Na/NiS cell, No. 365-132, was constructed with 0.30 g NiS (88.6 mA-hr/$1e^-$), and discharged and charged at 10 mA (1 mA/cm^2) at 165°C. The voltage limits were 1.7 and 3.0V. The first four cycles are shown in Figure 28. The capacity in the first discharge was 134 mA-hr, equivalent to a utilization of $1.52e^-/NiS$. The capacity increased to $1.8e^-/NiS_2$ in the second discharge and to $1.9e^-/NiS_2$ by the fourth. There was no further change in utilization. The cell was terminated at the end of the 10th discharge for X-ray analysis of the cathode. The capacity in the 10th discharge was $1.95e^-/NiS_2$.

The data in Figures 26 and 28 clearly illustrate the similarities in the discharge/charge profiles of NiS and NiS_2. They also substantiate that NiS is an intermediate in the discharge of NiS_2.

The first discharge of NiS shows two voltage plateaus; the first at ~2.3V, emcompassing ~$0.4e^-/NiS$, and the second at ~2.0V, yielding ~$1.1e^-/NiS$. These plateaus most probably correspond to the reduction of NiS to N_3S_2 and that of Ni_3S_2 to Ni, respectively. The X-ray data for the cathode from Cell No. 365-132, listed in Table 15, strongly support this. The pattern can be indexed for Ni_3S_2 and Ni; however, small amounts of β-Ni_7S_6 may also be present.

It should be noted that beginning with the second discharge of NiS, an additional plateau at ~2.7V, and a sloping voltage region between 2.7 and 2.4V appear. The combined capacities in these two regions equal ~20% of the total discharge capacity. It appears that the recharge of the cathode to 3.0V, oxidizes the material to a composition slightly richer in S than that in NiS.

Table 14

X-Ray Diffraction Data of the Cathode of Na/NiS_2 Cell No. 365-128

Cathode of Cell No. 128[a]		NiS	
d, Å	I/I_o	d, Å	I/I_o
4.81	20	4.81	60
4.43	10		
3.25[b]	50		
2.80[b]	100	2.78	100
2.52	20	2.51	65
2.40	10	2.41	12
2.31	10		
2.23	10	2.23	55
2.01[b]	90		
1.86	20	1.86	95
1.81	10	1.82	45
1.71	10	1.73	40
1.62[b]	80	1.63	18
		1.60	35
1.55	10	1.55	25
1.51	10		
1.41[b]	70		
1.30	10	1.30	10
1.27[b]	70		
1.15[b]	60		
1.11	10	1.11	16
1.10	20		
1.09	20		

[a]Cell ended on the second discharge at 2.1V, capacity 1.8 e^-/NiS_2.
[b]Also probably due to NaCl. The cathode had been washed only with CH_3CN.

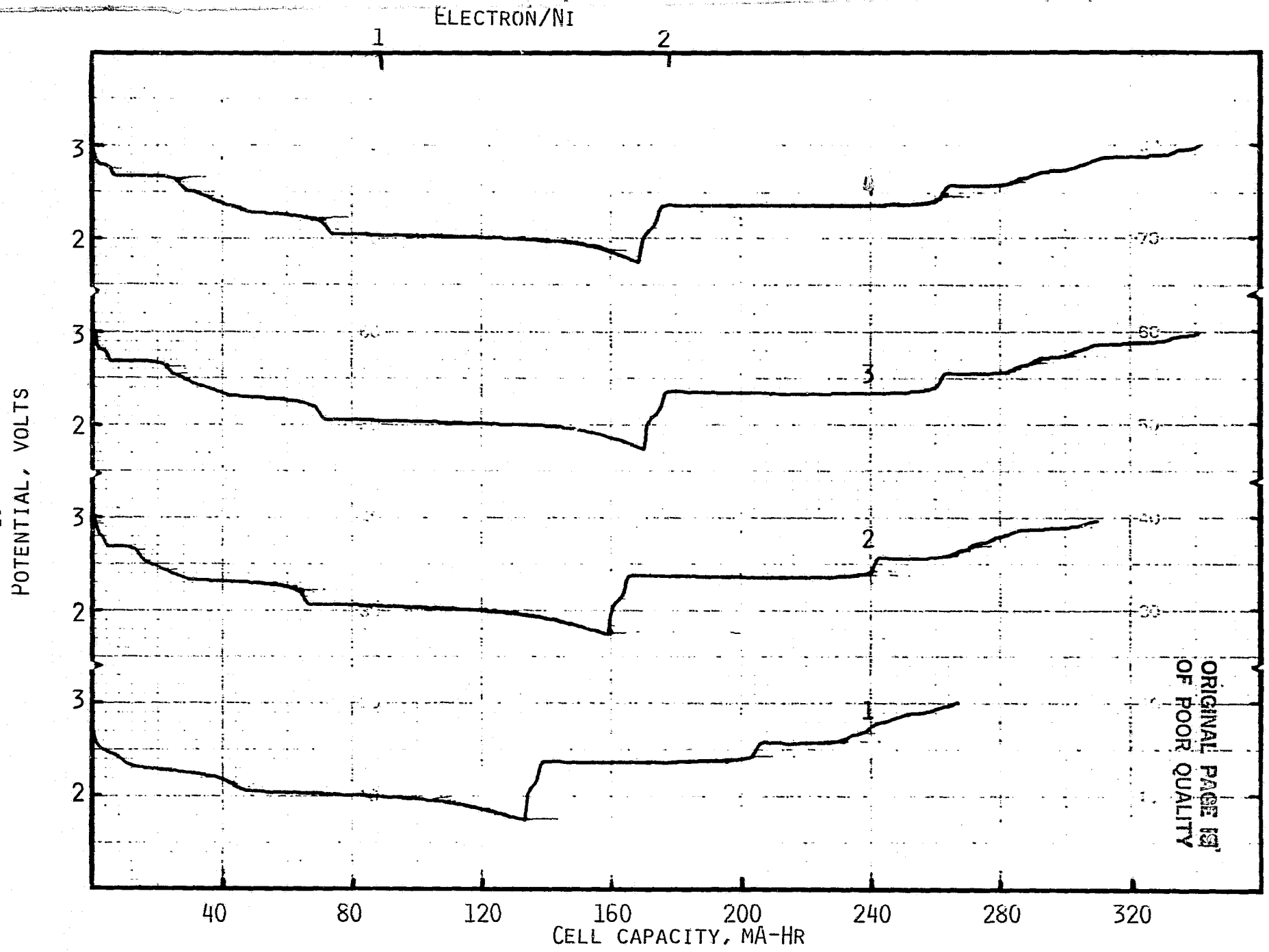

Fig. 28. The first four cycles of Na/NiS Cell No. 365-132 at 165°C. Current; id = ic = 1 mA/cm^2.

Table 15

X-Ray Diffraction Data of the Cathode of Na/NiS Cell No. 365-132

Cathode from Cell #365-132*		Ni		Ni_3S_2		Starting NiS	
d, Å	I/I_o	d, Å	I/I_o	d, Å	I/I_o	d, Å	I/I
5.47	10						
4.82	10						
4.05	10			4.1	70		
3.35	10						
						2.96	80
2.86	70			2.88	100		
2.78	20						
						2.58	70
2.51	10						
2.37	30			2.39	60		
				2.35	30		
2.22	10						
2.03	100	2.03	100	2.04	60		
						1.97	100
1.86	10						
1.82	20			1.83	100		
				1.81	100	1.71	80
1.77	80	1.76	42				
1.68	50			1.67	30		
				1.66	100	1.52	30
1.38	< 10			1.37	40	1.48	30
1.25	50	1.25	21	1.36	40	1.42	30
1.06	60	1.06	20	1.22	100	1.33	30
						1.29	60

*Some of the unaccounted for lines may be due to β-Ni_7S_6.

4.2.2.3 Cycling Behavior of the "Ni + Na_2S" Cathode

In an attempt to further elucidate the cathode reaction mechanism of the NiS_2 electrode, cell No. 345-32 was setup. Its cathode comprised a mixture of 0.15 g (2.5 mmoles) Ni powder and 0.4 g (5.1 mmoles) Na_2S. The open-circuit-voltage was 2.2V at 165°C. The theoretical capacity of the cell, based on a $4e^-$/Ni utilization, would be 274 mA-hr. The cell was cycled at a constant current of 10 mA (1 mA/cm^2) between voltage limits of 1.8 and 3.5V. The first cycle (beginning with a charge to 3.5V) and the fifth cycle are shown in Figure 29. The utilization in the first 10 cycles averaged ~$3.5e^-$/Ni. In Figure 29, the two cycles of this cell are compared with the 18th cycle of No. 302-149, presented earlier in Figure 27. Clearly, there are striking similarities in the voltage profiles of the two cells. The cycling reactions in the two cells are seemingly identical.

4.2.2.4 Cathode Reactions in the Na/NiS_2 Cell

Based on the evidences presented in the above sections, the NiS_2 positive electrode reaction may be represented as:

$$NiS_2 + 4Na^+ + 4e^- \underset{\text{Charge}}{\overset{\text{Discharge}}{\rightleftharpoons}} Ni + 2Na_2S \qquad [25]$$

As discussed in Section 3, the Na_2S would react with the electrolyte to form $NaAlSCl_2$ and NaCl so that the actual overall discharge/charge reaction may be that shown in equation [26].

$$NiS_2 + 4Na^+ + 4e^- + 2NaAlCl_4 \rightleftharpoons Ni + 2NaAlSCl_2 + 4NaCl \qquad [26]$$

The experimental results also indicate that the NiS_2 discharge involves the intermediate steps, shown in equations [27-30]. The latter correspond to the formation of the phases, Ni_3S_4, NiS and Ni_3S_2. Electrochemical reversibility for each step appears to be excellent.

$$3NiS_2 + 4Na^+ + 4e^- + 2NaAlCl_4 \rightleftharpoons Ni_3S_4 + 2NaAlSCl_2 + 4NaCl \qquad [27]$$

$$Ni_3S_4 + 2Na^+ + 2e^- + NaAlCl_4 \rightleftharpoons 3NiS + NaAlSCl_2 + 2NaCl \qquad [28]$$

$$3NiS + 2Na^+ + 2e^- + NaAlCl_4 \rightleftharpoons Ni_3S_2 + NaAlSCl_2 + 2NaCl \qquad [29]$$

$$Ni_3S_2 + 4Na^+ + 4e^- + 2NaAlCl_4 \rightleftharpoons 3Ni + 2NaAlSCl_2 + 4NaCl \qquad [30]$$

Note that reactions [29] and [30] are those involved in the cycling of NiS.

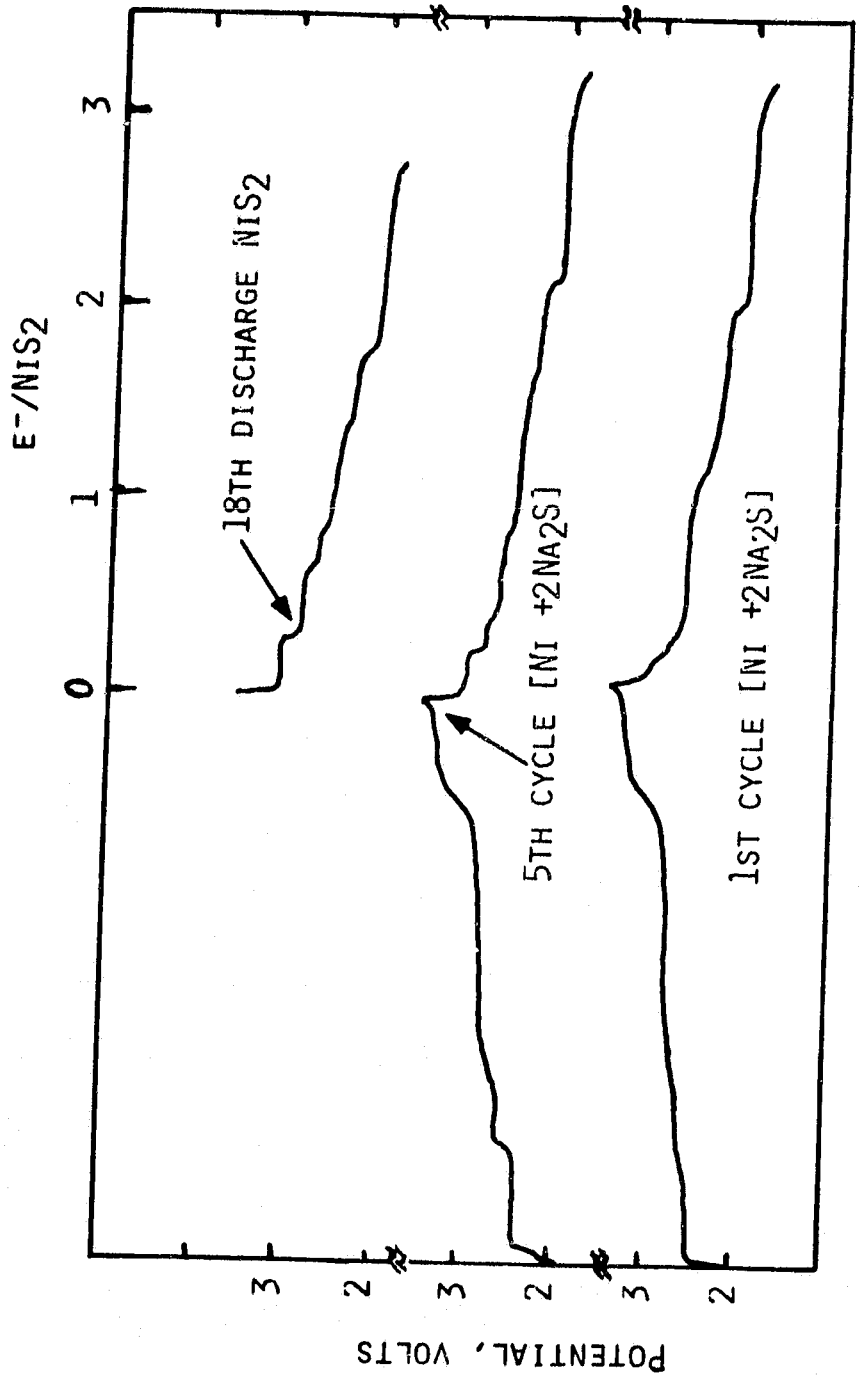

Fig. 29. A comparison of the cycles of cell No. 345-32 utilizing a mixture of [Ni +2Na_2S] with the 18th discharge of Cell No. 302-149 utilizing NiS_2.

4.2.3 Rechargeability of NiS_2 and NiS Cells

Most of the studies to-date have been carried out with NiS_2. It is rather obvious from the reaction mechanism discussed that an apparent reversibility for NiS_2, within limits of 1.8-3.5V, implies the same for NiS also. However, we have verified the latter by cycling NiS alone as the cathode. These various data obtained from NiS_2 and NiS cells are presented below.

4.2.3.1 Extended Cycling Studies of Na/NiS_2 Cells

The results obtained from the cycling of the following Na/NiS_2 cells are the most useful in assessing the rechargeability of the NiS_2 cathode.

Cell No. 365-61: The major purpose of this test was to assess the fundamental rechargeability of the NiS_2 cathode in molten $NaAlCl_4$ at a temperature in the range of 165-200°C. The NiS_2 to $NaAlCl_4$ mole ratio was maintained at 1:4 and a moderate loading capacity of ~50 mA-hr/cm^2 (based on a $4e^-/NiS_2$ theoretical utilization, and on the surface area of the β''-Al_2O_3 exposed to the carbon felt current collector containing the cathode material) was used. Thus, the cathode contained a mixture of 0.75 g (6.1 mmoles) NiS_2, 0.15 g Ni* and 4.7 g $NaAlCl_4$. The cell configuration was the same as that of the laboratory cells already described. The surface area of the β''-Al_2O_3 exposed to the carbon felt was 12.5 cm^2. The cell cycling was begun at a temperature of ~165°C. The OCV at 165°C was 2.90V.

A plot showing NiS_2 utilization versus cycle number is given in Figure 30. Some typical cycles are given in Figure 31. In the several initial cycles the current was varied to arrive at optimum discharge and charge current densities for the extended cycling. Thus, the first four cycles were performed at a constant current of 25 mA (2 mA/cm^2). Between cycles 5 and 54, the current was 50 mA (4 mA/cm^2). Beginning with cycle 55, the current density was 8 mA/cm^2 for discharge and 4 mA/cm^2 for recharge. Thereafter current was unchanged. The temperature was maintained at 165°C until the 184th cycle when it was raised to 190°C. All cycles subsequent to 184 were obtained at 190°C.

The cell was cycled 540 times before it was voluntarily terminated. The uninterrupted cycling took almost one year. The excellent rechargeability of NiS_2 has unequivocally been demonstrated by these data. The higher temperature of 190°C helped increase the cathode utilization; principally, the capacity of the 2.1V plateau. The cell temperature during the

*A small amount of Ni powder, 20-40 m/o of NiS_2, was found to improve the cathode rechargeability. The Ni powder helps improve the electronic conductivity of the cathode. It also facilitates NiS reduction by chemical reaction to form Ni_3S_2. The latter apparently is more easily reduced electronically.

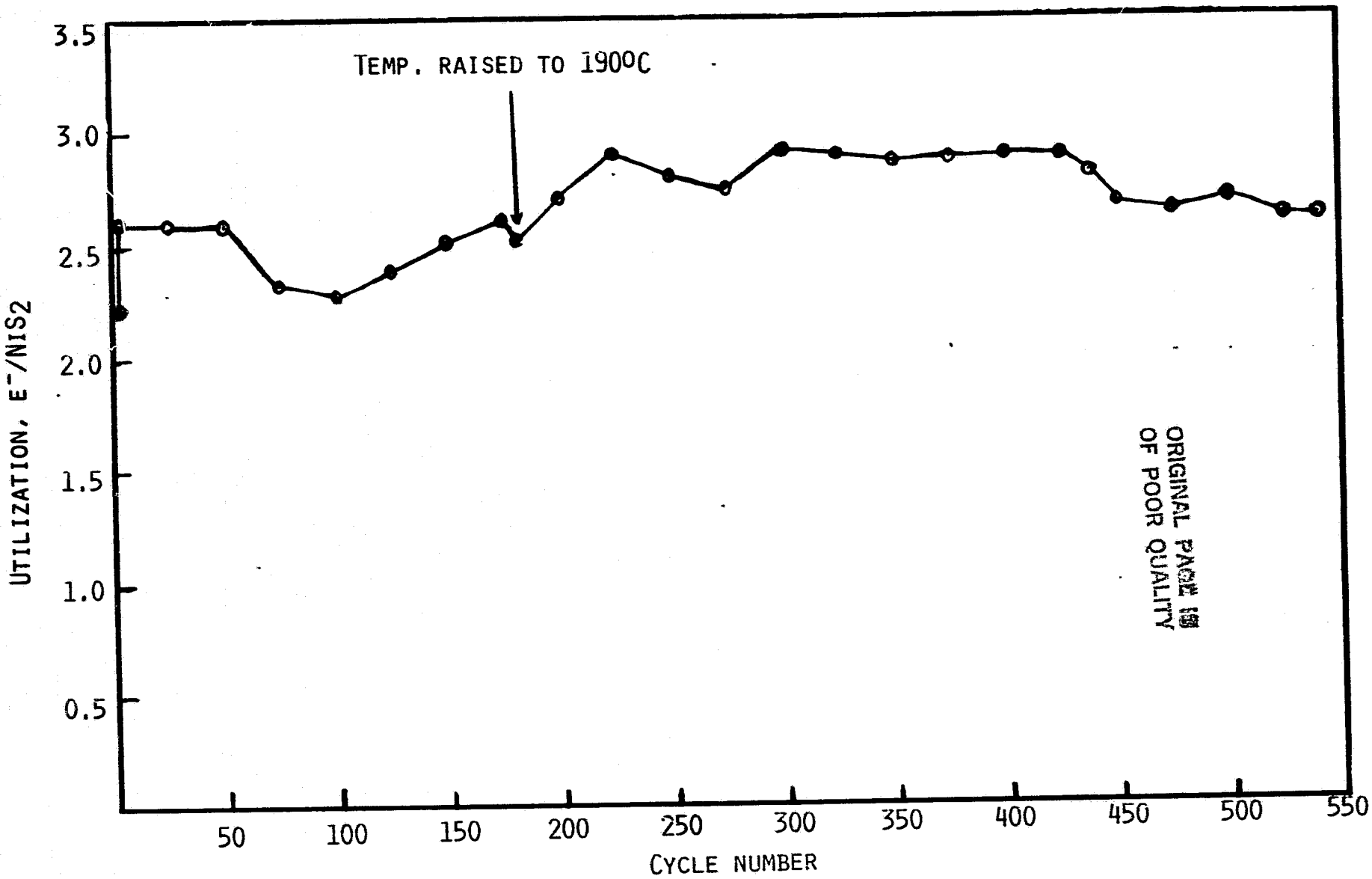

Fig. 30. Cathode utilization versus cycle number for Cell No. 365-61.

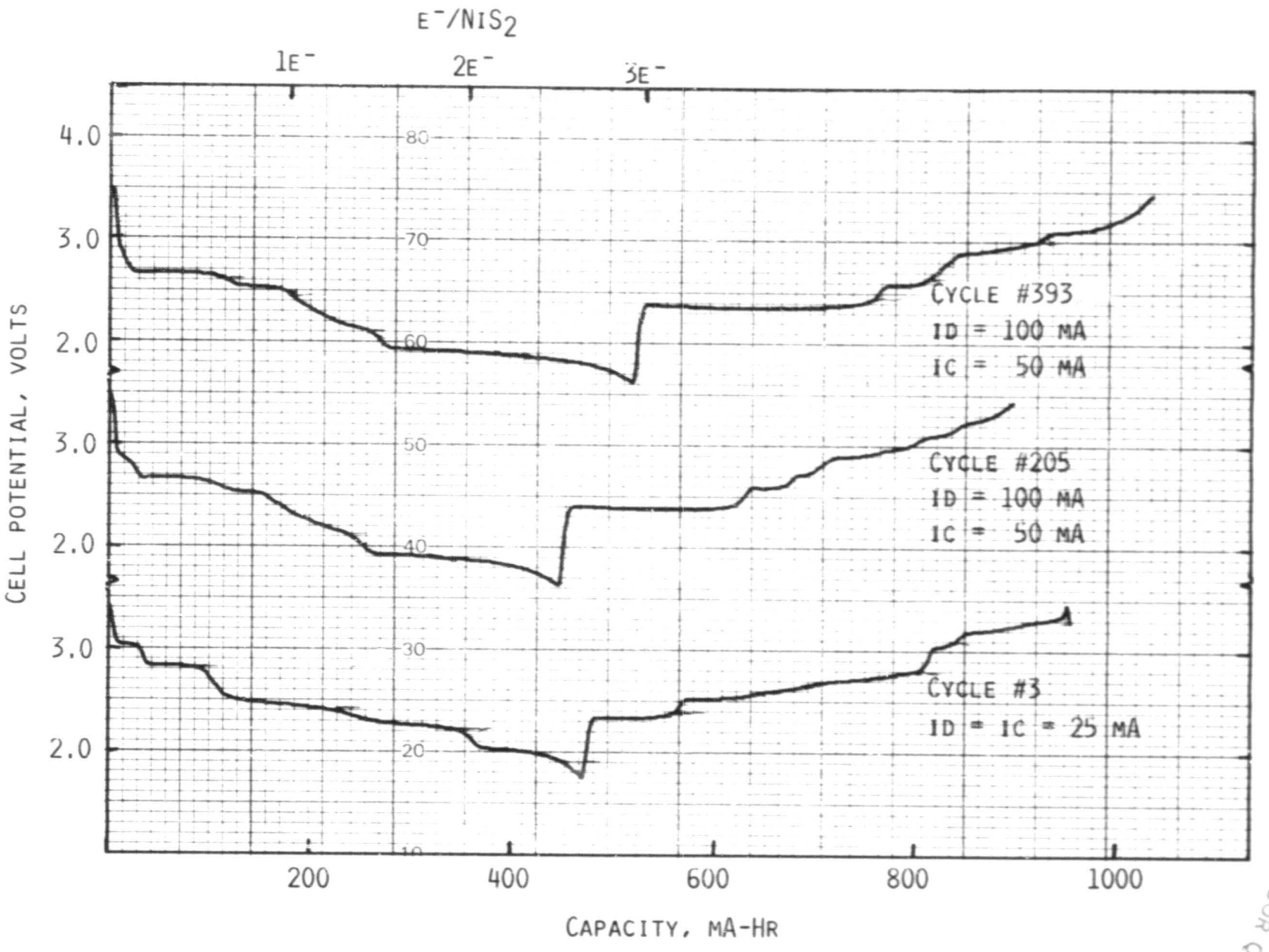

Fig. 31. Typical cycles of Na/NiS_2 Cell No. 365-61.

last eight months of cycling was the higher 190°C. The average NiS_2 utilization in the 540 cycles was ~2.6e^-/NiS_2. The latter corresponds to an average specific utilization of ~34 mA-hr/cm^2 of β"-Al_2O_3. The extended cycling has also demonstrated the excellent compatibility between β"-Al_2O_3 and molten $NaAlCl_4$. The cycling experiment was discontinued when the contract was completed.

Cell No. 365-75 with an Inside-Out Configuration: This cell was studied in order to ascertain the feasibility of cell construction and operation in the inside-out configuration, and to assess the effect of a loading capacity of ~100 mA-hr/cm^2 (of the β"-Al_2O_3) on the cathode's rechargeability.

The cell hardware was the same as that shown in Figure 22. However, while maintaining a loading capacity of ~100 mA-hr/cm^2 (of the β"-Al_2O_3 tube), the total cell capacity was limited to about 1 A-hr. Thus the cell utilized a cathode mix composed of 1.53 g NiS_2 and 0.30 g Ni. The mix was pressed into small discs, measuring ~13 mm diameter, and weighing ~120 mg each. There were 16 of these discs. Each disc was sandwiched between a pair of graphite felt wafers, measuring ~1.0 mm. The 16 sandwiches were stacked inside the β"-Al_2O_3 tube and ~8 g of $NaAlCl_4$ was added. The ratio of $NaAlCl_4$ to cathode active material was ~3.5:1. The theoretical cathode capacity based on 4e^-/NiS_2 was 1.33 A-hr which corresponds to a cathode loading of 158 mA-hr/cm^2.

The outer stainless steel Na container served also as the anode current collector. The cathode lead consisted of two tungsten wires, inserted through the silicone rubber seal at the mouth of the β"-Al_2O_3 tube and extending the entire length of the electrode stack assembly. All cycling was performed at 190°C. The initial OCV of the cell was 3.02V. The first four cycles were obtained at a current of 25 mA (3.0 mA/cm^2) for both discharge and charge between limits of 1.7 and 3.5V, respectively. Beginning with cycle 5, the currents were 100 mA (12 mA/cm^2) for discharge and 50 mA (6 mA/cm^2) for charge; the voltage limits were 1.7 and 3.5V. Some typical cycles are given in Figure 32. A plot of capacity versus cycle number is given in Figure 33.

The initial NiS_2 utilization is lower than in Cell No. 365-61. This probably reflects the higher loading capacity and/or the different cathode structure in the present cell. However, the utilization continued to increase, reaching 2e^-/NiS_2 by the 40th cycle. The fact that there are no significant differences in the voltage profiles of the early and later cycles seems to indicate that the higher capacity in the later cycles is due to an increased material utilization. This is illustrated in Figure 34, depicting cycles 4, 50 and 87. The 2e^-/NiS_2 utilization is equivalent to a specific utilization of ~80 mA-hr/cm^2 (of the β"-Al_2O_3).

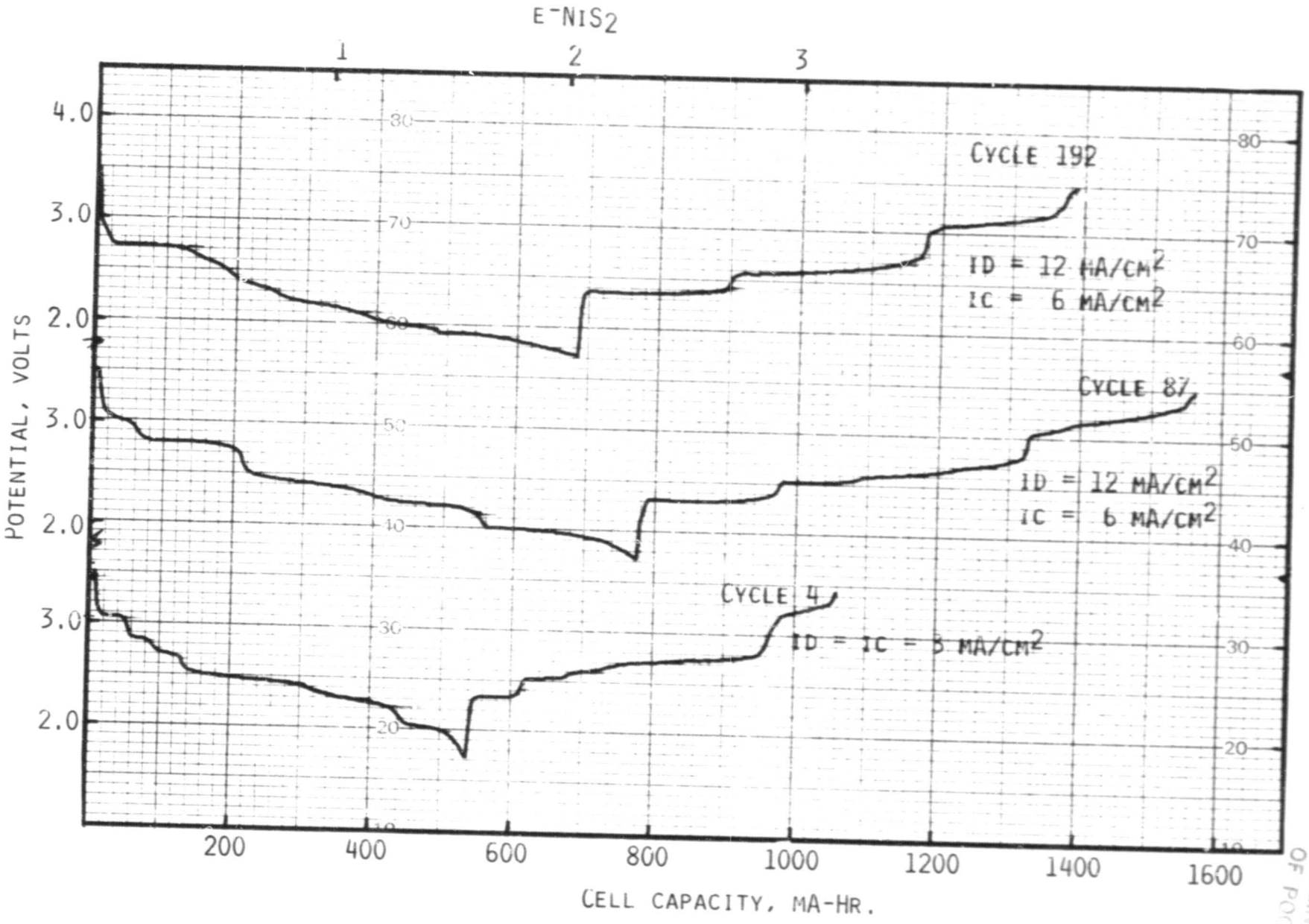

Fig. 32. Typical cycles of Na/NiS_2, Cell No. 365-75.

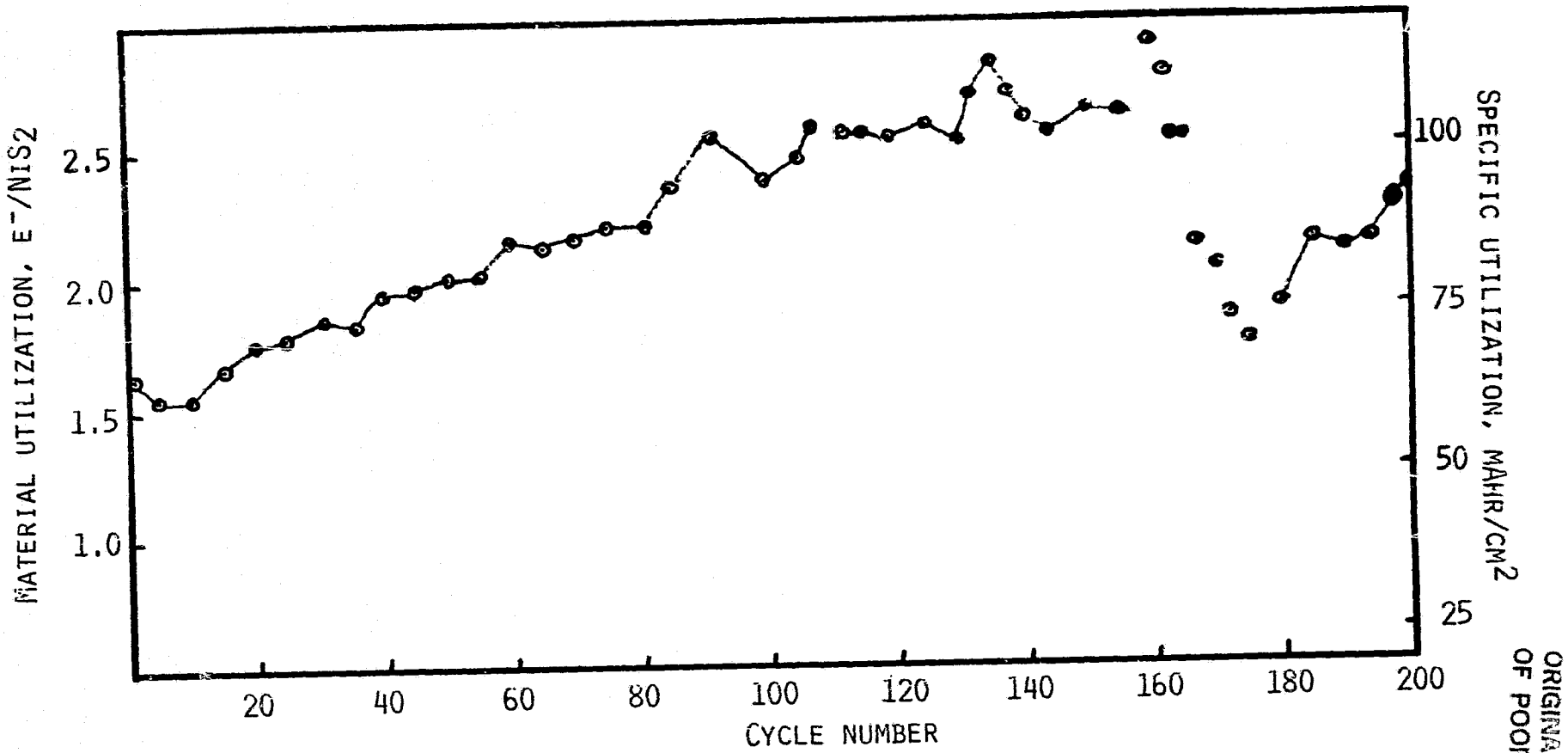

Fig. 33. Cathode utilization versus cycle number for Cell No. 365-75. Cycles 1-4, id = ic = 3 mA/cm^2. Cycles 5-159, id = 12 mA/cm^2, ic = 6 mA/cm^2. The currents were varied in cycles 160-180.

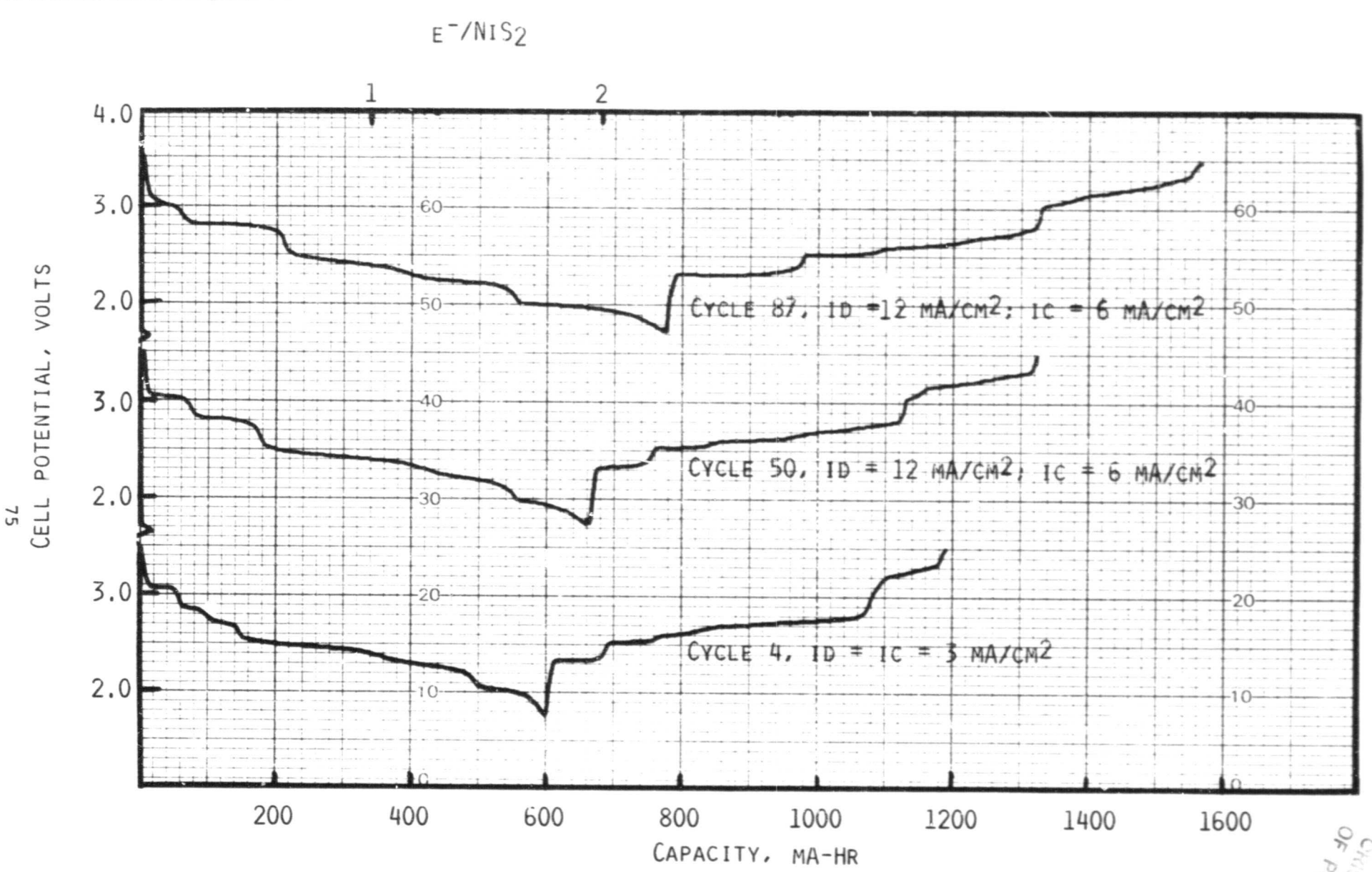

Fig. 34. Early cycles of Na/NiS_2 Cell No. 365-75.

The cathode utilization reached a high value of ~2.5e⁻/NiS_2 by the 90th cycle and remained relatively steady thereafter.

In cycles 108-110, we evaluated the effect of a 3.0V recharge limit on NiS_2 utilization. The result is shown in Figure 35. The discharge capacity decreases by ~25% as a result of the lower recharge voltage limit. The capacity involved in the first plateau at ~2.8V is not accessible if the recharge is not continued to a limit of 3.5V. Cycling of the cell was resumed within the voltage limits of 1.7 and 3.5V.

Beginning with cycle 160, the cell capacities were evaluated at a series of current densities between 3 and 27 mA/cm^2. The rate/capacity data are given in Figure 36. Some discharges at the higher current densities are given in Figure 37. Evidently, the rate-capacity behavior of the NiS_2 cathode remains good, irrespective of its cycle life.

The cell test was terminated upon completion of 200 deep discharge/charge cycles. The feasibility of cell fabrication in the inside-out configuration and the accessibility of high NiS_2 utilization in such cells at high loading capacities and current densities have been demonstrated.

Cell No. 365-103 with a 2:1 $NaAlCl_4$ to NiS_2 Mole Ratio:

Because of the participation of $NaAlCl_4$ in the discharge process (through reaction with Na_2S to form $NaAlSCl_2$ and NaCl) the initial $NaAlCl_4$ to NiS_2 ratio is believed to have a significant effect on the capacity, rate capability and rechargeability of the Na/NiS_2 cell.

Cell No. 365-103, constructed in the normal configuration with Na inside the β''-Al_2O_3 tube, utilized 1.53 g NiS_2, 0.31 g Ni and 4.78 g $NaAlCl_4$. Thus, the $NaAlCl_4$ to NiS_2 mole ratio was 2:1. The theoretical cathode capacity, based on $4e^-/NiS_2$, was 1.33 Ah. The cell exhibited an initial OCV of 2.90V at 190°C. The cycling data are given in Figure 38. Some discharge/charge curves are given in Figure 39. The cell was subjected to more than 200 deep discharge/charge cycles, most of which were confined to the limits of 1.7 and 3.5V. A few early cycles were also obtained within voltage limits of 1.7 and 3.0V.

The average NiS_2 utilization obtained at id = 8 mA/cm^2 and ic = 4 mA/cm^2 is ~1.5e⁻/NiS_2. The related specific energy, based on all active materials, including Na and $NaAlCl_4$, is ~170 Whr/Kg.

As was found in the previous cell, the utilization decreases by ~25% if the recharge limit is lowered to 3.0V. The capacity corresponding to the 2.8V plateau becomes inaccessible.

Beginning with cycle 140, rate/capacity relationships were evaluated for current densities between 4 and 22 mA/cm^2. The data are given in Figures 40 and 41. Even with a restricted amount of $NaAlCl_4$, the rate capability of NiS_2 appears to remain excellent during the long life of the cell.

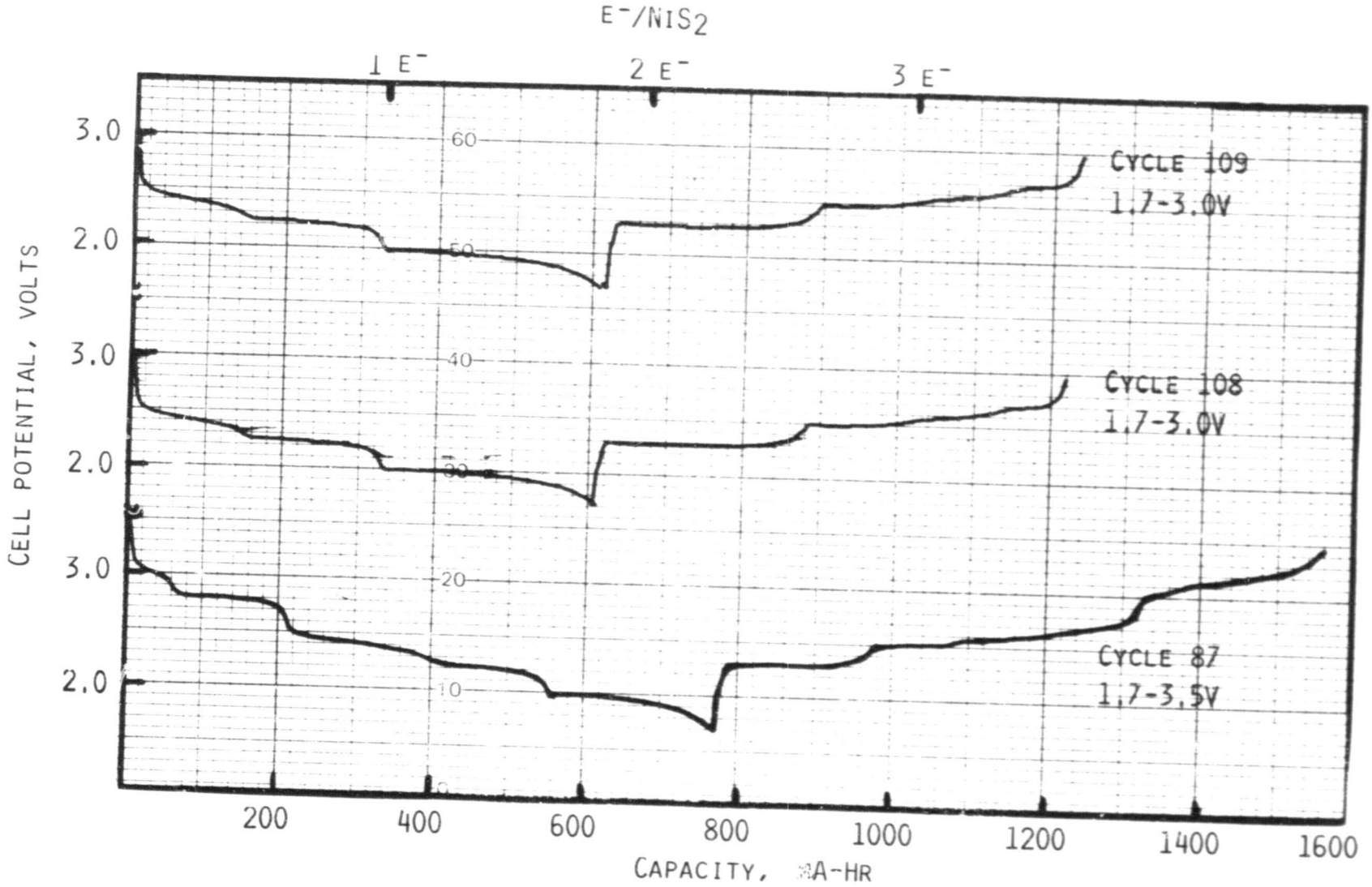

Fig. 35. Effect of recharge voltage limits on NiS_2 utilization in Cell No. 365-75. All cycles are at same currents; id = 12 mA/cm^2, ic = 6 mA/cm^2.

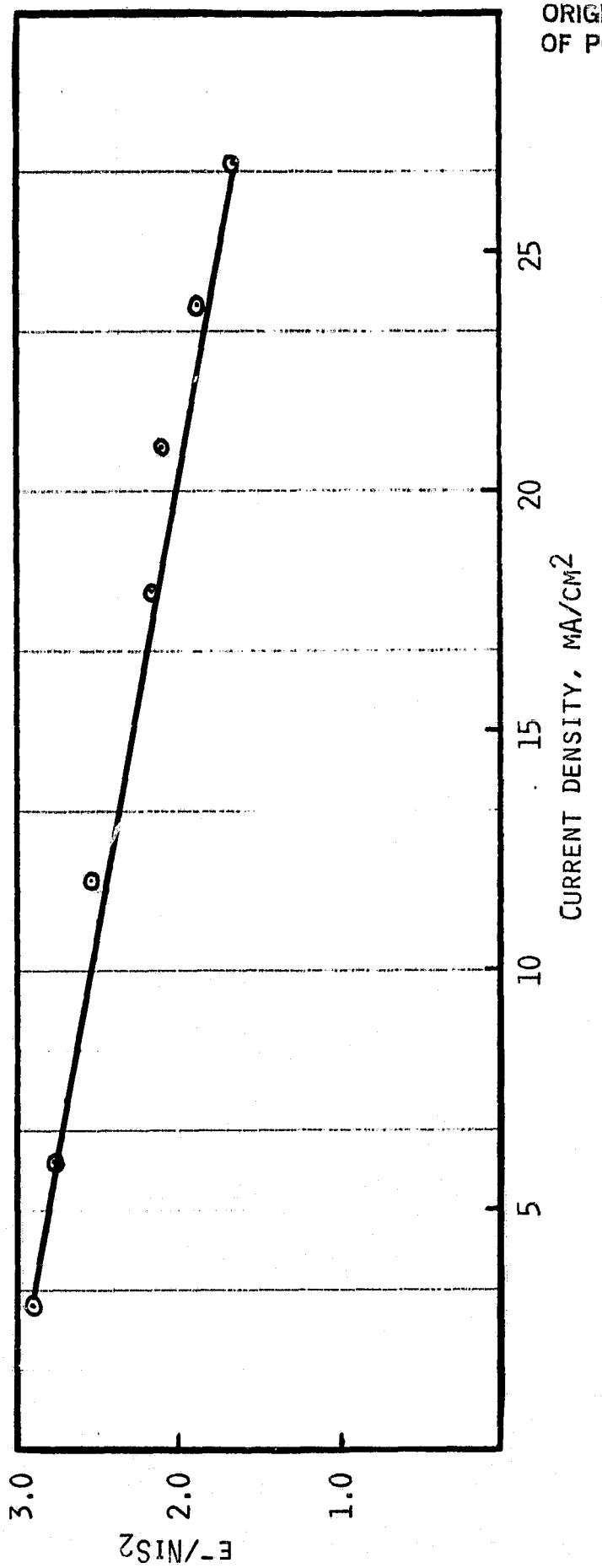

Fig. 36. Capacity versus current density in Cell No. 365-75 beginning with cycle 160. Each discharge was followed by a charge at 2 mA/cm^2. Temperature, 190°C.

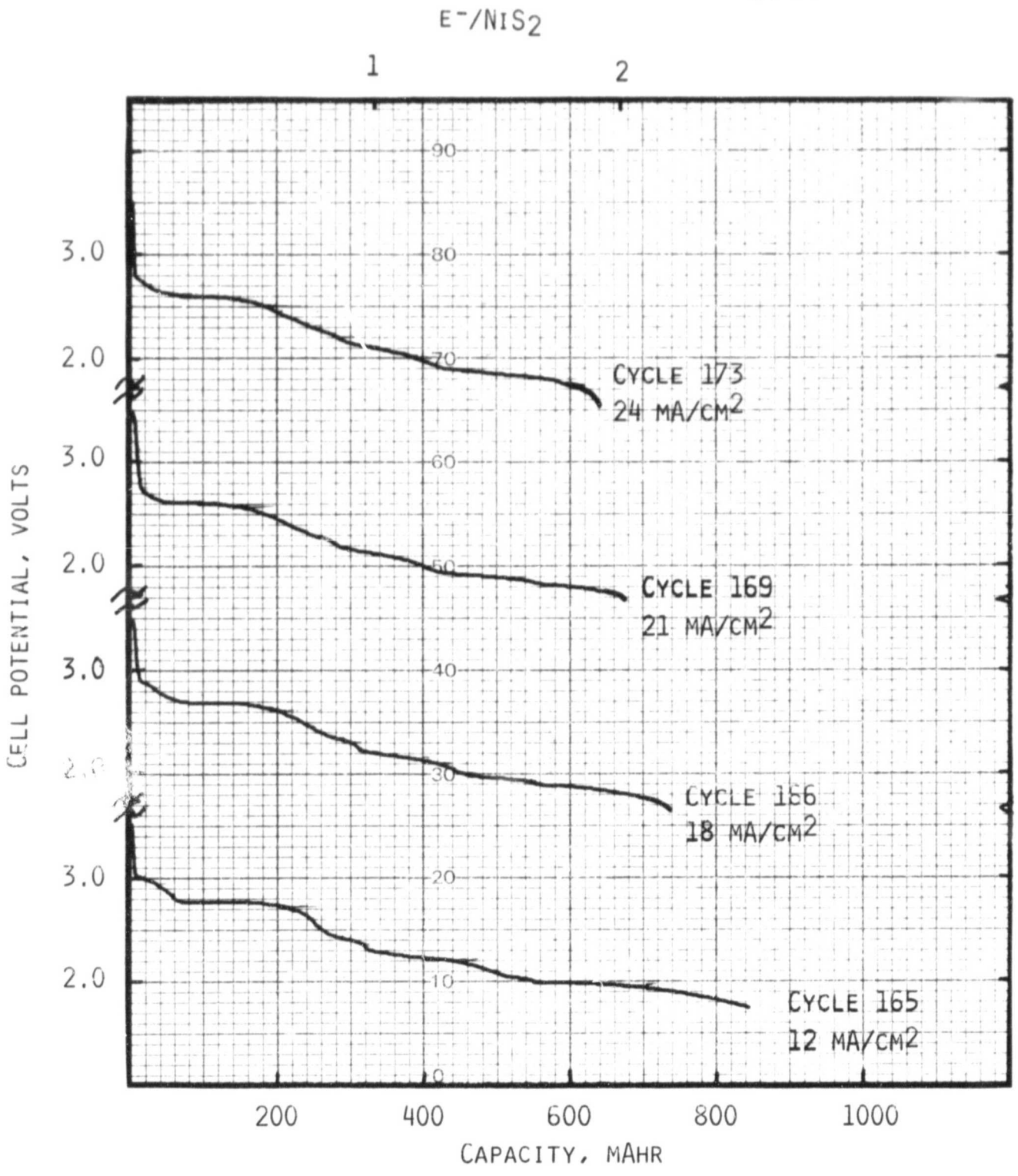

Fig. 37. Discharges of Cell No. 365-75 at various current densities. The cell had completed 160 cycles.

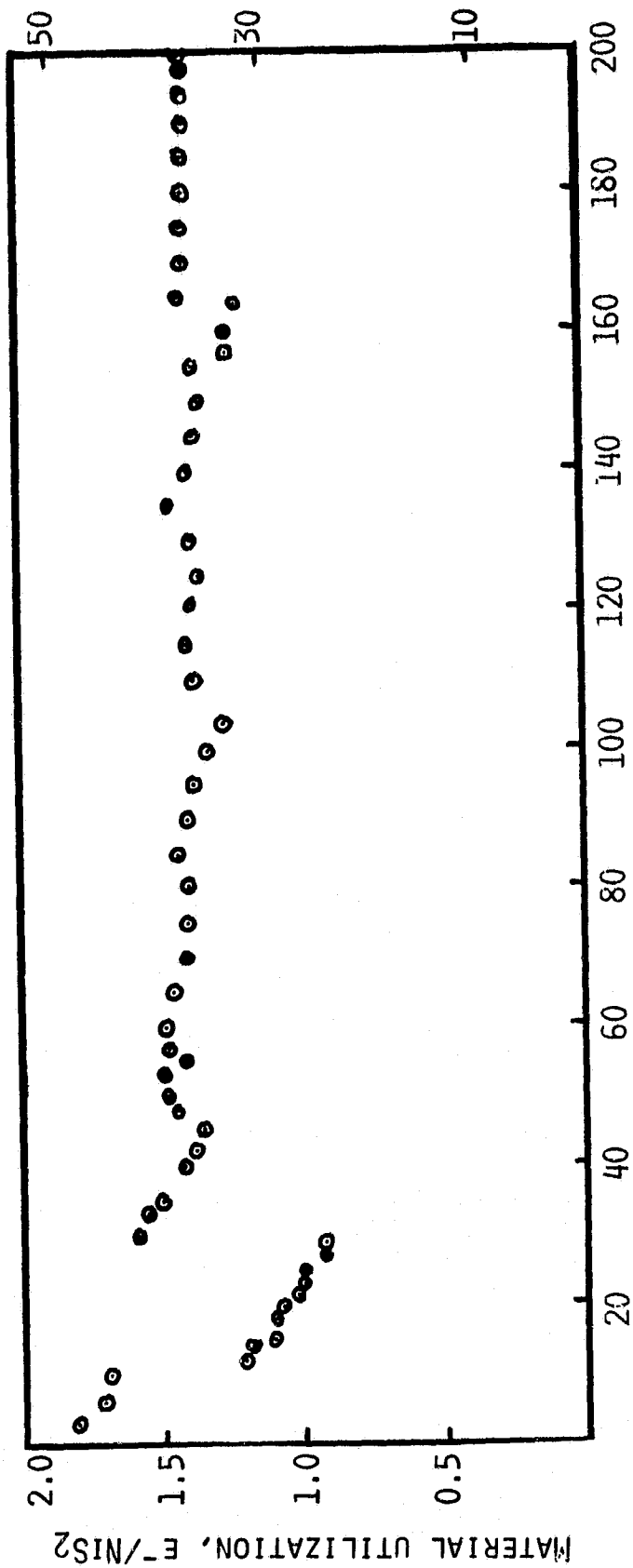

Fig. 38. Utilization versus cycle number in Na/NiS_2 Cell No. 365-103. Voltage limits: 1.7-3.5V, except in cycles 10-27 in which the recharge limit is 3.0V. Current: cycles 1-4, id = ic = 2 mA/cm^2; cycles 5-24; id = ic = 4 mA/cm^2; cycles 25-46 id = ic = 8 mA/cm^2; cycles 47-200 id = 8 mA/cm^2, ic = 4 mA/cm^2.

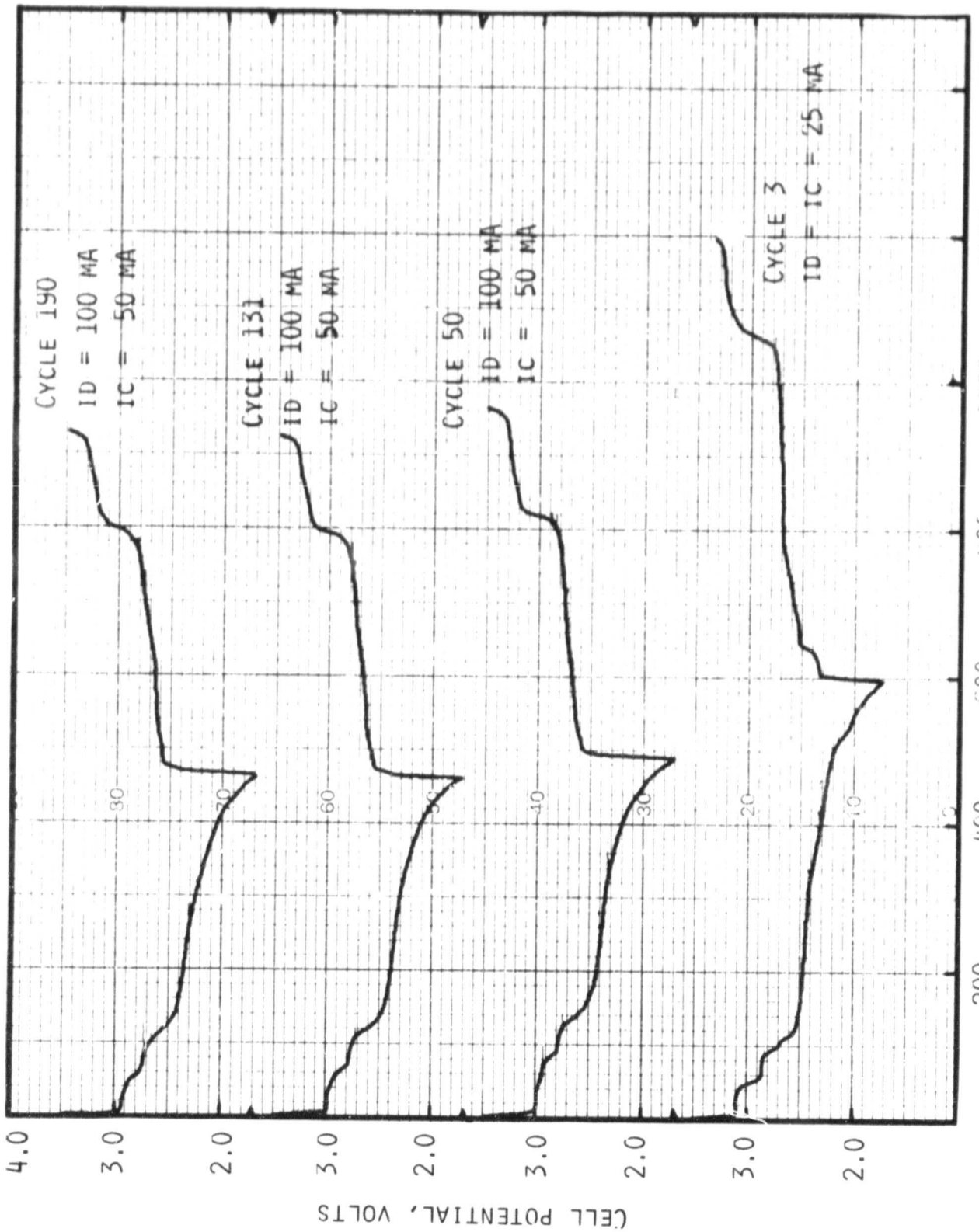

Fig. 39. Typical cycles of Cell No. 365-103.

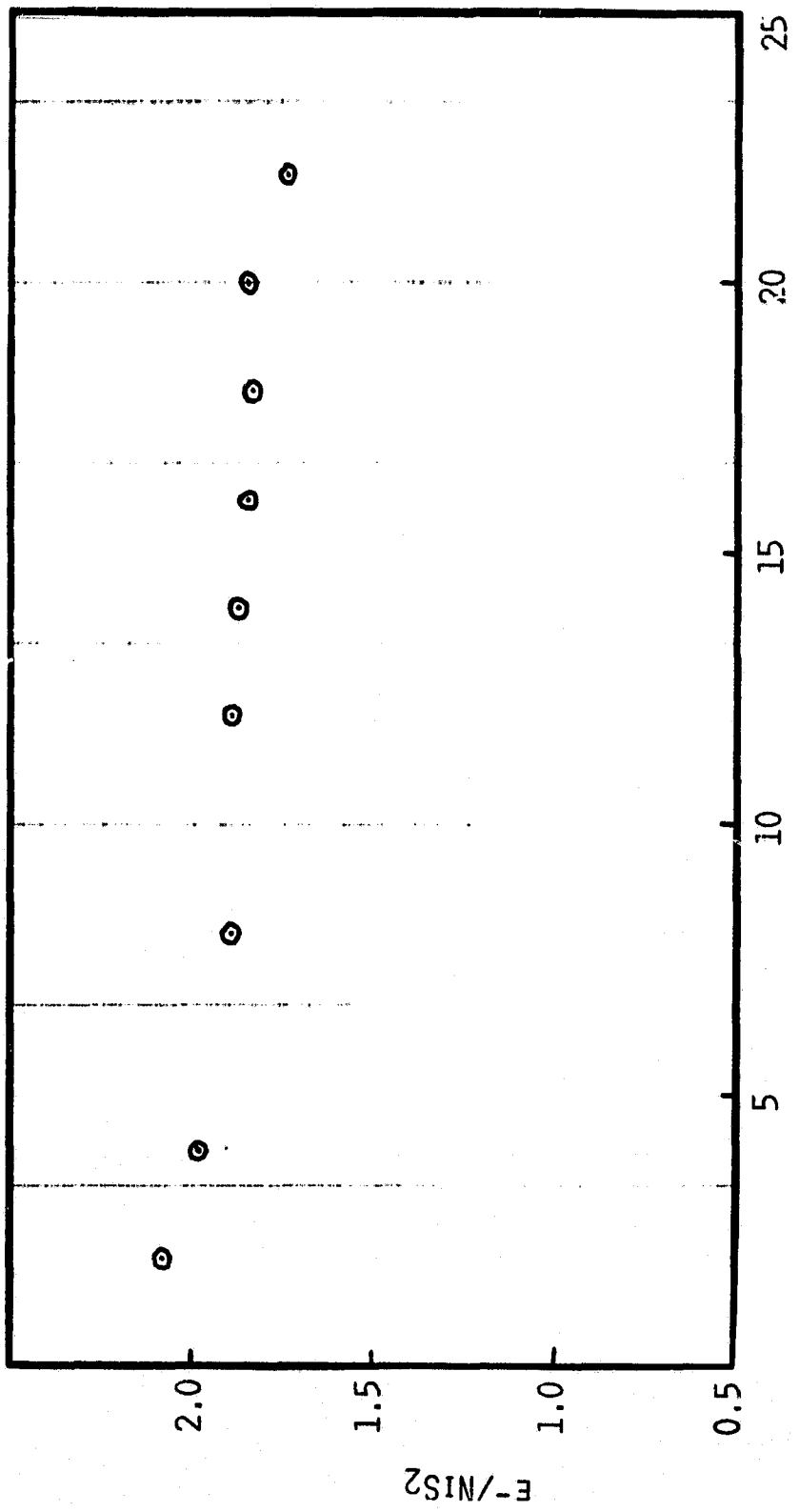

Fig. 40. Capacity versus current density in Cell No. 365-103. Temperature 190°C. The cell had completed 140 cycles. Each of the discharge was followed by a charge at 2 mA/cm^2.

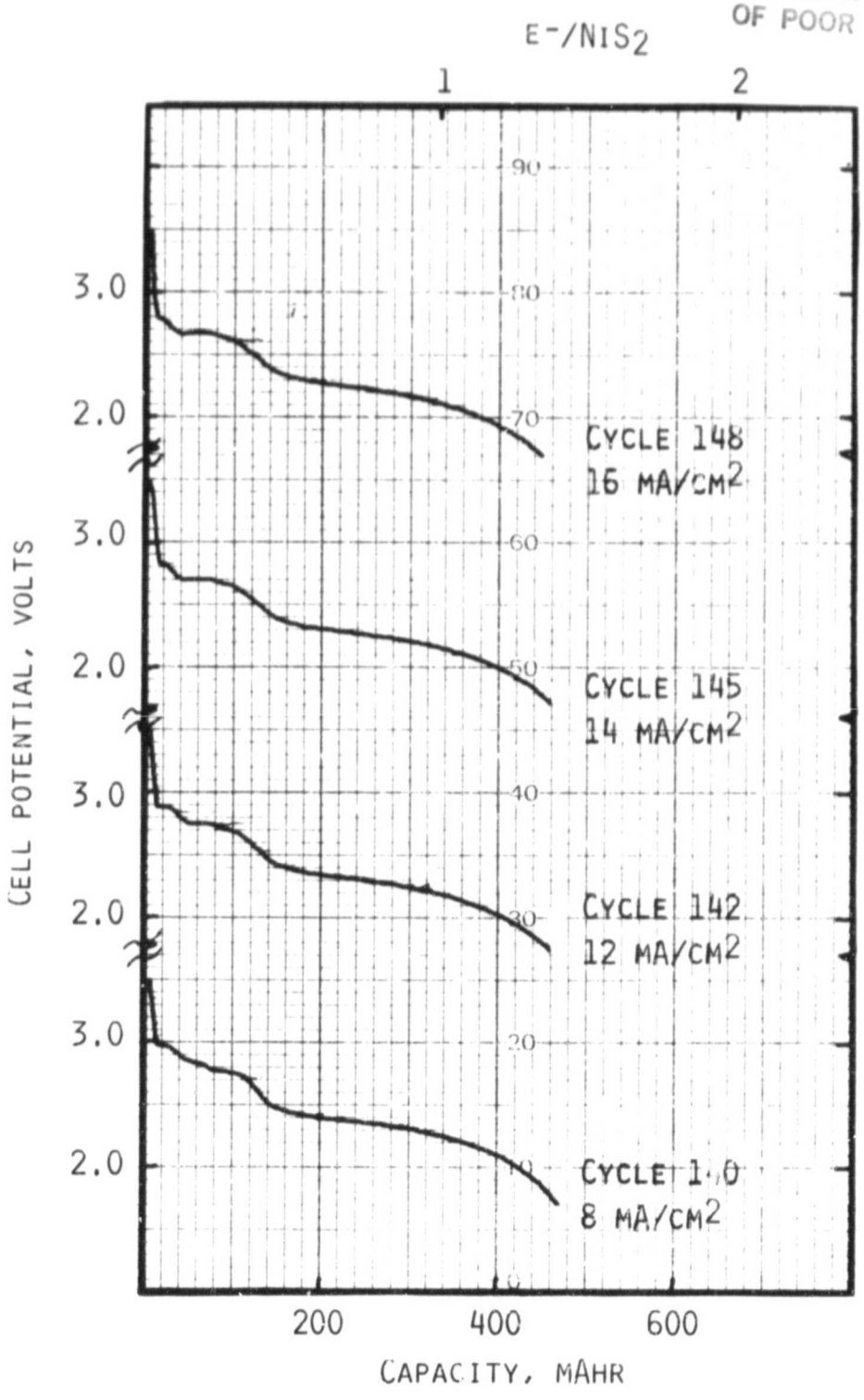

Fig. 41. Discharges of Cell No. 365-103 at various current densities.

4.2.3.2 Extended Cycling of A Na/NiS Cell

Cell No. 365-136 was constructed with 1.1 g NiS in contact with 4.7 g $NaAlCl_4$. The NiS was initially mixed with ~70 mg carbon black in an agate mortar and the mixture was then dispersed into a graphite-felt sheet which in turn was wrapped around the β''-Al_2O_3 tube. The cell exhibited an OCV of 2.9V at 190°C, the temperature at which the entire cycling was performed.

The cycling data are given in Figures 42, and 43. More than 100 cycles were demonstrated before the experiment was voluntarily terminated. The cell, cycling between the limits of 1.5 and 3.0V, and at the currents of 50 mA (4 mA/cm^2) for discharge and 25 mA for charge, exhibited an average capacity of ~400 mA-hr. The latter correspond to a utilization of ~1.3e^-/NiS. This is about 35% lower than found in the previous NiS cell (see Section 4.2.2.2), setup with a much smaller cathode loading capacity. It appears that further optimization of the cathode current collector structure would be necessary in order to obtain a significant portion of the theoretical 2e^-/NiS capacity at relatively high electrode loadings and current densities.

The specific energy achieved in the present cell, based on the weights of NiS, Na and $NaAlCl_4$, and a mid-discharge voltage of 1.9V is ~125 W-hr/Kg. Obviously, this specific energy is less than that in Na/NiS_2 cells, in which an experimental value of ~200 W-hr/Kg is possible.

4.2.4 Effects of Overdischarge and Overcharge on the Performance of NiS and NiS_2 Cells

4.2.4.1 Overdischarge

Sodium cells utilizing $NaAlCl_4$ possess a remarkable overdischarge safety mechanism. When the cell is discharged down to ~1.6V versus Na^+/Na, a reversible process involving the reduction of the electrolyte occurs.

$$NaAlCl_4 + 3Na^+ + 3e^- \rightarrow Al + 4NaCl \qquad [31]$$

We have found that these cells can be overdischarged for extended periods of time without any apparent effect on their subsequent cycle performance. In fact, the capacity corresponding to the overdischarge process can also be harnessed practically, thus increasing the energy densities of cells which contain electrolyte in excess of the theoretical minimum. The cycle of a Na/NiS_2 cell, shown in Figure 44, illustrates this chemistry.

We have already seen the effect of recharge voltage limits on the NiS_2 cell capacity. Obviously, recharge voltage limits up to 3.5V have no deleterious effects on the performance of the cell.

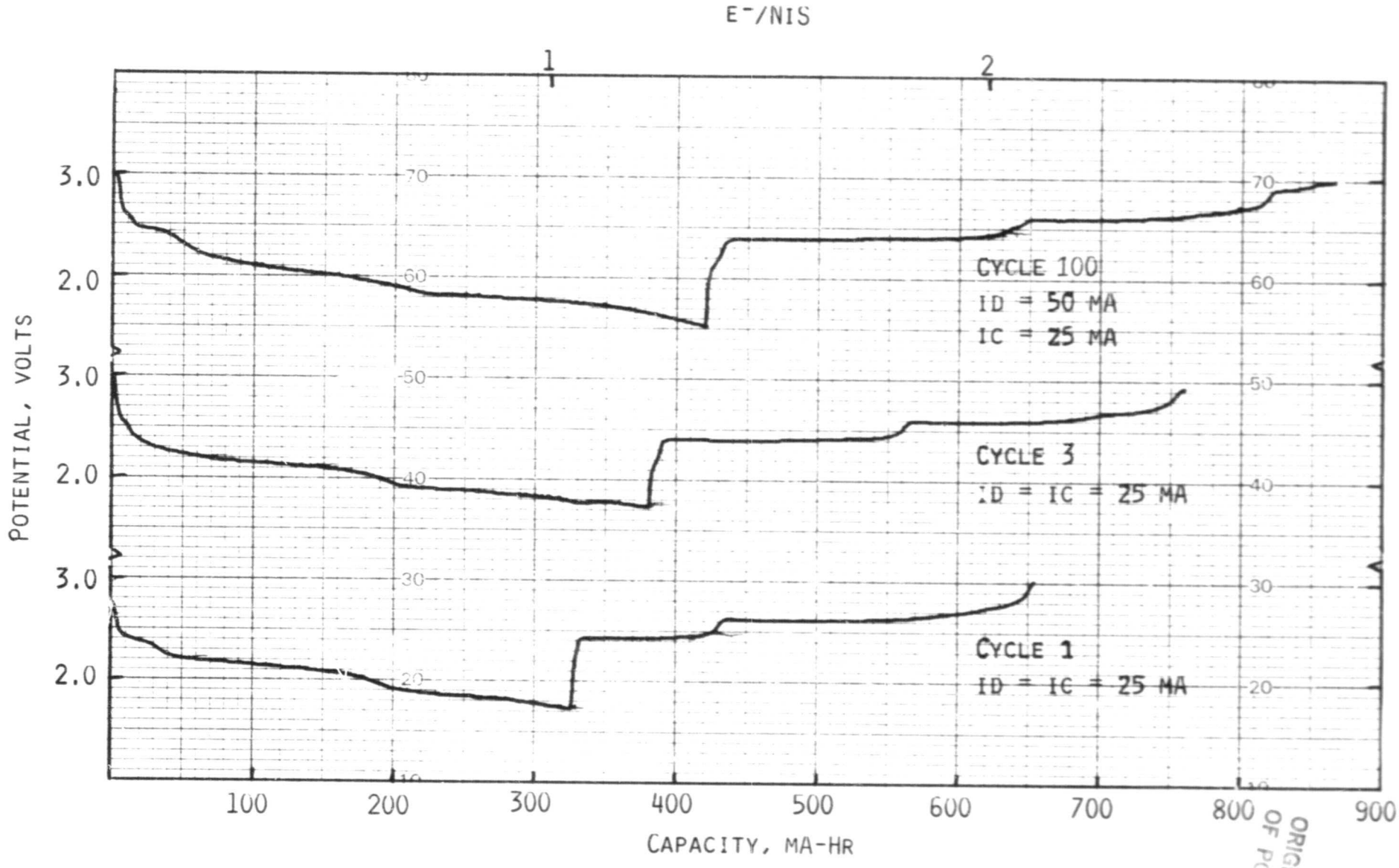

Fig. 42. Typical cycles of Na/NiS Cell No. 365-136.

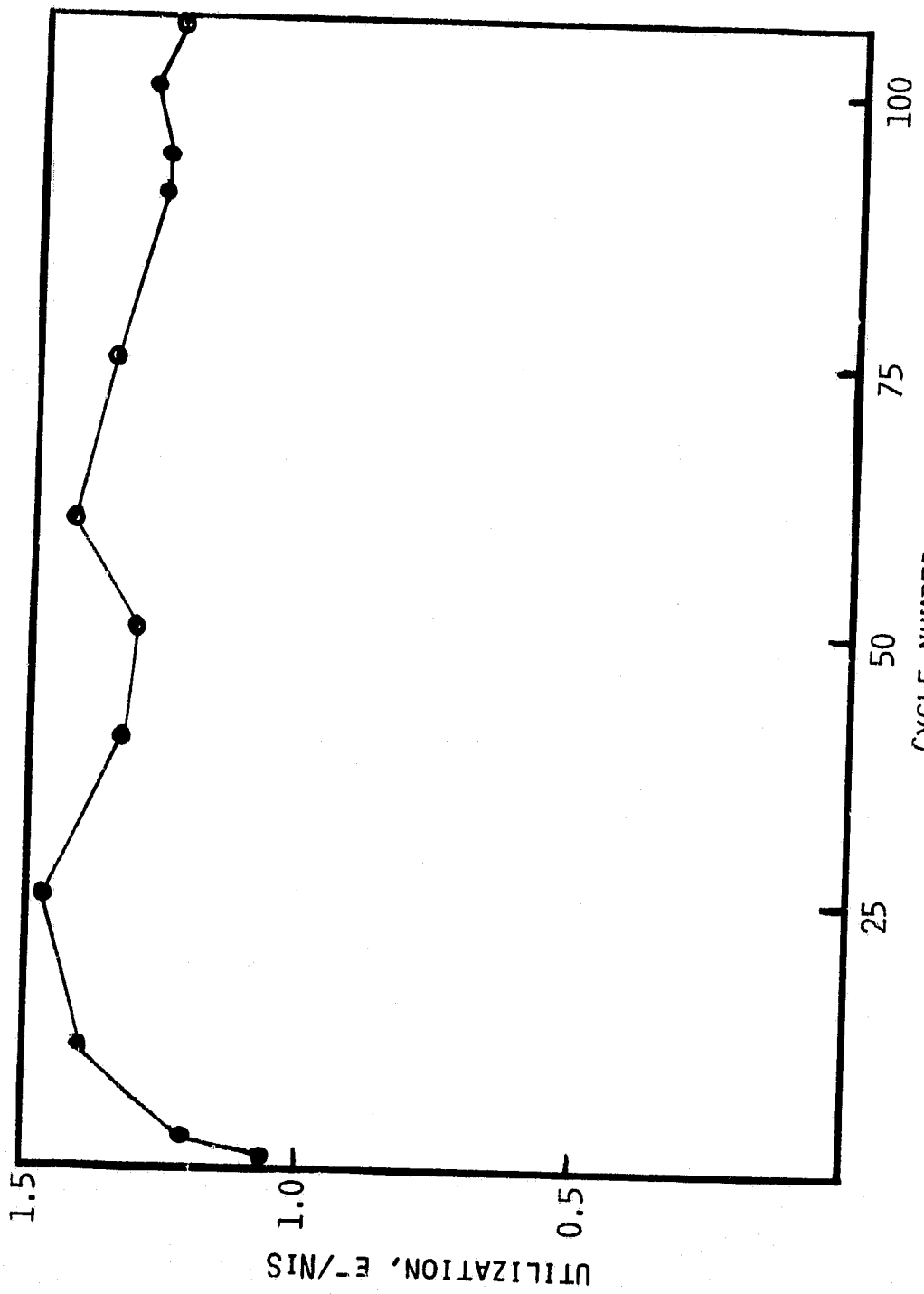

Fig. 43. Utilization versus cycle number in the Na/NiS Cell No. 365-136. Temperature 190°C.

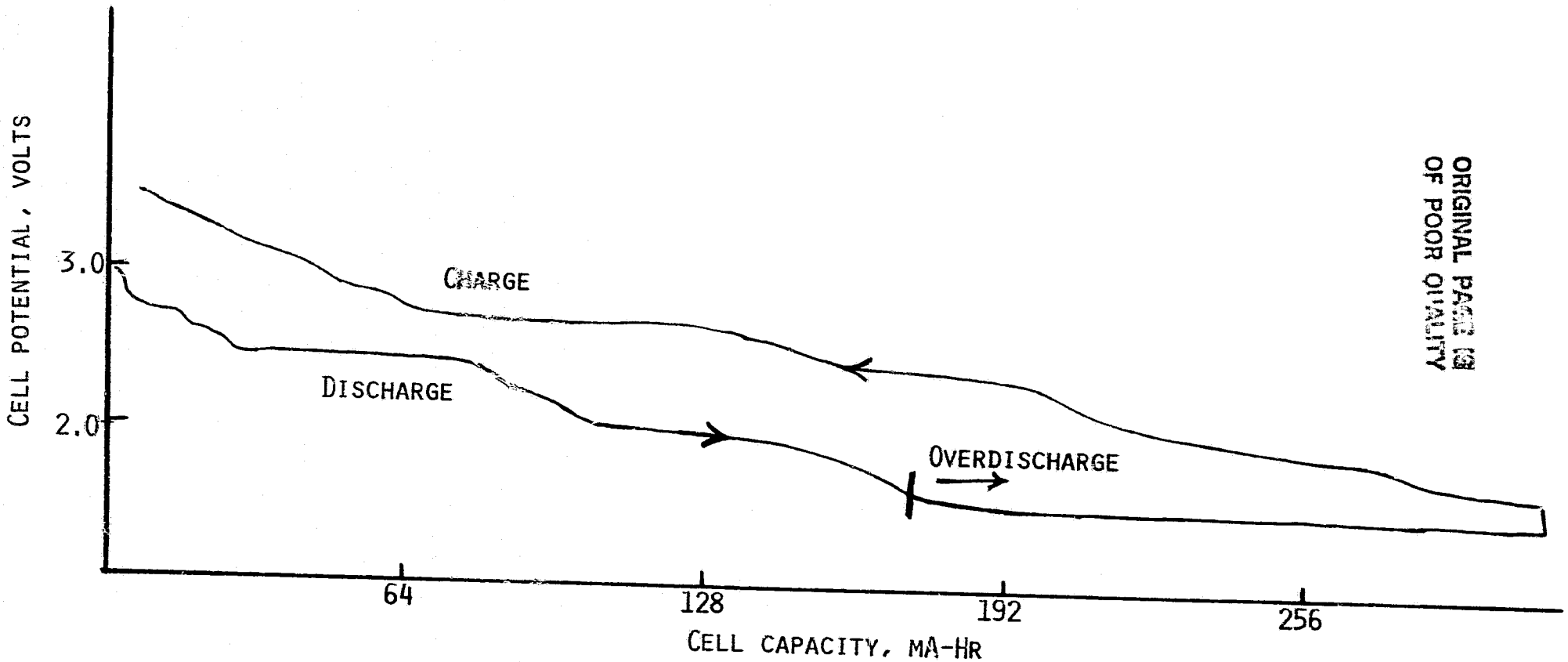

Fig. 44. A galvanostatic cycling curve including a substantial overdischarge in a $Na/NaAlCl_4$, NiS_2 cell at 165°C.

• Overcharge: In one experiment a Na/NiS_2 cell was repeatedly overcharged to a potential of 4.0V with no detrimental effects on its subsequent cycle performance. The overcharge between 3.5 and 4.0V occurred in a sloping potential region with the associated capacity showing some variations from cycle to cycle. When the recharge potential limit was lowered to 3.5V, after the overcharge cycles, the cell resumed cycling with capacity and voltage characteristics typical of those which were never overcharged.

The most likely reaction at the cathode during overcharge to 4.0V is

$$2AlCl_4^- \rightarrow 2AlCl_3 + Cl_2 + 2e^- \quad [32]$$

The Cl_2 would dissolve in the electrolyte, or it would react with the cathode material. Another possible reaction during overcharge is the oxidation of NiS_2 to form S and $NiCl_2$.

In discharges following an overcharge to 4.0V a fraction of the capacity appeared at a potential of ~3.4V. This is likely associated with the reduction of Cl_2 dissolved in the electrolyte.

An overcharge to 4.5V also proceeds with a sloping potential profile similar to that seen in the region between 3.5 and 4.0V. The OCV of cell after the charge to 4.5V was 3.8V indicating Cl_2 in solution. Again no detrimental effect of any sort on cell performance was observed.

In practical cells which would contain some Ni powder as an additive in the cathode, the Cl_2 would react with the Ni forming $NiCl_2$ which can be reduced during discharge.

Based on presently available data it can be concluded that the Na/NiS_x cells utilizing $NaAlCl_4$ possess excellent built-in overdischarge and overcharge protection mechanisms due to reversible chemical processes in addition to those associated with the redox reactions of the sulfides.

4.2.5 Prototype Cell Construction and Testing

A large NiS_2 cell, No. 365-128, having approximately 4 A-hr nominal capacity was constructed in the inside-out configuration. Except for its larger size, the cell is identical to the inside-out cell, No. 365-75, discussed earlier, and shown schematically in Figure 22. The 'NiS_2 plus Ni powder' mix was deposited on layers of graphite felt discs vertically stacked inside the β''-Al_2O_3 tube. The latter is the standard tube we have been using in all our Na cell experiments; Ceramatec Cat. No. CT16A, 16 mm OD, 13 mm ID and 20 cm length.

The cell utilized 8.1 g NiS_2, 1.62 g Ni and 29 g $NaAlCl_4$. The NiS_2 to $NaAlCl_4$ mole ratio was 1:2.3. The cathode mix and the graphite felt when

C-2

placed inside the $\beta"$-Al_2O_3 tube had a height of ~10 cm. The surface area of the $\beta"$-Al_2O_3 tube facing the circumference of the cylindrical cathode structure was ~40 cm^2. A vitreous carbon rod extending the full inside length of the $\beta"$-Al_2O_3 tube served as the cathode lead.

The cell was cycled at 190°C. Initially, the currents were kept low. The first four cycles were performed at 100 mA or a current density 2.5 mA/cm^2. In cycles beginning with the 9th discharge, the discharge current was changed to 300 mA or 7.5 mA/cm^2 and the charge current to 3.75 mA/cm^2. The voltage limits were 1.5 and 3.5 volts. The cell was cycled over 75 times. A few cycles are given in Figure 45. The highest capacity of the cell was 3.7 A-hr, corresponding to a NiS_2 utilization of ~$2e^-$ /NiS_2. The latter performance was realized rather earlier in the cycling, at a current density of 4 mA/cm^2. A plot of cell capacity versus cycle number is given in Figure 46. Continued cycling of the cell led to a gradual loss in capacity. The major cause of this capacity loss appeared to be a relatively high cell resistance. The initial cell resistance at the operating temperature of 190°C was ~1.1Ω. It seems that significant improvements will have to be made in current collector designs in order to achieve full practical potentials for the system. An examination of the data in Figure 45 indicates that very little of the capacity involved in the 2.0V plateau has been realized.

The specific energy achieved in Cell No. 365-128, based on the observed capacity of 3.7 A-hr and a mid-discharge voltage of 2.3V, is 190 Whr/Kg. Only the weights of the $\beta"$-Al_2O_3 and the can are excluded in this calculation.

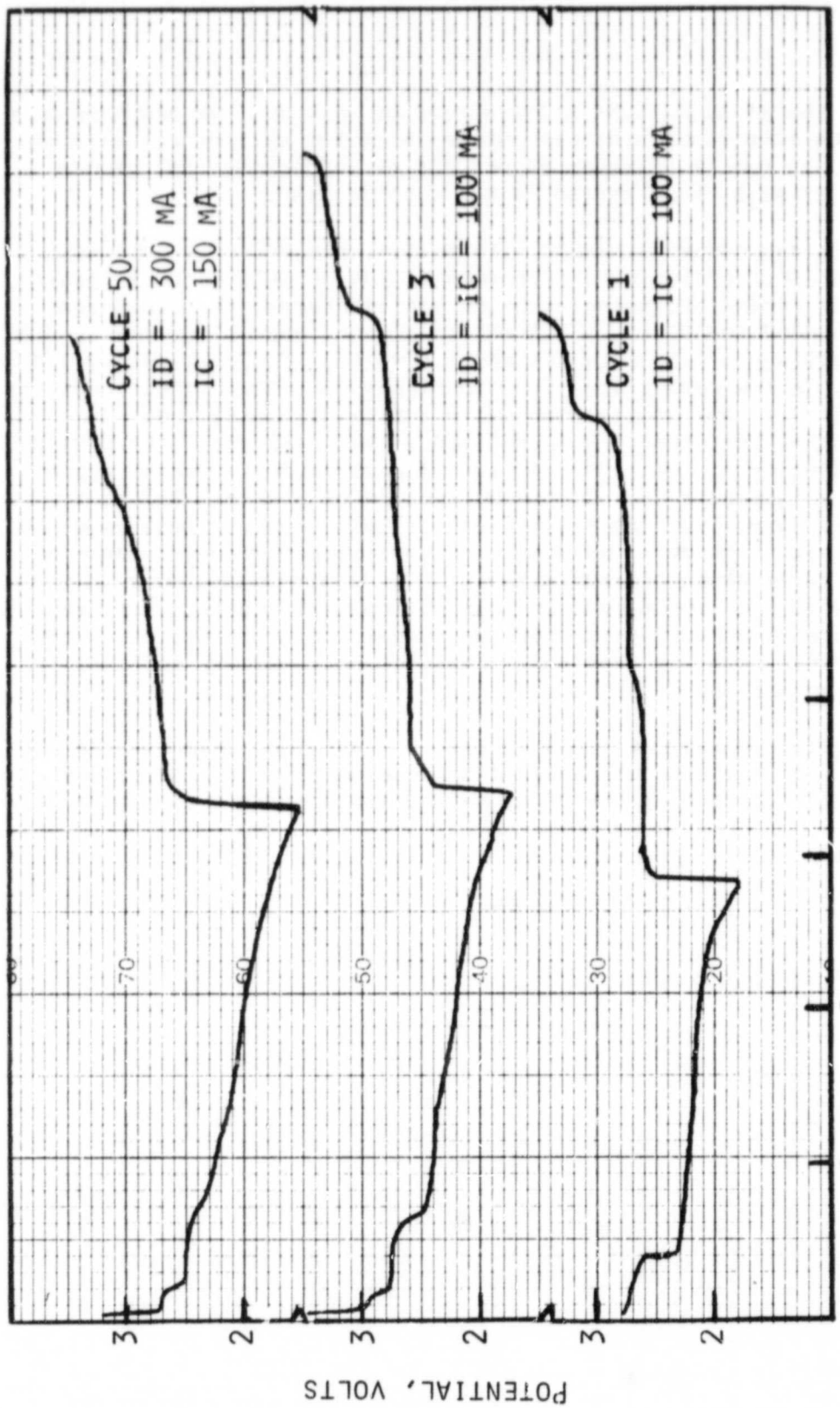

Fig. 45. Some cycles of prototype Cell No. 365-128.

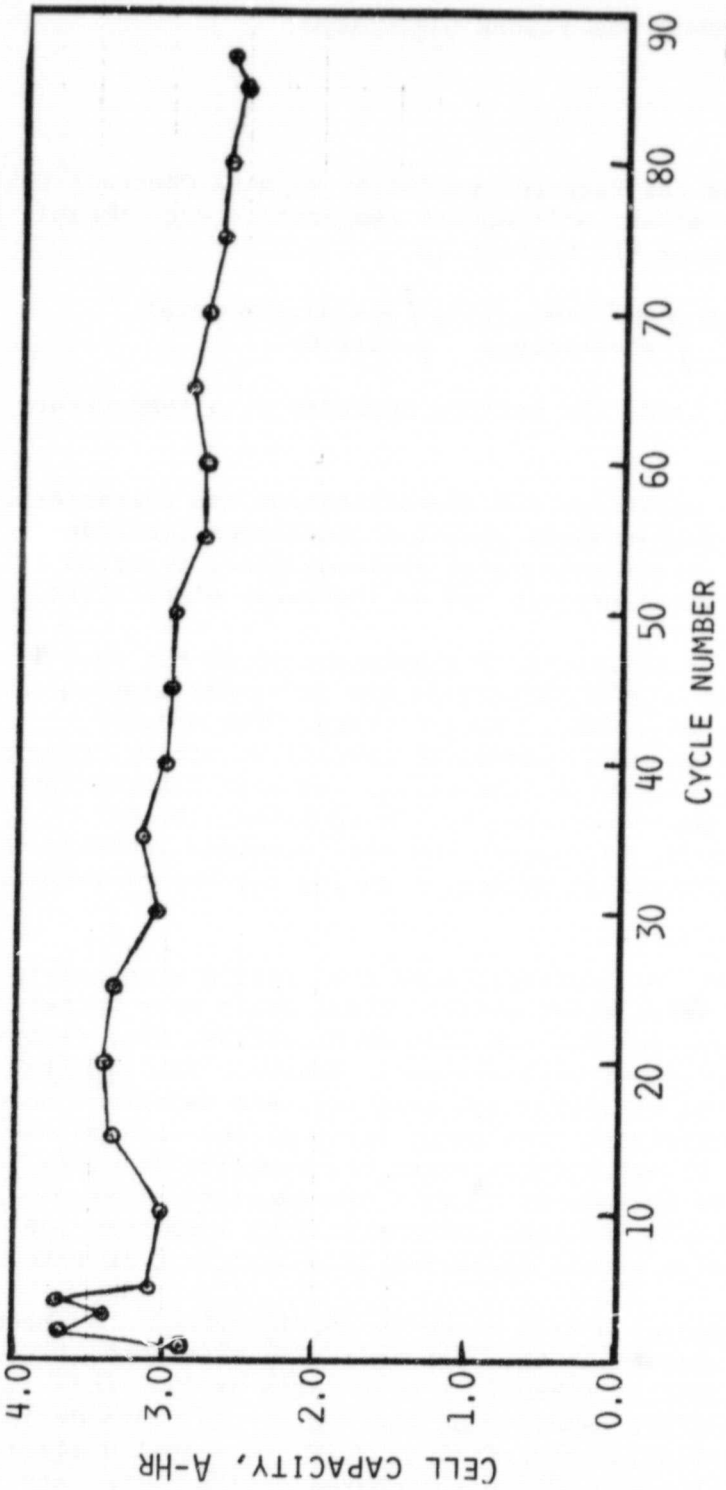

Fig. 46. Cell capacity versus cycle number in Cell No. 365-128.

5.0 SUMMARY AND FUTURE DIRECTIONS

This report summarizes the research performed on NASA Contract NAS3-21726, dealing with the development of moderate temperature rechargeable Na batteries. The configuration of the battery is

$$\text{Liquid Na} \,/\, \beta''\text{-}Al_2O_3 \,/\, \begin{matrix}Na^+\text{-containing} \\ \text{electrolyte}\end{matrix} \,/\, \begin{matrix}\text{Transition metal} \\ \text{sulfide}\end{matrix}$$

Depending on the electrolyte used, the battery operates at a temperature in the range of 130-200°C.

A major aspect of the work involved identification and characterization of high energy density rechargeable positive electrodes (cathodes). Na^+- intercalating, layered, transition metal chalcogenides, typified by VS_2, have been studied in both an organic and an inorganic electrolyte.

The organic electrolyte consisted of a solution of IM NaI in triglyme. Cells were operated at ~130°C, utilizing the Na^+-intercalating cathodes, VS_2, TiS_2, $Cr_{0.5}V_{0.5}S_2$, NbS_2, $TiSe_2$ or VSe_2. The organic electrolyte has been identified with inadequate thermal stability, causing restrictions on long term operations of the cells, and with limited rate capabilities because of its poor conductivity. In addition, the Na^+-intercalation reaction at 130°C, in most of the chalcogenides investigated, results in nucleation of irreversible phases, reducing the energy densities of the cells.

In order to circumvent the limitations of the organic electrolyte, we have used molten $NaAlCl_4$ as an alternative. These cells were operated at 165-190°C. We have discovered that the layered disulfide, VS_2, reacts with $NaAlCl_4$ during early stages of cell cycling. However, the <u>in situ</u> formed VS_xCl_y cathode material exhibits high capacity, and excellent rate and rechargeability characteristics. The composition of the cathode material approximates VS_2Cl. It exhibits a reversible capacity of ~2.8e^-/vanadium and a mid-discharge voltage of ~2.6V. The excellent reversibility of the positive electrode has been demonstrated by more than 100 deep discharge/charge cycles in a cell operating at about the C/10 rate.

A simple method to produce a high capacity VS_xCl_y cathode has been developed. It consists of assembling the cell initially with a positive electrode composed of VCl_3 and S, taken in a mole ratio of 1:2, and $NaAlCl_4$. The theoretical specific capacity of the "VCl_3 + 2S" cathode is 4e^-/vanadium, and the mid-discharge potential is 2.6V. One cell utilizing this electrode has exceeded 300 deep discharge/charge cycles. Its rate capability compares with that of the <u>in situ</u> formed VS_xCl_y cathode.

The non-Na^+-intercalating nickel sulfides, NiS_2 and NiS, have been identified as highly reversible positive electrodes in molten $NaAlCl_4$. These cells were operated at ~190°C. The cathode reactions involve a displacement process, resulting in Na_2S and Ni or a lower nickel sulfide as the products. The theoretical capacity of NiS_2 is $4e^-$/Ni and that of NiS, $2e^-$/Ni. The mid-discharge potential of the Na/NiS_2 cell is 2.4V and that of the Na/NiS cell 2.1V. A Na/NiS_2 cell, cycling at the C/5 rate, has exceeded 500 deep discharge/charge cycles. The average NiS_2 utilization in this cell was ~$2.5e^-$/Ni.

Reversibility of the NiS cathode has been demonstrated by more than 100 deep discharge/charge cycles in a Na/NiS cell.

A prototype Na/NiS_2 cell having a nominal capacity of 4 A-hr has been constructed and tested at 190°C. This cell was repeatedly discharged and charged more than 80 times, before being voluntarily terminated due to insufficient time left in the contract. Cathode structure improvement has been identified as a key item for further development of the Na/NiS_2 battery.

Quasi theoretical specific energies of moderate temperature Na cells utilizing the four cathodes, VS_xCl_y, "VCl_3 + 2S", NiS and NiS_2, are compared in Table 16. Specific energies realized to date are those shown in the last column in Table 16. In practical cells it should be possible to achieve 25-33% of these specific energies. Thus, long cycle life Na batteries based on either the "VCl_3 + 2S" or the NiS_2 cathode should deliver 100-150 Whr/Kg. Major developments required are in areas of cathode structure, and cell and battery hardware.

Table 16

Energy Densities of Moderate Temperature Sodium Cells

Cathode	Capacity, e^-/metal	Mid-Discharge Voltage	Specific Energy (W-hr/Kg) Excluding Electrolyte	Specific Energy (W-hr/Kg) Including* Electrolyte
VS_xCl_y	2.8	2.6	780	375
"VCl_3 + 2S"	4.0	2.6	890	395
	3.0		720	358
NiS_2	3.0	2.4	1005	397
NiS	1.75	2.1	751	331

*Based on 1 mole of electrolyte per each mole of Na_2S, according to: $NaAlCl_4 + Na_2S \rightarrow NaAlSCl_2 + 2NaCl$. This is the actual specific energy possible in the $NaAlCl_4$ medium.

6.0 REFERENCES

1. R. A. Harlow, Report on "Sodium-Sulfur Battery Development", DOE Contract No. DE-AM02-79-CH10012, October 1980.

2. K. M. Abraham, Solid State Ionics, 7, 199 (1982).

3. K. M. Abraham, L. Pitts and R. Schiff, J. Electrochem. Soc., 127, 2545 (1980).

4. K. M. Abraham and L. Pitts, J. Electrochem. Soc., 128, 1060 (1981).

5. K. M. Abraham and L. Pitts, J. Electrochem. Soc., 128, 2574 (1981).

6. R. Morassi, G. Mamantov and J. Q. Chambers, J. Electrochem. Soc., 123, 1128 (1976).

7. R. R. Chianelli and M. B. Dines, Inorg. Chem., 17, 2759 (1978).

8. A. J. Jacobson, R. R. Chianelli, S. M. Rich and M. S. Whittingham, Mat. Res. Bull., 14, 1437 (1979).

9. V. H. Schafer and W. Beckman, Z. Anorg. Allg. Chem., 347, 225 (1966).

10. M. Nakano-Onoda and M. Nakahira, J. Solid State Chem., 30, 283 (1979).

11. R. W. Berg, S. Von Winbush and N. J. Bjerrum, Inorg. Chem., 19, 2688 (1980).

12. M. Armand, L. Coic, J. Rouxel and J. Portier, Mat. Res. Bull., 13, 221 (1978).

13. "Comprehensive Inorganic Chemistry", Vol. 3, J. C. Bailar, Jr. et al. eds., Pergamon Press, NY (1973) p. 491.

14. A. J. Jacobson, R. R. Chianelli, S. M. Rich and M. S. Whittingham, Mater. Res. Bull., 14, 1437 (1979).

15. S. K. Preto, Z. Tomczuk, S. Winbush and M. F. Roche, J. Electrochem. Soc., 130, 264 (1983).

16. Z. Tomczuk, L. Redey and D. Vissers, J. Electrochem. Soc., 130, 1074 (1983).

17. S. M. Smitsyna and N. A. Bukhteoeva, Russian J. Inorg. Chem., 20, 1267 (1975).

APPENDIX

Solid State Ionics 7 (1982) 199–212
North-Holland Publishing Company

REVIEW

INTERCALATION POSITIVE ELECTRODES FOR RECHARGEABLE SODIUM CELLS

K.M. ABRAHAM
EIC Laboratories, Inc., 67 Chapel Street, Newton, Massachusetts 02158, USA

Received 13 September 1982

ABSTRACT

This paper summarizes studies of intercalation compounds as positive electrodes for rechargeable Na cells. The layered transition metal dichalcogenides have received the greatest attention to date. The basic and applied research aspects of Na intercalation positive electrode chemistry are in their early stages, offering many opportunities for future studies. Some directions for future research are indicated.

1. INTRODUCTION

Rechargeable batteries with Li or Na negative electrodes (anodes), because of their potentially high energy densities, have been actively pursued in recent times for applications such as electric vehicles, electrical load-levelling and space modules. Some of the popular systems which have been under development are: the ambient temperature rechargeable Li batteries utilizing organic electrolytes (1); the high temperature rechargeable Li batteries with Li-Al alloy anodes and inorganic molten salt electrolytes (2); and, the moderate to high temperature rechargeable Na batteries with liquid Na anodes utilizing a Na^+ permeable solid electrolyte such as Na-β-Al_2O_3 or Na-β"-Al_2O_3 (3-7). In all cases an important aspect of the battery development concerns the positive electrodes (cathodes) (8,9).

2. INTERCALATION COMPOUNDS AS BATTERY CATHODES

Highly reversible cathodes based on compounds undergoing the intercalation reaction have been characterized for both the ambient and high temperature Li batteries (8,9). Well known examples are the layered transition metal chalcogenides, in particular the disulfides and diselenides (8,9), and the transition metal oxides having the rutile- and perovskite-type three dimensional network structures (9,10).

An intercalation reaction involves the interstitial introduction of a guest species (Li^+ or Na^+ in the present context) into a host crystal lattice, as depicted in equation 1.

$$xA^+ + xe^- + MY_n \underset{\text{charge}}{\overset{\text{discharge}}{\rightleftharpoons}} A_xMY_n \qquad (1)$$

An ideal intercalation reaction, by definition involving little or no structural change of the host, is highly reversible because similar transition states are readily achieved for both the forward and backward reactions, leading to close compliance with the thermodynamic principle of microscopic reversibility. In actual reactions, the bonding within the host lattice may be slightly perturbed, a slight expansion of the host lattice may occur, and crystallographic phase changes of the host compound may take place. Depending upon the extent of the structural perturbations, the reaction may be reversible, partially reversible or irreversible.

The following basic requirements have been proposed for intercalation cathodes (10).

i) A large free energy of reaction, ΔG, affording a high cell voltage.

ii) A wide compositional range, i.e., x in equation 1, resulting in high cell capacities.

iii) High diffusivity of the guest species (Na^+ or Li^+) in the host, allowing high power densities.

iv) Good electronic conductivity over a wide range of x.

v) Minimal structural changes with the degree of intercalation, resulting in a reversible reaction and long cycle life.

0 167-2738/82/0000 0000/$ 02.75

Some of the properties of Li and Na intercalates of TiS_2 and TaS_2, listed in Table I, illustrate the compliance of the layered metal chalcogenides with many of these requirements, however, certain structural aspects of the

Table I. Some Properties of A_xTiS_2 and A_xTaS_2; A = Li or Na (13).

Compound	ΔG (kcal/mole)*	Composition Range, x	Maximum D (cm^2/S)**
Li_xTiS_2	-57.4	0<x<1	$\sim 6\times10^{-9}$
Li_xTaS_2	-50.5	0<x<1	$\sim 3\times10^{-8}$
Na_xTiS_2	-48.4	0<x<1	$\sim 10^{-9}$
Na_xTaS_2	-42.9	0<x<1	$\sim 3\times10^{-8}$

*For x=1 in A_xMS_2.
**Diffusivity at or near room temperature.

host compound and the relative sizes of Li^+ and Na^+ ions distinguish the choice of intercalation cathodes for Li and Na batteries.

A structural aspect of the cathode material is concerned with whether it is of the layered or of the three dimensional network type. The layered chalcogenides with Van der Waals gaps, the well known examples being the dichalcogenides typified by TiS_2, have considerable structural flexibility. This is mainly due to the two dimensional characteristics of the layers which permit the insertion of the relatively large Na^+ ($rNa^+ = 0.98\AA$) as well as the smaller Li^+ ($rLi^+ = 0.71\AA$) with similar ease. A larger lattice expansion does occur in Na_xMY_2 than in Li_xMY_2. In many compounds comprised of a three dimensional network oxide lattice, the faces of the cavities usually have the right dimensions to permit diffusion of Li^+ but not of larger ions such as Na^+ and K^+. Thus, intercalation of Na may be difficult in these compounds or the reaction may involve large structural perturbations such as partial or complete breakage of the M-O bond. The result is poor capacity and/or irreversibility. A special case among the oxides, however, is MoO_3, which has a layered structure (10). It should be noted that rigid lattice network compounds based on sulfides or selenides may exhibit geometric features more favorable for Na intercalation.

It is apparent that intercalation compounds which merit immediate consideration for Na battery applications are those having layered structures with Van der Waals gaps. The most prominent among these are the transition metal disulfides and they, indeed, have received the greatest attention to date.

3. STRUCTURAL ASPECTS OF Na_xMS_2 TERNARIES

A brief look into the structural aspects of Na_xMS_2 ternaries is useful in order to understand the electrochemical results. Three factors have been judged to be of importance in determining the co-ordination site of the intercalated alkali metal ion (11,12): the nature of the slabs of the layered host, the size of the alkali metal ion and the amount of intercalation.

Sodium being too large, it is difficult for it to enter the dichalcogenide lattice without an initial expansion of the Van der Waals gap. As this expansion must consume some energy, ~4 kcals/mole, sufficient Na must be incorporated before the intercalate can form (12). Thus a miscibility gap or phase region is expected at low Na values. This miscibility gap can be minimized by the formation of staged compounds, that is, where only every n^{th} layer is intercalated. Thus one expects to see a two phase region, a staged compound (or several), a two phase region, and then a compound in which every layer contains Na^+ ions. Another consequence of the initial expansion of the chalcogenide slabs is a sliding motion of the layers making it possible for the Na^+ to occupy different sites. Usually a trigonal antiprismatic (TAP) co-ordination is found for large values of intercalation and a trigonal prismatic (TP) co-ordination for low to intermediate values of sodium. The structural data on several sodium intercalated dichalcogonides shown in Table II illustrate this.

These structural changes may have several consequences on cathode applications in Na cells. The diffusivity of Na^+ has shown variations with its co-ordination (13). Thus, higher diffusivities have been measured in the TP than in the TAP phase. This may affect both the extent and rate of discharge. The appearance of many phases also requires the chalcogenide to undergo repeated structural changes during cell cycling, probably affecting both the utilization and reversibility of the cathode. Both of these effects have been seen experimentally (vide infra).

The use of a strictly stoichiometric chalcogenide is also important in electrode applications. In $M_{1+x}Y_2$, non-stoichiometric compounds, the excess metal cations reside in the Van der Waals gap. The excess metal will impede the diffusion of Na^+; they also link the slabs, negating to a large extent the advantage of having a two dimensional structure. This has been very nicely demonstrated in Li/TiS_2 cells (17).

4. Na CELLS WITH INTERCALATION CATHODES

Before reviewing the results, it is useful to examine some practical aspects of cell studies, in particular, cell and cathode fabrication.

Table II. Phase-Structure Relationship in Na Intercalates of Metal Chalcogenides

Chalcogenide	Transition Metal Site Symmetry in the Chalcogenide	Na_xMY_2, Compositions	Phase
TiS_2	O	$0.17 < x \leq 0.3$	2nd stage compound
		$0.38 < x \leq 0.72$	1st stage TP
		$0.79 < x \leq 1$	1st stage TAP
$TiSe_2$	O	$x < 0.32$	2nd stage compound
		$0.68 < x \leq 0.74$	1st stage TP
		$0.82 < x \leq 0.91$	1st stage TAP
ZrS_2	O	$x < 0.32$	2nd stage compound
		$0.64 < x \leq 1$	1st stage TAP
VS_2	O	$x < 0.3$	2nd stage compound
		$0.3 < x \leq 0.8$	1st stage TP
		$0.8 < x \leq 1$	1st stage TAP

O = Octahedral
TP = Trigonal prismatic
TAP = Trigonal antiprismatic or elongated O

4.1 Cell Configuration

Conceptually, it is possible, as in ambient temperature rechargeable Li batteries (1), to construct cells in which Na is in direct contact with a non-aqueous electrolyte with the cathode and anode separated by an electrically insulating separator. There has been one published cycling study by Newman and Klemann (14) using this type of cell with TiS_2 cathode and an electrolyte comprising sodium triethyl (N-pyrrolyl) borate in dioxolane. A potential problem with this type of cell is the high reactivity of Na with the organic solvent, leading to questions of Na electrode rechargeability and safety. In the absence of major breakthroughs, it appears that the major application of this cell configuration would be in basic studies of positive electrodes.

An alternative cell construction uses solid electrolytes such as β-Al_2O_3 or β''-Al_2O_3 to isolate the Na. The cell configuration is,

Liquid Na / β''-Al_2O_3 / Na^+-containing electrolyte / Metal chalcogenide

All of the work from the author's laboratory (3, 15-17), discussed in this account, has been carried out in this type of cell. Major concerns relate to the electrolyte. It is necessary to have an electrolyte which has good Na^+ conductivity, is thermally stable, is non-reactive with the chalcogenides at elevated temperatures and has a suitable electrochemical window. An organic electrolyte consisting of a 1 molar solution of NaI in 1,2-Bis(2-methoxyethoxy)ethane (triglyme), has been satisfactorily used in all our studies. The cells with this electrolyte were operated at ~130°C.

Another electrolyte we have used in some studies at 130°C with TiS_2 and TaS_2 is dimethylacetamide (DMAC)/NaI(1M) (18). This electrolyte, however, appeared less satisfactory.

More recently we have used molten $NaAlCl_4$ in cells operating between 165-200°C (3). We have found molten $NaAlCl_4$ to react with sulfides such as TiS_2 and VS_2. But, to our surprise, the resulting reaction products, MS_xCl_y, have exhibited much higher capacities, and excellent rechargeability and rate capabilities (see later).

Recently Zanini and co-workers reported (19,20) on studies of intercalation cathodes, also in a cell utilizing β''-Al_2O_3, without a liquid electrolyte. From a practical standpoint, it would be difficult to achieve acceptable rate capabilities in such cells at high cathode loadings. However, studies of intercalation reactions in the absence of liquid electrolytes are useful to ascertain the effects of solvents on electrode reactions.

4.2 Cathode Structure

An important practical aspect which is not often discussed in accounts of intercalation electrochemistry concerns electrode structure. Usually the electrode comprises a matrix of the chalcogenide powder bonded to a metallic grid with Teflon or other binders. During cathode cycling the chalcogenide crystallites undergo expansions and contractions. In most cases the binders do not have ideal elastic properties, so an initially optimized electrode structure changes even after the first discharge/charge cycle. A loss of particle-to-particle or particle-to-grid contact may occur, resulting in diminished material utilizations. The deleterious effects of electrode structure on utilization can often times be minimized by properly constraining the electrode in the cell, and using low-density filler additives such as carbon in the electrode. It should be noted that electronically conducting materials such as TiS_2 and VS_2, in principle, do not require a conductive additive; but, as we found in our studies of Li intercalation cathodes (21,22), better material utilization can be achieved in presence of carbon in the electrode. The carbon ensures electrical continuity and probably greater porosity.

4.3 Cathode Cycling Results

The transition metal dichalcogenides have received the greatest attention to date. The results with these materials will be reviewed first. Some data are available on two trichalcogenides, TiS_3 and MoS_3. We have evaluated $NiPS_3$ and the one dimensional chain-type compounds NbS_2Cl_2 and MoS_2Cl_2. These data are presented. Finally, we shall summarize the results of our recent cycling studies of transitional metal chalcogenides in molten $NaAlCl_4$.

4.3.1 Transition Metal Dichalcogenides

Among the numerous dichalcogenides, TiS_2, VS_2, $Cr_{0.5}V_{0.5}S_2$, NbS_2, TaS_2, VSe_2, $TiSe_2$ and $NbSe_2$ have been investigated to varying degrees.

TiS_2: The cycling behavior of TiS_2 has been evaluated at 25, 130 and 280°C. Newman and Klemann cycled (14) an ambient temperature TiS_2 cell with an electrolyte comprising sodium triethyl (N-pyrrolyl)borate in dioxolane and a solid sodium anode. At a discharge current density of 2.5 mA/cm^2, a capacity of 0.8e$^-$/TiS_2 has been obtained with a limiting cathode composition of $Na_{0.8}TiS_2$. The discharge is characterized by two voltage plateaus, one at ~1.9V and the other at ~1.5V. The former plateau spans the Na composition range x, in Na_xTiS_2, at $0<x\leq0.4$, and the latter at $0.4<x\leq0.8$. The two voltage plateaus correlate reasonably well with the first two phases in the Na_xTiS_2 ternary listed in Table II as well as the EMF-composition curve reported by Winn et al. (23). In continued cycling at ambient temperature, Newman et al. found a gradual loss in the capa-

city of the upper plateau so that after 8 cycles only ~5% of the upper plateau could be reproduced. The capacity of the lower plateau was maintained even after 16 cycles. Some typical cycles of this cell are shown in Figure 1.

Our discharge of a Na/β"-Al_2O_3/TiS_2 cell at 130°C gave a similar two step first discharge with a limiting capacity of $Na_{0.85}TiS_2$. The upper voltage plateau encompassed the Na range, $0<x\leq0.3$, and the lower, $0.3<x\leq0.85$. We too found that the capacity of the first phase gradually decreased with cycling. However, even after eight cycles about half of the capacity in the upper plateau was reversibly utilized along with all of the capacity in the lower plateau. Our data at 130°C indicated an average rechargeable capacity of $0.65e^-/TiS_2$ with a 1.7V mid-discharge, corresponding to a specific energy of 215 Whr/kg.

It appears from the data at 25 and 130°C that it is difficult to intercalate Na electrochemically into the TAP phase. This finding is in agreement with the observations of Whittingham et al. (24) who found that in the preparation of Na_xTiS_2 from TiS_2 and Na-naphthalide, even with a large excess of the latter reagent, the ternary with the maximum Na content was $Na_{0.8}TiS_2$. The lack of Na intercalation into the TAP phase could be attributed to the lower diffusivity of Na^+ in this phase. In the TAP phase, Na^+ has to pass through small tetrahedral co-ordination sites, whereas in the TP phase such sites are much larger, enabling better Na^+ diffusion.

The cycling of an Na/TiS_2 cell with a β"-Al_2O_3 solid electrolyte has also been investigated at temperatures between 230 and 280°C by Zanini and co-workers (19,20). In contrast to the results at 25 and 130°C, this cell was was found to be rechargeable for x between 0.0 and 0.95. The difference could be attributed to higher Na^+ diffusivities at higher temperatures, to the extremely low TiS_2 loading capacity employed in that study, or to the different phase regions observed at these higher temperatures. The Na composition ranges of the three plateaus at 280°C were observed at $0<x\leq0.2$, $0.2<x\leq0.69$ and $0.69<x\leq0.95$. It is interesting to note that Zanini et al. have not used a liquid electrolyte in the cathode compartment of their cell. It appears that at temperatures near 300°C, a higher specific energy, corresponding to ~337 Whr/kg is possible with TiS_2.

Very little data are available on the rate-capability of TiS_2 in Na cells. The relatively high sodium diffusivities (~10^{-9} cm^2/second at 27°C in Na_xTiS_2, $0.25<x\leq0.6$) suggest a potentially high rate capability at least up to x = 0.8. We, however, found better rechargeabilities in electrodes incorporating carbon (15).

VS_2: We have cycled VS_2 at 130°C (15). The Na/VS_2 cell had an open-circuit-voltage (OCV) of 2.30V. Its first discharge to a 1.0V cutoff yielded a capacity of $1e^-/VS_2$.

The discharge was characterized by three voltage regions spanning x in Na_xVS_2 at $0<x\leq0.28$, $0.28<x\leq0.85$ and $0.85<x\leq1.0$. The rechargeable capacity decreased with cycling, but much of this loss occurred in the 2nd discharge and seemed to involve mostly the capacity in the first plateau. An average capacity of $0.7e^-/VS_2$ was obtained in 40 cycles. Some typical cycles of the Na/VS_2 cell are shown in Figs. 2 and 3.

It is interesting that Na intercalation in VS_2 has been achieved up to the theoretical maximum. The three potential regions found in the first discharge of the Na/VS_2 cell correlate fairly well with the three phase regions of the Na_xVS_2 ternary depicted in Table II. Our X-ray diffraction data for a sample of electrochemically prepared $Na_{1.0}VS_2$ exhibited lattice parameters, a = 3.22 Å and c = 7.30 Å, identical to those reported by Wiegers for the hexagonal $Na_{1.0}VS_2$ isostructural with Li_xTiS_2 (25). It thus appears that the third phase in the electrochemical reaction is not a true TAP phase as in $NaTiS_2$ or $NaCrS_2$ but rather a hexagonal form with a higher c/a ratio. The activation energy for Na intercalation usually decreases with increasing c/a ratio. The c/a ratio in hexagonal $NaVS_2$ is 2.26 whereas that in the TAP $NaTiS_2$ is 1.9. It should be noted when $Na_{1.0}VS_2$ is prepared in Na-naphthalide, both the TAP (a = 3.54 Å and c = 19.74 Å) and the hexagonal (a = 3.22 Å and c = 7.30 Å) compounds are formed (17). Apparently electrochemistry discriminates between these structures.

Unlike TiS_2, where the limiting composition $Na_{0.8}TiS_2$ could be obtained both with and without carbon in the electrode, we could obtain a capacity of only ~$0.7e^-/VS_2$ with VS_2 electrodes having no carbon in them (15). Resistivity measurements of chemically prepared $Na_{0.8}VS_2$ and $Na_{1.0}VS_2$ indicated that this distinction might be due to increased resistivities of Na_xVS_2 with high Na contents.

The specific energy of the Na/VS_2 system with an average capacity of $0.7e^-/VS_2$ and a mid-discharge voltage of 1.8V is 258 Whr/kg.

$Cr_{0.5}V_{0.5}S_2$: This material was of interest because of its mixed metal composition, possibly leading to unusual structural and electrochemical properties. However, both structural and electrochemical data indicated (17) many similarities to TiS_2 and VS_2. Cycling results indicated a rechargeable capacity of $0.7e^-/Cr_{0.5}V_{0.5}S_2$ with a mid-discharge voltage of 1.9V, yielding a specific energy of 273 Whr/kg.

NbS_2: We cycled $Nb_{1.1}S_2$ at 130°C (15) and Zanini et al. obtained (20) cyclic voltammetric data at 320°C.

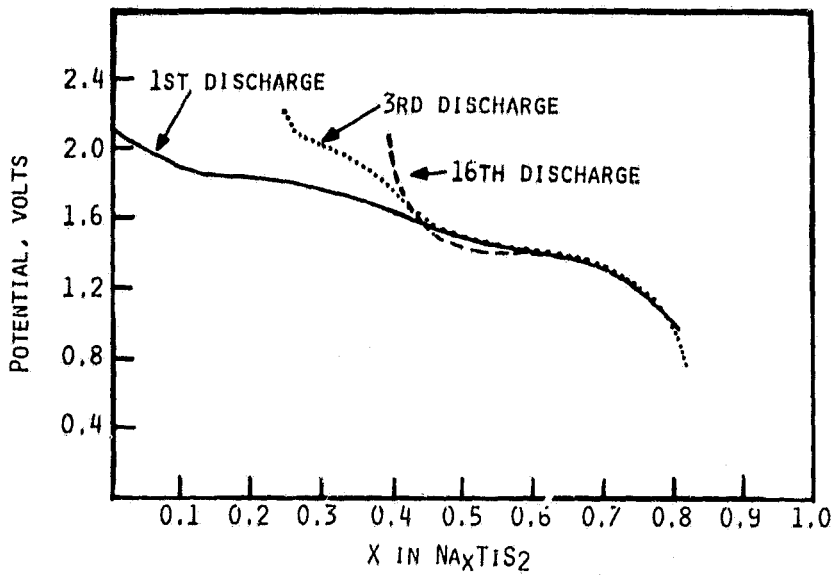

Fig. 1. Discharges of Na/organic electrolyte/TiS_2 cell at 25°C. From ref. 14.

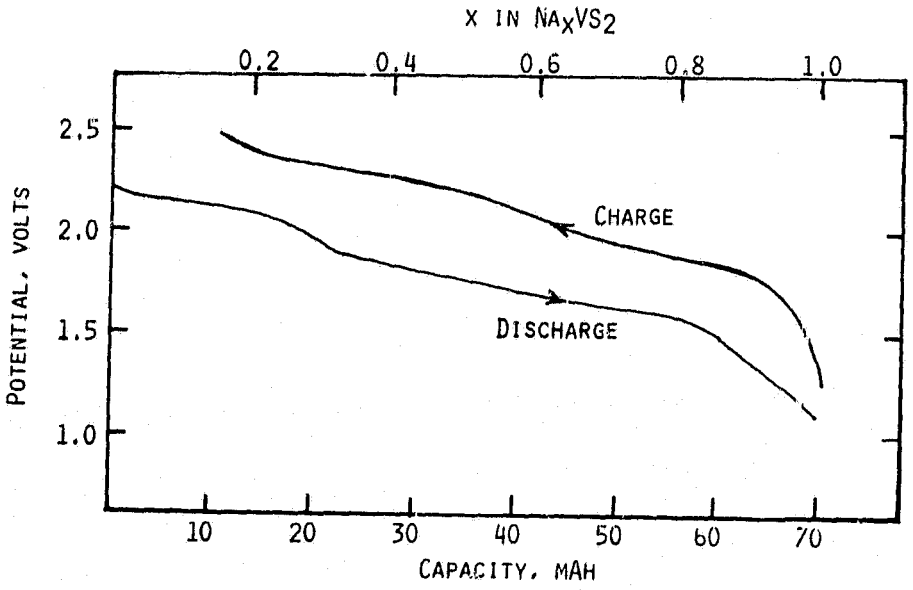

Fig. 2. The first cycle of a liquid Na/β"-Al_2O_3/triglyme, NaI/VS_2 cell at 130°C. From ref. 15.

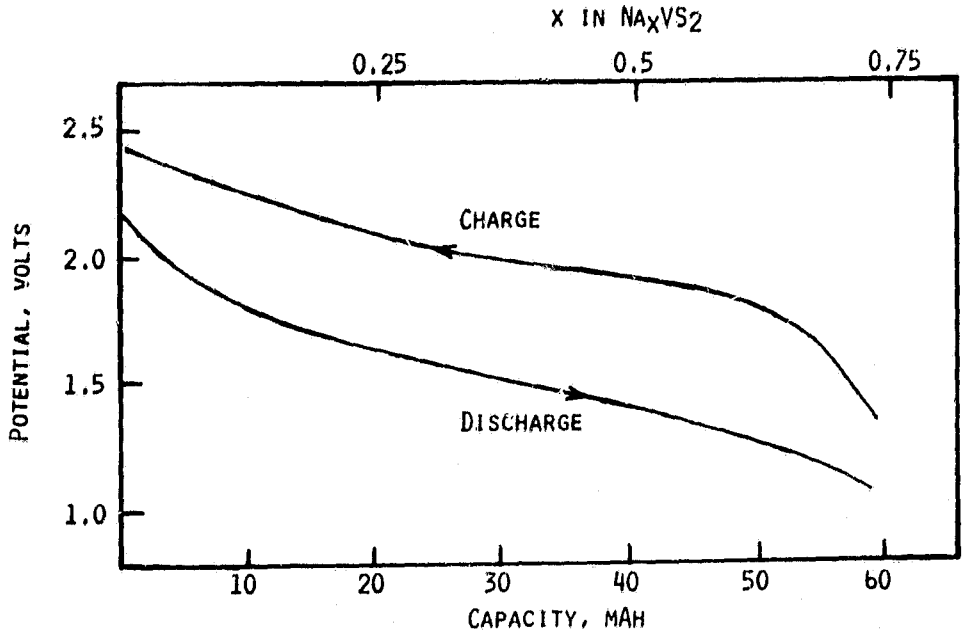

Fig. 3. The 22nd cycle of the same Na/VS_2 cell as in Fig. 2.

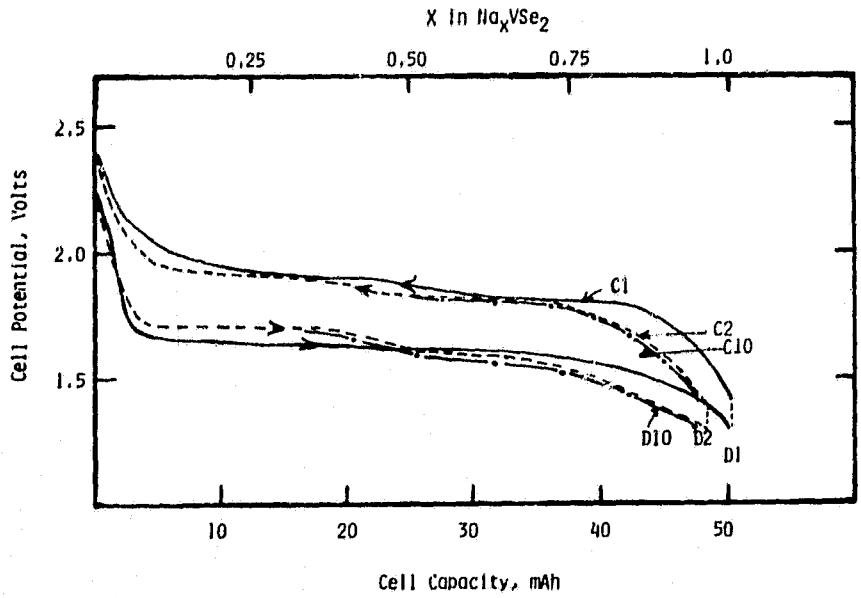

Fig. 4. Typical cycles of a liquid $Na/\beta''-Al_2O_3$/triglyme, NaI/VSe_2 cell at 130°C. From ref. 16.

The OCV of a Na/$Nb_{1.1}S_2$ cell at 130°C was 2.2V. However, the first discharge proceeded from ~1.7V with the potential remaining at ~1.4V during most of the discharge. The discharge to a 1.0V cutoff yielded a capacity of 0.72e^-/$Nb_{1.1}S_2$. In contrast to the discharge, the first charge exhibited a more linear voltage-time behavior, with a much higher slope than the discharge. The charge to 2.3V corresponded to 0.54e^-/$Nb_{1.1}S_2$. All subsequent discharges and charges exhibited slopes similar to the first charge with ~0.5e^-/$Nb_{1.1}S_2$ capacity. On the basis of our cycling results we have suggested that the 3R-$Nb_{1+x}S_2$ structure at the end of the first cycle is converted to 2H-$Nb_{1+x}S_2$, with little change thereafter.

The discharge capacity and rechargeability of $Nb_{1.1}S_2$ at 320°C was strongly dependent on the cutoff voltage. Thus, to a 1.7V cutoff the Na uptake was ~0.45 with 90-95% reversibility. If the cutoff voltage was set lower, Na uptakes exceeding one were possible, but with substantial irreversibility.

The specific energy of the Na/$Nb_{1.1}S_2$ cell with 0.5e^-/$Nb_{1.1}S_2$ and 1.5V is 119 Whr/kg. Obviously, it is much inferior to the three disulfides discussed earlier.

TaS_2: The EMF-composition data obtained by Nagelberg and Worrell (26) for 2H-TaS_2 in a Na cell at room temperature indicated a linear profile in the range $0<x\leq1$. These authors interpreted this to mean a single phase ternary for all values of Na. We have cycled a TaS_2 cathode at 130°C (18). To a 1.0V cutoff we found a limiting composition of $Na_{0.8}TaS_2$. Furthermore, the discharge deviated from a linear behavior probably indicative of different phases at the low and high Na levels.

Cyclic voltammetric data with 2H-TaS_2 at 280°C indicated at least four phases in the Na/2H-TaS_2 system (26). Interestingly enough, reversibility for Na was found in all of the four phases. The high temperature data, obtained with very low cathode loadings, indicate a specific energy of 185 Whr/kg for the Na/TaS_2 couple.

4.3.2 Transition Metal Diselenides

We have cycled three diselenides, VSe_2, $TiSe_2$ and $NbSe_2$ in a Na cell utilizing triglyme/NaI(1M) at 130°C (16,28).

VSe_2: Typical cycling curves for VSe_2 are given in Fig. 4.

Although the OCV of the Na/VSe_2 cell was 2.32V, the cell rapidly polarized upon discharge to ~1.7V, and the discharge proceeded with a voltage plateau at ~1.6V. The discharge showed a definite end-point when a capacity equivalent to 1e^-/VSe_2 has been reached. The cell exhibited 100% rechargeability in the first charge and with repeated cycling, the 1e^-/VSe_2 utilization was maintained.

A break in the discharge curve, which becomes more pronounced in the second and subsequent discharges, is observed at $Na_{0.48}VSe_2$. From a comparison of the X-ray data of discharged cathodes with those of the previously identified Na_xVSe_2 phases (27), we have assigned the first plateau in the discharge to a two-phase region comprising VSe_2 and a Type I Na_xVSe_2 rhombohedral phase ($a = 3.48$ Å and $c = 7.41$ Å). The second plateau apparently corresponds to further intercalation of Na into the Type I Na_xVSe_2 phase with both Type I and Type II rhombohedral ($a = 3.73$ Å and $c = 6.88$ Å) phases co-existing at high values of x.

Preliminary potentiostatic experiments indicated higher rate capabilities for VSe_2 than for TiS_2 and VS_2. A capacity equivalent to 0.72e^-/VSe_2 was obtained at a current density of 5 mA/cm^2. The specific energy of the Na/VSe_2 couple based on the observed cell voltage (1.6V) and capacity is 185 Whr/kg. Although this energy density is lower than in TiS_2 and VS_2 cells, its higher rate capability and excellent reversibility at moderate temperatures would make VSe_2 a practically attractive material.

$TiSe_2$: The discharge of a $TiSe_2$ cathode at 130°C proceeded in two distinct potential plateaus at ~1.75V and ~1.4V with a capacity of 1e^-/$TiSe_2$. The recharge in the first cycle was 100% efficient. The second and subsequent discharges, however, proceeded at lower potentials with the apparent absence of the two plateaus seen in the first discharge. The capacity in the sixth discharge was still 0.88e^-/$TiSe_2$. Apparently, a structural change of the host lattice occurs in the first cycle with little change thereafter. Although, we found reversibility for ~0.85 Na/$TiSe_2$, the lower cell voltages beginning with the second discharge do not make this material as attractive as VSe_2.

$NbSe_2$: This material exhibited a cycling behavior much inferior to VSe_2 and $TiSe_2$. The first discharge corresponded to a capacity of only ~0.3e^-/$NbSe_2$ with a mid-discharge potential of ~1.5V. This capacity was reversible for many cycles (28).

4.3.3 Transition Metal Trisulfides

Some preliminary results are available for two trisulfides, namely, TiS_3 and amorphous MoS_3.

TiS_3: This compound, although it has a layered structure related to TiS_2, contains two types of sulfur species, S^{-2} and S_2^{-2}. When TiS_3 is discharged in a Li cell, a capacity of 3e^-/TiS_3 is obtained. But, two of these electrons are involved in the irreversible reduction of S_2^{-2} (1).

Zanini et al. (19) found an irreversible discharge of TiS_3 in Na cells also. At 230°C, they obtained a capacity in the first discharge of $2.4e^-/TiS_3$ at 0.1 mA/cm^2. In the second cycle, however, the capacity decreased to less than $1e^-/TiS_3$ and the discharge curve resembled that of TiS_2. Their evidence indicate that TiS_3 transforms to TiS_2 during cycling at 230°C.

MoS_3: Intercalation of amorphous MoS_3 in Na-naphthalide resulted in Na uptakes of up to 4 Na/MoS_3 (29). The ambient temperature discharge of a Na/MoS_3 cell utilizing an organic electrolyte resulted in a capacity of nearly $3e^-/MoS_3$ with a mid-discharge voltage of ~1.5V. However, little data are available on cathode rechargeability. We have cycled a-MoS_3 in a cell utilizing molten $NaAlCl_4$ at 165°C and the results are discussed in a later section. Many amorphous metal sulfides have exhibited unusual Li intercalation behavior compared with their crystalline analogs (12). It appears that both the structural and electrochemical studies of Na intercalation compounds of amorphous metal chalcogenides would be a fruitful research area.

4.3.4 Nickel Phosphorus Trisulfide

The transition metal phosphorus trichalcogenides, MPX_3, where M = Fe or Ni and X = S or Se, apparently have structures similar to that of TiS_2. The transition metal atoms and P-P pairs occupy sites that Ti would fill in the TiS_2 structure.

We have evaluated the cycling behavior of $NiPS_3$ at 130°C (30). Figure 5 shows a few cycles. The first discharge to a 1V cutoff yielded a capacity of $2e^-/NiPS_3$ with a mid-discharge voltage of 1.8V. Preliminary X-ray data of a discharged cathode indicated no Na_2S and the line positions were shifted only slightly from $NiPS_3$, apparently indicating an intercalation reaction. However, the capacity showed a continuous decrease with cycling, diminishing to ~$0.4e^-/NiPS_3$ by the 20th cycle. Further work is required to fully understand the behavior of this class of compounds in Na cells. Thus, it would be useful to obtain information on the role of the metal, Fe vs. Ni, and the role of the chalcogenide, S vs. Se, on the cathodic behavior of this class of compounds.

4.3.5 One Dimensional Chain-Type Compounds

This class of compounds potentially offers a higher degree of structural flexibility for Na intercalation than the two dimensional layered dichalcogenides (11). We have carried out a preliminary study of NbS_2Cl_2 and MoS_2Cl_2.

X-ray diffraction data of $Na_2NbS_2Cl_2$, prepared in Na-naphthalide with stoichiometric quantities of the reagents, indicated X-ray lines not significantly different from those in NbS_2Cl_2. But, for preparations with a large excess of Na-naphthalide, X-ray data indicated Na_2S. It appeared that the following reactions occurred.

$$NbS_2Cl_2 + 2Na\text{-}Naph \rightarrow Na_2NbS_2Cl_2 + 2Naph. \quad (2)$$

$$Na_2NbS_2Cl_2 + 2Na\text{-}Naph. \rightarrow 2Na_2S + NbCl_2 + 2Naph. \quad (3)$$

We also investigated the cycling behavior of NbS_2Cl_2 and the related MoS_2Cl_2 in a Na cell utilizing triglyme/NaI(1M) at 130°C. The discharges are shown in Fig. 6. Capacities of $0.95e^-/NbS_2Cl_2$ and $1.05e^-/MoS_2Cl_2$ with mid-discharge voltages of 2.0 and 1.8V respectively, were obtained in the first discharge to a 1.3V cutoff. The rechargeabilities, however, of both of these compounds were poor. Interestingly enough, we have found excellent reversibility for NbS_2Cl_2 in a Na cell with molten $NaAlCl_4$ electrolyte at 165°C. This is discussed in the next section.

4.3.6 Transition Metal Chalcogenides in Molten $NaAlCl_4$

In order to take advantage of the higher thermal stability and ionic conductivity of inorganic molten salts, we have investigated the cycling behavior of metal chalcogenides in molten $NaAlCl_4$. A preliminary account of the results has been reported (3). A basic melt prepared from 51 mole-percent NaCl and 49 mole-percent $AlCl_3$ was used. Some surprising results, but practically more useful than with organic electrolytes, have been obtained. A brief discussion of the results with VS_2, MoS_2 and NiS_2 would be useful as an introduction into this chemistry.

Unlike in the organic electrolyte, the first discharge of VS_2 seem to involve a displacement process, forming V_2S_3 and Na_2S, with a capacity between 0.90 and 0.70 e^-/VS_2 at current densities between 1 and 5 mA/cm^2. Upon allowing the discharged cathode to stand on open-circuit (for ~72 hrs), an apparent reaction of V_2S_3 with $NaAlCl_4$ occurs. This leads to a large increase in the following recharge capacity. During the next few cycles, larger increases in the discharge capacity occur with a maximum of ~2.6 to $2.8e^-$/vanadium by the 5th to the 8th cycle. The cycling of the cell then becomes 100% coulombically efficient. The mid-discharge voltage is ~2.5V and the mid-charge voltage is ~2.8V. The cell exhibits excellent rechargeability. One cell has been cycled more than 100 times with very little capacity loss.

Analysis of solid cathodes from several cells, subsequent to cycling and removal of $NaAlCl_4$ by washing with CH_3CN, indicated that the higher capacities apparently result from the cycling of an *in situ* synthesized compound of the apparent composition $VS_{2.7}Cl_{1.6}$. The cycling behavior of the latter is quite similar to that of NbS_2Cl_2 (Fig. 7).

Cycling of MoS_3 in presence of $NaAlCl_4$ at 165°C resulted in a highly reversible $1e^-/MoS_3$

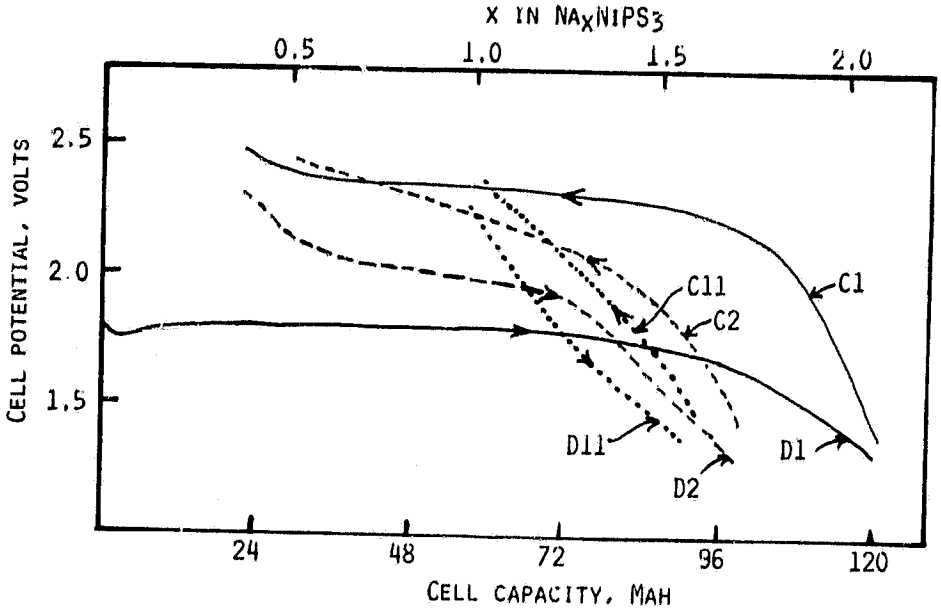

Fig. 5. Some typical cycles of a liquid Na/β'-Al_2O_3/triglyme, NaI/$NiPS_3$ cell at 130°C. current density: discharge, 1 mA/cm^2; charge, 0.5 mA/cm^2. Curves marked D's are discharges and those marked C's are charges.

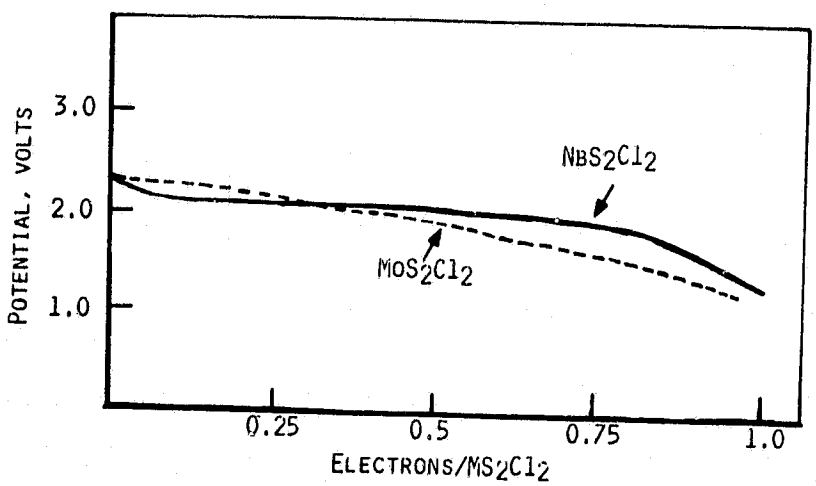

Fig. 6. Discharges of NbS_2Cl_2 and MoS_2Cl_2 at 130°C.

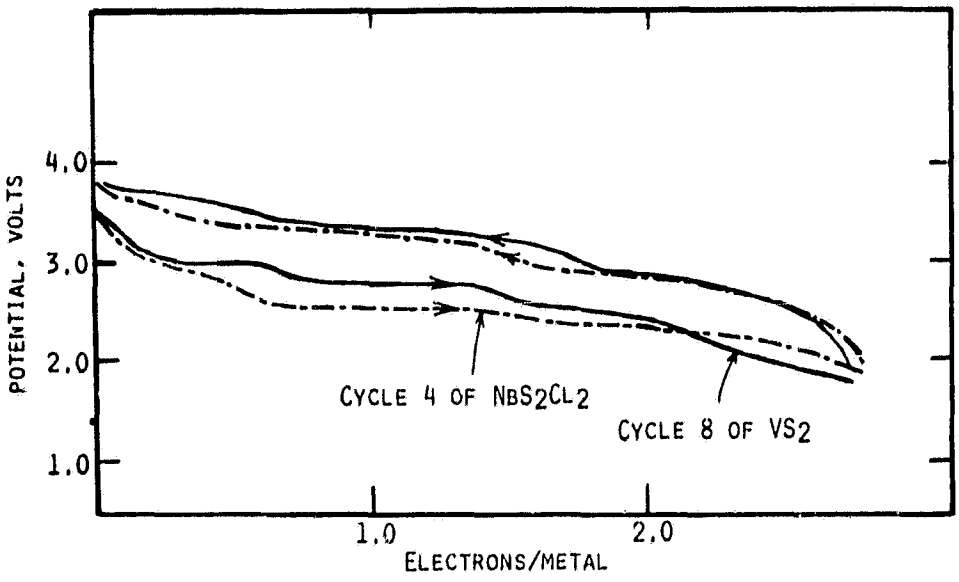

Fig. 7. Cycles of liquid Na/β"-Al_2O_3/$NaAlCl_4$/VS_2 or NbS_2Cl_2 cells at 165°C. From ref. 3.

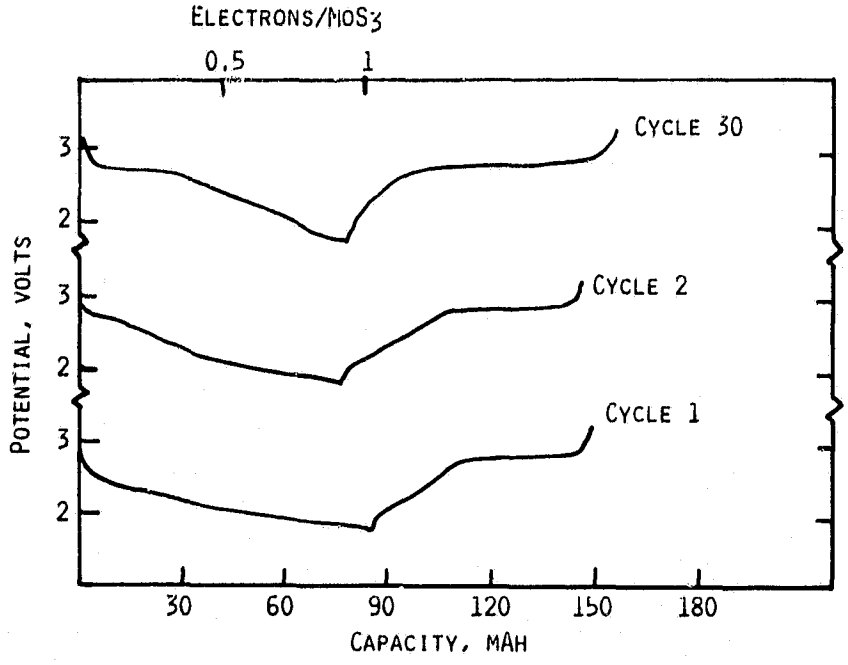

Fig. 8. Typical cycles of a liquid Na/β"-Al_2O_3/$NaAlCl_4$/MoS_3 cell at 165°C.

Table III. Quasi-Theoretical Energy Densities* of Na/Metal Chalcogenide Couples

Metal Chalcogenide	Temperature (°C)	Capacity, e^-/Chalcogenide	Mid-discharge Voltage (V)	Specific Energy (Whr/Kg)
TiS_2	25	0.40	1.5	140
	130	0.65	1.7	215
	280	1.0	1.8	360
VS_2	130	0.70	1.8	258
$Cr_{0.5}V_{0.5}S_2$	130	0.70	1.9	273
$Nb_{1.1}S_2$	130	0.50	1.5	119
TaS_2	280	1.0	1.8	185
VSe_2	130	1.0	1.6	185
$TiSe_2$	130	1.0	1.4	162

*Based on reversible capacities.

capacity to a discharge limit of 1.7V (Fig. 8). The higher voltages than in organic electrolyte cells (27) suggest a probable displacement type discharge process. Interestingly enough, further reactions of the discharge product with $NaAlCl_4$, as in the case of VS_2, did not seem to occur.

The behavior of MoS_3 resembled that of non-Na intercalating materials such as NiS_2 which undergo displacement type electrode reactions without direct interaction with $NaAlCl_4$ (31). The reasons for the differences in the electrochemistry of Na intercalating chalcogenides in organic and molten $NaAlCl_4$ electrolytes, as well as the differences in the behavior of VS_2 versus NiS_2 in molten $NaAlCl_4$ are not clearly understood.

5. SUMMARY AND FUTURE DIRECTIONS

The quasi-theoretical energy densities of some of the relatively well characterized Na/metal chalcogenide couples are listed in Table III. The data seem to indicate that the energy densities approach theoretical values as the temperature is increased to relatively high values. However, non-reactive electrolytes would be required to preserve the intercalation reaction.

At ambient to moderately high temperatures the rechargeability of many materials is limited by crystallographic phase changes in the intercalation products. Further exploration of the structural and electronic properties of the intercalates, especially the multistage compounds at low Na contents, is required to fully understand the causes of the irreversibilities and to possibly overcome them. In this respect, further studies of chalcogenides of the type, $M_nN_{1-n}S_2$ and MS_nSe_{2-n} would be valuable.

Very little work has so far appeared dealing with the general class of amorphous compounds. Opportunity for both structural and electrochemical studies exist in this area.

As has been found in Li battery cathode studies (1), metal selenides such as $NbSe_3$ and $MoSe_3$ may show considerably different and more desirable Na intercalation properties than TiS_3. This would be worth exploring.

The scope of rigid lattice transition metal oxides as rechargeable positive electrodes for Na cells remains to be assessed.

The results with NbS_2Cl_2 and MoS_2Cl_2 indicate some potential opportunities with one dimensional chain-type materials as cathodes.

Finally, as we have found with $NaAlCl_4$, novel electrolyte-dependent chemistry might be possible with many of these chalcogenides as well as with other electrolytes.

6. ACKNOWLEDGEMENT

The experimental work at EIC on Na Intercalation Cathodes was funded by National Aeronautics and Space Administration.

7. REFERENCES

(1) K. M. Abraham and S. B. Brummer, Chapter 14 in "Lithium Batteries", J. P. Gabano, ed, Academic Press, London (book in print).

(2) "Annual DOE Review of the Li/Iron Sulfide Battery Program", Argonne National Laboratory, June 20-21, 1979 and June 25-26, 1980.

(3) K. M. Abraham, M. W. Rupich and L. Pitts, J. Electrochem. Soc., 128, 2700 (1981).

(4) G. Mamantov, R. Morassi, M. Matsunaga, Y. Ogato, J. P. Wiaux and E. J. Frazier, J. Electrochem. Soc. 127, 2319 (1980).

(5) J. J. Auborn and S. M. Granstaff, Proc., 15th IECEC, 575 (1980).

(6) A. M. Chreitzberg, EPRI EM-751, April (1978).

(7) I. W. Jones, Electrochim Acta, 22, 681 (1977).

(8) M. S. Whittingham, Progress in Solid State Chem. 12, 41 (1978).

(9) K. M. Abraham, J. Power Sources 7, 1, (1981/82).

(10) D. W. Murphy and P. A. Christian, Science 205, 651 (1979).

(11) J. Rouxel, Physica 99B, 3 (1980).

(12) M. S. Whittingham, J. Electroanal. Chem. 118, 229 (1981).

(13) W. R. Johnson and W. L. Worrell, Synthetic Metals 4, 225 (1982).

(14) G. H. Newman and L. P. Klemann, J. Electrochem. Soc. 127, 2097 (1980).

(15) K. M. Abraham, L. Pitts and R. Schiff, J. Electrochem. Soc. 127, 2545 (1980).

(16) K. M. Abraham and L. Pitts, J. Electrochem. Soc. 128, 1060 (1981).

(17) K. M. Abraham and L. Pitts, J. Electrochem. Soc. 128, 2574 (1981).

(18) K. M. Abraham, R. Schiff and S. B. Brummer, Final Report, NASA Contract NAS3-21028, Report No. CR159469 (1979).

(19) M. Zanini, J. L. Shaw and G. J. Tennenhouse, J. Electrochem. Soc. 128, 1647 (1981).

(20) M. Zanini, J. L. Shaw and G. J. Tennenhouse, "Proc. International Conference on Fast Ion Transport in Solids", Gatlinburg, TN (1981).

(21) K. M. Abraham, J. L. Goldman and M. D. Dempsey, J. Electrochem. Soc. 128, 2493 (1981).

(22) K. M. Abraham, J. L. Goldman and D. L. Natwig, J. Electrochem. Soc. in press.

(23) D. A. Winn, J. M. Shemilt and B. C. H. Steele, Mater. Res. Bull., 11, 559 (1976).

(24) B. G. Silbernagel and M. S. Whittingham, Mater. Res. Bull. 11, 29 (1976).

(25) G. A. Wiegers et al. Mater. Res. Bull. 9, 1261 (1974).

(26) A. S. Nagelberg and W. L. Worrell, "Electrode Materials and Processes for Energy Conversion and Storage," J. D. E. McIntyre, S. Srinivasan, and F. G. Will, Editors, p. 487, The Electrochemical Society Softbound Proceedings Series, Princeton, NJ (1977).

(27) J. R. Bloembergen, R. J. Haange and G. A. Wiegers, Mater. Res. Bull., 12, 1103 (1977).
(28) K. M. Abraham, EIC Laboratories, Inc, unpublished results.
(29) A. J. Jacobson, R. R. Chianneli, S. M. Rich and M. S. Whittingham, Mater. Res. Bull. 14, 1437 (1979).
(30) K. M. Abraham, unpublished data.
(31) K. M. Abraham, M. W. Rupich and J. Elliott, paper presented at the fall Meeting of the Electrochemical Society, Detroit, MI (1982).